BSc Thesis

DC Grid Design

Paul Kluge
Jesse Richter

Group O
Distribution of the electricity grid of a tiny house community

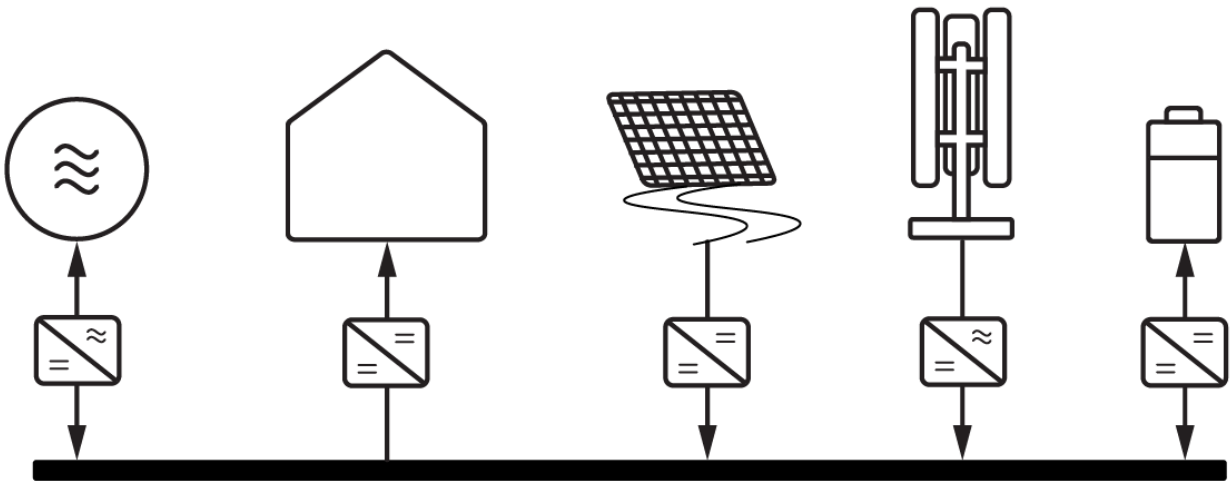

TU Delft

BSc Thesis

DC Grid Design

by

Paul Kluge
Jesse Richter

Students:	P.M. Kluge	4915593
	J.O. Richter	4862236
Project duration:	April 19, 2021 – July 2, 2021	
To be defended on:	June 28th, 2021	
Thesis committee:	Dr. R.A.C.M.M. van Swaaij,	chair
	Dr. P.P. Vergara Barrios,	supervisor
	Dr. M. Taouil	
	Dr. S. Du	

TU Delft

Abstract

This thesis covers the top-level design of a DC microgrid of a tiny house community on the roof of a high-rise building in Rotterdam. This DC microgrid consists of 12 tiny houses, a common usage area, Renewable Energy Supply (RES) methods, using solar and wind energy, and an Energy Storage system (ESS). This design is part of a complete DC smart grid for such a community with two other subgroups focusing on the control and software, the CNS group, and power line communication, the PLC group.

In this thesis, three design phases are discussed; demand estimation, storage & supply design, and topology design. Subsequently, the resulting grid design is validated. The first phase resulted in an estimation of hourly, daily, and monthly energy usage. Using a model of the generation, 61.2 m^2 Photo-Voltaic (PV) panels and 6 Vertical Axis Wind Turbines (VAWT)s were selected. In order to handle the varying energy generation of the RESs, different ESS options are considered, and 4 Li-Ion batteries are chosen. This combination of storage and supply resulted in a grid availability of 93.73%. In the last design phase, the topology of the community is designed, which resulted in a 400 VDC unipolar ring-based series-connected multi-bus configuration, which effectively operates in radial form to reduce complexity and enables easier fault location detection. The topology design also considers the converter requirements, wiring, and stability and safety considerations. A cost analysis is made of the entire grid resulting in an estimated total cost of around €100,000. Lastly, design verification is performed on the proposed design, which resulted in functional results during 100% demand, with a maximum voltage drop of 1.82% and during 150% demand, with a maximum voltage drop of 2.80%.

Preface

The basis for this research stems from an initial minor project of one of our colleagues, Pieter van Santvliet. Our interest in sustainability and our background in electrical engineering motivated us to continue his project. Without our four highly motivated colleagues who tackled two other essential aspects of the design, this project would not have been possible.

Our special thanks goes to our motivated and open-minded supervisor, Dr. P.P. Vergara Barrios, who was always able to guide us and propose alternatives during times of difficulty.

We would like to thank our thesis committee consisting of the chair Dr. R. van der Swaaij, our supervisor Dr. P. P. Vergara Barrios, Dr. M. Taouil, and Dr. S. Du.

Furthermore, we would like to express our gratitude to Dr. A. Lekić who was able to help us tremendously during the design validation.

Our thanks also go to J. Antonisse and A. Mensink for answering our large number of initial questions and giving us a perspective on usage, generation, and storage in a tiny house community.
We would like to also thank T. Tajiri for providing us with anonymous monthly energy usage data from several houses in the 'Minitopia' tiny house community.

Additionally, we would like to thank the residents of the tiny house communities 'Pionierskwartier' in Delft and 'Minitopia' near Den Bosch for their cooperation in our surveys.

Lastly, we would like to thank Dr. I.E. Lager for the excellent organization and fluency during the COVID-19 pandemic of the Bachelor Graduation Project, as well as his willingness to answer all our questions regarding the project.

Paul Kluge and Jesse Richter
Delft, June 2021

Contents

1 Introduction

With climate change being a more pressing matter than ever, many people are looking for ways to minimize their ecological footprint. One of the most effective ways for individuals to reduce their impact on the environment is sustainable living. In the last two decades, sustainable housing has been gaining popularity with at the forefront of the movement a concept called 'tiny houses' [1]. According to the US-based International Residential Code (IRC) a tiny house is as a dwelling that has a floor area of less than 37 m^2 [2]. This description, however, is insufficient as tiny houses can not be described merely by their size. Tiny houses are commonly designed to achieve efficient use of internal space, greater environmental sustainability and the ability to live off-grid while minimizing possessions [3]. This is mainly achieved by multi-functional interior design, minimizing energy demand, and operating on green energy by using Renewable Energy Source (RES)s. As space is scarce, many tiny house users put or build their tiny houses in communities to share resources. According to [4], one of the key motivators for people deciding to live in a tiny house is being part of a community. And while these communities are connected socially, many of them consist of separately built homes that each have their own energy generation and storage.
Designing a tiny house community that can collaborate on a technical level was the goal of the tunus project [5].

1.1. Tunus

In the tunus project, first, the design of a single tiny house was made. This tiny house was called tunus. Then, the electricity, heat, and water grids of 12 tuni - the plural of tunus - were connected. Besides the tiny houses, a common area (or central hub) was added to the tiny house community. It consists of batteries, a controller, and washing machines.

The tunus community is designed to be on top of high-rise buildings in the city of Rotterdam. Power is provided by PV panels and VAWTs and distributed by an intelligent DC Grid (DCG), as on top of these buildings wind and sun is plenty. Batteries are used to store or provide extra power.

This thesis elaborates on the tunus project [5]. Whereas the tunus project mainly discussed the concepts of all technical aspects, for this thesis, the focus is on only the electricity grid of the community. A top-level design of this grid will be made and presented in this report.

It is likely no coincidence that the project coincides with an increasing interest in microgrid technology. Cambridge Dictionary defines a microgrid as "an electricity grid system of electricity wires for a small area, not connected to a country's main electrical grid" [6], which clearly includes both the tunus project and the scope of this thesis. Now, a situation assessment and state-of-the-art analysis of microgrids are made.

1.2. Microgrid Analysis

For the past decades, the electricity grid has functioned on centralised generation, and transmission using Alternating current (AC) [7]. Generation mainly was done using fossil fuels. This meant large

generators and long transmission lines. The first renewable energy sources connected to the grid were hydroelectric, which is often also generated far from cities and thus requires transmission. Although these big interconnected AC networks were and still are the global standard, it is vital to remember that ”AC electrical energy is a transportation medium and not a commodity in itself” [8].

According to the International Energy Agency (IEA), the energy consumption is expected to grow by 4.6% in 2021. 70% of this growth is projected to be in emerging economies [9]. To accommodate this kind of growth, all losses should be minimised. In Europe, losses in transmission and distribution stages can be up to 11% of the total energy consumption [10]. To combat these losses, new methods are introduced. One relatively new method that is increasingly used is microgrids. Microgrids are relatively small to medium-sized energy supplying systems operating within the framework of clearly defined boundaries for the generation, storage, transmission, and distribution of energy [11]. They can decrease the losses in the overall system by spatially reducing the distance between generation and consumption. Perhaps the most crucial advantage of microgrids is their ability to integrate residential RESs without drastically interfering with the AC main grid. The current main grid is not explicitly designed to accommodate for smaller amounts of energy supplied by many residential nodes even though the use of residential RESs is quickly increasing. Due to the reduction of price and improvement of quality of PV panels and more development in smaller VAWTs, these renewable and decentralised generation methods become more affordable and accessible. However, these renewable sources do present issues, as discrepancies between generation and demand can occur. New developments in energy storage technology and control strategies are improving the feasibility of these microgrids, and their use cases are growing. This can help the transition from the old centralised fossil fuel-based system to a new, more sustainable decentralised system. Besides improving the integration of RESs and reducing losses, microgrids can also improve reliability by operating in islanded mode when the grid goes down, reduce emissions when making use of renewable sources and in larger cities reduce costs by relieving the grid at critical areas [12].

Optimizing control strategies in order to make microgrids ’smart’ will further improve usability and thus popularity. Another important upcoming trend is the use of DC grids instead of AC as this technology is more compatible with PVs and battery systems which both operate on DC. As DC is gaining in popularity, the market for DC appliances is growing as well [13]. These trends make for a promising future as a DC microgrid with DC appliances is estimated to be more than 30% more energy efficient compared to the current grid and appliances [14]. Especially in more remote areas, microgrids can be a more efficient way to provide reliable electricity to consumers. According to the IEA, microgrids are the most economical way to expand access to energy in remote regions and regions which lack electricity infrastructure [15]. They predict that by 2030, 30–40% of people living in developing countries will be supplied by microgrids based on renewable energy sources.

1.3. Problem Definition

It is clear that microgrids will play an essential role in the future. This project will contribute to this future by building on the work of the tunus project, though only the electricity grid will be considered. This means that several of the designs and design choices that were made for the tunus project will be kept here. These include the location (on a Rotterdam rooftop), the heat grid, and the design of a single tiny house. Unsolved or unfinished characteristics of these topics will not be treated here as they are of little relevance. For example, how to get on the roof is not part of this project’s scope. The topology and control system are subject to change, as well as the choices on electricity generation and demand and the grid connection.

The result of this project should be a design of the DC smart grid of a tunus tiny house community. It should serve more as a Proof of Concept (Poc) than a finished design or instruction manual. Further, it should contribute to the development of microgrids, for tiny house communities and elsewhere.

1.4. Subdivision

The design of the microgrid is split into three parts. A different subgroup treats each part. The first part considers the hardware of the microgrid. It treats the design choices for all the components used in the grid, responsible for energy demand, generation, storage, and distribution. It considers the topology and layout of the microgrid, including its safety and stability. This part is done by the DC Grid (DCG) subgroup.

The second part considers the control and software of the microgrid. It discusses the forecasting of energy generation and demand using ANNs. This forecast is used in combination with the measurements performed by the DCG subgroup to control the microgrid. This part also treats the design of this control algorithm. This part is done by the Control & Software (CNS) subgroup.

The third part considers the communication within the microgrid. It treats the communication over the DC power line. It discusses the modulation technique, error detection, bit rate, and transmission and receiver module. Lastly, it considers the communication protocol. This part is done by the Power Line Communication (PLC) subgroup.

1.5. Thesis Outline

This thesis covers the Bachelor Graduation Project of the DCG subgroup. Chapter 2 presents the PoR of the DC grid design, indicating all that is required for this design to be deemed completed.

In Chapter 3, the energy demand of the tiny house community will be estimated and modelled. Based on these models, the appropriate methods for generating and storing energy can be selected. The process of selecting and sizing the energy supply and storage of the community is covered in Chapter 4. To interconnect the loads of the tiny houses, energy generation, storage system, and the AC main grid, a topology design is proposed in Chapter 5. In Chapter 6, a simulation is made to validate the design of the proposed DC grid. Finally, Chapter 7 contains the conclusion of the project. A discussion and some recommendations for future work are also provided here. Figure 1.1 shows how each chapter contributes to the entire DC grid design.

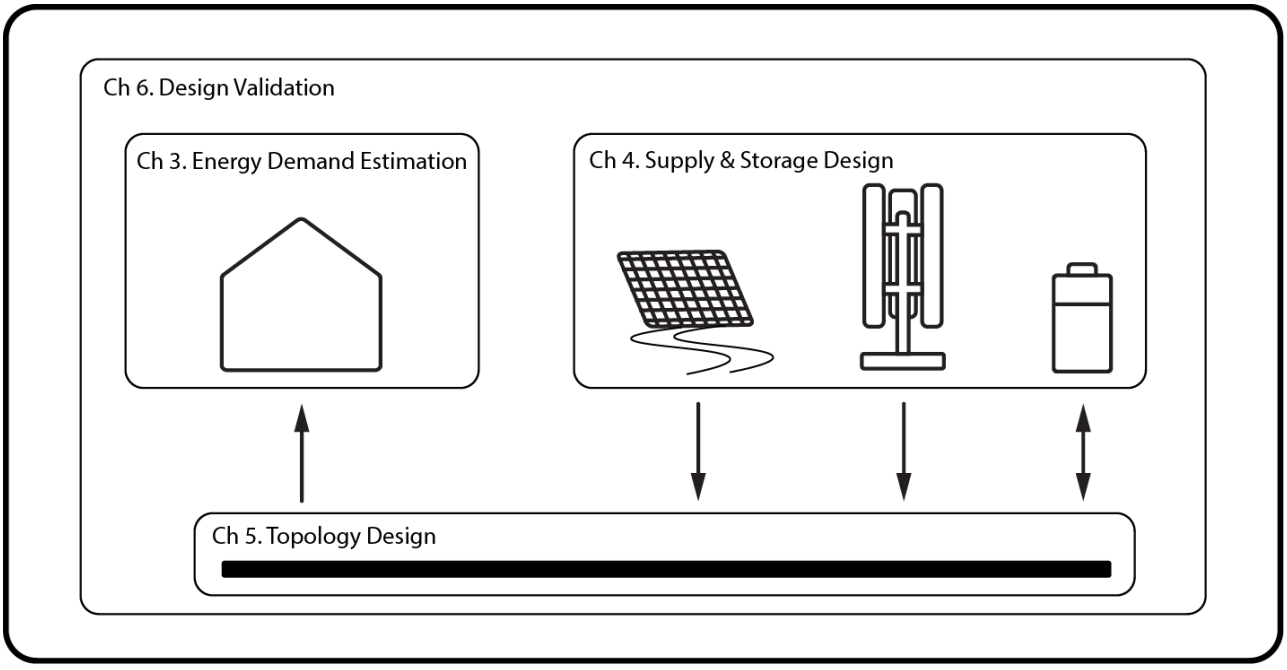

Figure 1.1: Schematic overview of the thesis outline

2

Program of Requirements

The following chapter specifically covers the requirements of the DC grid design sub system. The top-level system requirements of the Bachelor Graduation Project 'Distribution of the electricity grid of a tiny house community' can be found in Appendix A. The top-level requirements relevant to the DCG subgroup have been rephrased and integrated into the subgroup requirements shown below.

The MoSCoW method [16] will be used to prioritize requirements. The method involves dividing requirements into 'Must have', 'Should have', 'Could have' and 'Won't have'. Must haves are essential requirements (primary). Should haves are secondary and will be done after primary requirements are achieved. Could haves are nice to have (tertiary/bonus requirements). Won't haves will not be implemented in this subsystem.

Must have

- **RQ-M.DCG.1:** The microgrid, which is defined as the interconnection between the RESs, ESS, main grid and loads of both the tiny houses and tunect, must operate at DC.
- **RQ-M.DCG.2:** The microgrid must be able to supply a certain amount of the peak demand of the 12 tiny houses combined. This amount has yet to be determined.
- **RQ-M.DCG.3:** The nanogrid, which is defined as the residential grid of a tiny house which is connected to the microgrid. must be able to supply a certain amount of the peak demand of all the appliances combined. This amount has yet to be determined.
- **RQ-M.DCG.4:** Users must be able to use all needed appliances in their homes. This implies that both AC and DC appliances need to be considered.
- **RQ-M.DCG.5:** The microgrid must have an availability of at least 90% throughout the year. The availability is defined as the amount of time in which the microgrid is able to supply the demand of the community without needing energy from the main grid. The microgrid is then considered (partly) unavailable if either a fault in the microgrid (or nanogrid) or overconsumption occurs.
- **RQ-M.DCG.6:** In case of overconsumption or faults, the microgrid must be connected to the main grid in order to supply the necessary power.
- **RQ-M.DCG.7:** In case of overproduction, the microgrid must facilitate this overproduction by either delivering back to the main grid or diverting power using to be determined methods.
- **RQ-M.DCG.8:** The generation of the community must consist solely of more than one RES.
- **RQ-M.DCG.9:** The energy storage system (ESS) must be able to supply the peak power demand.
- **RQ-M.DCG.10:** The power lines must be able to handle the maximum current and voltage at the chosen peak demand at all times.

- **RQ-M.DCG.11:** The DC/DC and AC/DC converters of the entire system must be able to handle the maximum rated input and output power of their respective connection points.
- **RQ-M.DCG.12** The design must include a heating grid based on the heat grid designed in [5].
- **RQ-M.DCG.13:** The voltage buses of the microgrid and nanogrid must remain at a constant optimally chosen voltage with minimum and maximum fluctuation of a to be determined percentage.
- **RQ-M.DCG.14:** Hourly measurements of power usage must be available for the communication to the control & software group.
- **RQ-M.DCG.15:** The design must be validated with power analysis simulation software. Minimum and maximum demand must show functional results.

Should have

- **RQ-S.DCG.1:** The balance between the overall cost of the entire DC grid and its functionality should be optimized.
- **RQ-S.DCG.2:** Each tiny house and the common usage load should have an interface for users to view the usage.
- **RQ-S.DCG.3:** The amount of any type of converter should be kept as low as possible in order to minimize costs and to optimize efficiency.
- **RQ-S.DCG.4:** A fault in one location of a nanogrid should not hamper the operation of the other houses.
- **RQ-S.DCG.5:** A to be determined control algorithm should be used for each of the converters of the RESs for optimal power extraction.
- **RQ-S.DCG.6:** The entire microgrid should comply with the safety regulations of the EU in association with Dutch regulations and safety and connection standards for DC grids.

Could have

- **RQ-C.DCG.1:** The microgrid could operate completely islanded.
- **RQ-C.DCG.2:** Appliances in the houses could operate completely at DC.
- **RQ-C.DCG.3:** The tiny houses could share power with each other.
- **RQ-C.DCG.4:** Design validation could be done for excessive scenarios of maximum power demand.
- **RQ-C.DCG.5:** Primary control methods could be defined and compared for this implementation.
- **RQ-C.DCG.6:** In case of overproduction, supplying excessive energy back to the main grid could be minimized in order to minimize grid connection.

Won’t have

- **RQ-W.DCG.1:** This design will not include the design of a primary control system.
- **RQ-W.DCG.2:** This grid design will not include optimal design of circuitry, only top-level design.
- **RQ-W.DCG.3:** This design will not include an in-depth design of a protection system. Thus only the grounding, overall safety and a general protection protocol will be considered.

3

Energy Demand Estimation

The first step of this grid design is to estimate the demand of the loads connected to the microgrid. These loads consist of the nanogrids of the 12 tiny houses and the common hub referred to as 'tunect'. The establishment of the energy demand of the community is needed for determining which RESs are the optimal choice for this grid design, how many RESs are needed, and what ESS needs to be chosen to obtain the required 90% availability. Furthermore, the scenario in which all appliances are on needs to be researched to properly size the system to be able to handle the peak power in order to meet RQ-M.DCG.2 and RQ-M.DCG.3. This includes the power cables, converters, and the total generation capacity of the RESs and the power output of the ESS. This chapter covers how the energy demand of the community has been estimated and modeled.

In Section 3.1 an initial estimation of the usage has been done by considering what appliances and electronics are likely to be used in the community. In this initial estimation, most appliances are AC as DC appliances are still rarely found. Then, in Section 3.2, it is discussed whether AC or DC appliances are to be used in the design and what effect the use of DC appliances might have on the demand. This section also covers modifications of the initial demand calculations based on design choices and information obtained from an interview with two tiny house owners and a questionnaire that has been sent to several tiny house communities. Finally, in Section 3.3 the demand of the community is established and modeled for various time scales.

3.1. Initial Calculations

As the community consists of 12 tiny houses and tunect, this section will consider the energy demand of one tiny house and tunect separately. In the final model, the demand of each tiny house is assumed to be similar while scaling the usage of tunect appropriately. All initial calculations are based on information found in datasheets of AC appliances found in Appendix B.1 and average time usage of appliances in common households provided by energy companies in [17] and [18]. All tables, data sheets and product references can be found in Appendix B.1 and Appendix B.2.

3.1.1. Tiny House Calculations

The types of appliances have been divided into four different categories. The base load indicates electricity usage, which draws power for almost all of the operating time. This demand should always be available to the user via storage or generation methods. Kitchen appliances consist of all appliances which could be used in a kitchen environment and which most people would own. The heating of both a tiny house itself and the hot water it uses is considered apart. This is because these systems are designed in the report of [5], and hence, need a separate section for proper elaboration. Lastly, the usage of some remaining appliances is covered, which are other minor appliances that do not fall under the previous three categories.

Base Load
The first category is the baseload and is summarised in Table B.1. In this table, the appliances are listed, together with their power rating, the time usage, and lastly, the energy consumption per day, which is calculated by multiplying the power rating times the usage in hours. The baseload of a conceptual tiny house would thus be equal to $80.68W$ and the total idle energy consumption per day equal to $435.61Wh/day$.

Kitchen Appliances
For the kitchen appliances, the same analysis has been made. Now a subtle difference can be made for some appliances between maximum and average power rating. For the energy usage in Wh, the average power rating is taken for the calculation. The maximum power rating is used to establish the peak demand. The results of the initial kitchen appliance usage are summarised in Table B.2. As can be seen from the table, the maximum power demand is equal to $12110W$, the average demand to $9210W$, and the energy consumption to $3041.58Wh/day$.

Heat Regulation
The heating of the houses themselves and their water usage is considered separately from the other demand. This is due to part of the heating regulation being based on the heat grid designed in [5]. Using Photo-Voltaic Thermal (PVT) panels, energy can be captured in the form of heat, which can be stored in newly developed heat batteries. This solves a significant demand problem as the majority of the used energy in a household is spent on heating. The heat grid and how it exactly operates will be discussed more in-depth in Section 4.1.1. On an average day, each house needs an additional $1700Wh$ for the boiler. Furthermore, it has been found that the setup in [5] had disregarded the need for a water pump, which has now been included in order to get a more realistic estimation of the energy demand. The water pump uses an additional $369.6Wh$.
The same sustainable shower system of [5] will be used in this design. This shower pumps 35 liters of water per minute but only uses 10 l/min as it filters and reuses its own water. This system requires an additional $30Wh$ a day, given that two users each take a shower of 6 minutes per day and the water has been heated by the previously mentioned boiler. Finally, air conditioning will add another $450Wh/day$. The total energy consumption of the heat regulation is then equal to $2549.6Wh/day$ with a peak power demand of $2644W$. These results are summarised in Table B.3.

Remaining Appliances
For the other usage, appliances used in the bathroom, the charging of a mobile phone and a laptop, an LED television, and a vacuum cleaner are considered. The peak demand, average demand, usage per day, and the energy consumption are listed in Table B.4. The peak and average demand are equal as the used appliances are either on or off with no intermediary modes (standby modes are not considered for the television and laptops). One exception has been made for phone chargers, where the average demand is set to older models which use $5W$ and the peak demand to more recent chargers of $10W$ or higher. For these appliances, the peak demand and average demand are equal to $2634W$ and $2629W$ respectively, and the energy consumption per day is equal to $566.99Wh/day$.

Initial Estimation of the Total Usage of a Tiny House
Until now, an initial model of the usage for the tiny house has been made. The total power consumption per house, excluding the tunect usage, can be calculated with these initial calculations. The results are shown in Table 3.1. This peak demand is very high, as a common household is able to handle 9.2 kW [19]. Moreover, this peak demand is not realistic as not all appliances will be used at once.

Table 3.1: Usage of all appliances in the tiny house combined.

Category	Peak power [W]	Wh/day	kWh/month	kWh/year
Idle	80.86	435.61	13.25	448.86
Kitchen	12110.00	3041.58	92.51	3134.10
Other	2634.00	566.99	17.25	584.23
Heating regulation	2644.00	2549.60	77.55	930.60
Total usage	17468.68	6539.79	200.56	5097.8

3.1.2. Tunect Calculations

Besides the usage of a tiny house, the usage of tunect is being defined externally. This common usage accommodates some appliances that will be used by all households and will thus be scaled to 12 users. The initial appliance selection of tunect consists of a washing machine, a dryer, and a printer. Tunect will also accommodate the control unit required to control the electricity grid. Furthermore, the community will need some outdoor lighting which will be powered by tunect.
These modules are installed at a central point accessible to all of the tiny house community members. The peak demand, average demand, usage per day, and energy consumption per day can be found in Table B.5. The average demand is only different for the printer, as the low power consumption of 0.3 W in idle mode is incorporated in the average usage calculation, being able to print when needed. In addition, 20 outdoor lights are deemed sufficient for providing enough light. As a result, the peak demand is equal to 3142 W, the average demand is equal to 3130.79 W, and a daily demand of 8550.41 Wh/day.

3.2. Demand Modifications

Now that an initial selection of appliances has been made, it is shown that the average usage and especially the peak demand is relatively high compared to a regular household [19]. One of the central values of a tiny house community is to live in a more sustainable way. Besides, designing a grid that must be able to supply the calculated peak demand will be both expensive and unnecessary, as the peak demand for all 12 houses will rarely be reached. Hence, in the design, a trade-off will be made between the demand and costs of the grid. The design choices for demand are based on experiences of tiny house users and research of existing and developing technologies.

3.2.1. Appliance Selection Based on Tiny House Users

In order to establish a better understanding of what tiny house owners actually use, some people from the tiny house community have been contacted. As mentioned in the previous sections, a survey was sent to two tiny house communities, and an interview was conducted with two tiny house owners that built their own homes. The results of the survey can be found in [20] and the notes of the interview in Appendix B.3. Note that only the appliance usage of houses with a living area smaller than 40 m^2 has been considered as anything larger has not been regarded as 'tiny'.
It is decided to find a balance between the minimalist approach of some of the owners and the somewhat abundant design of [5]. This way, the users of our tiny houses will live sustainably without giving up much comfort.

The usage of the baseload remains unchanged after modification. Even though the wifi router was indicated (in the survey) to be used less than expected, it is decided to use one as it may be needed for the smart control.
The most significant savings have been made by discarding kitchen appliances. It is decided to replace the coffee machine and kettle by simply boiling water on the stove as both interviewees stated they did and, as the survey indicated, were less commonly used. This choice has been compensated by adding time to stove usage. This way, energy savings are not too significant, but estimated peak demand is lowered remarkably. Then, the oven and microwave were chosen to be a combination unit which lowers peak demand, and the kitchen machine has been discarded as it is quite a luxury item.
All design choices for heating remain the same as those are very case-specific, and the current heat grid is considered fittingly sustainable.
The decision was made to discard the television and hairdryer as both are indicated to be used very little. Additionally, the vacuum cleaner is switched for a much more sustainable handheld model, which will suffice for cleaning a house of tiny proportions. Finally, the use of a dryer is unsustainable and excessive and thus discarded. However, it is decided to add an extra washing machine as the visited tiny house village had two for the same amount of households. The resulting usage is shown in Table B.10.

To conclude, the energy demand of a more sustainable household has been estimated. The tables can be found in Appendix B.4 and the final usage is shown in Table 3.2. Also, a comparison is made between the initial usage and the sustainable modified usage, which is shown as the percentual decrease in power and energy usage in the sustainable estimation after the modifications.

Table 3.2: The estimation of the total usage of one tiny house with a sustainable selection of appliances, including the percentual decrease in usage with respect to the initial estimation.

Categories	Peak power [W]	Wh/day	kWh/month	kWh/year
Idle	80.68	435.61	13.25	159.00
Kitchen	6450.00	1910.00	58.10	697.15
Other	172.00	117.27	3.57	42.80
Heating regulation	2194.00	2099.60	63.86	766.35
Total usage	8896.68	4562.48	138.78	1665.31
Decrease	49.07%	30.81%	30.81%	30.81%

3.2.2. The Effect of DC Appliances

In this design, one of the primary objectives of this system is to minimize main grid connection and thus optimize independence thereof. For this reason, simply choosing AC appliances because of standardization is not a valid argument. Besides, the microgrid to which the nanogrid of the tiny houses will be connected to is required to be operating on DC as stated in the PoR.
A standalone DC grid with RESs and its own ESS has some major advantages over AC microgrids, some of which are the fact that PV systems are a DC power source and ESSs like batteries and supercapacitors have DC characteristics as well.

Furthermore, the use of a residential DC grid has additional advantages including efficiency improvement, absence of losses due to reactive power, and great reduction of Electro-Magnetic Interference (EMI) [21]. One of the causes of this efficiency improvement is the fact that most residential appliances already operate on DC internally, meaning these appliances make use of an internal AC-DC converter also resulting in losses [22]. Garbesi et al. [13] state that these internal inverters are very inefficient and that avoiding its use throughout the residence can save up to 12% on conversion losses only. Making use of highly efficient DC heaters which are in development can save an additional 50% on heating [13] and using brushless DC motors instead of commonly used induction motors can save an additional 24% in some appliances [22]. Overall, the use of DC appliances only on a DC grid can result in energy savings of more than 30% according to [14], [13] and [21].

Even though the current market of DC appliances is still in its early phases and has some barriers to overcome, there are some clear indications that the sector has significant potentials [13], [14]. Based on what has been stated in this section and the ambition for this design to be innovative and technologically progressive, it is decided to assume DC appliances will be used in this grid design. RQ-C.DCG.2, which states that the appliances in the houses could operate completely at DC, is hereby fulfilled.
As these energy savings are still an educated approximation and speculation, the energy demand will not be scaled down by 30%. Instead, these potential energy savings will be used as the safety margin of the energy demand to account for potential underestimation of the energy demand and losses such as converter inefficiencies and wire losses. Meaning adding energy use to the currently calculated demand average will not be necessary as this is accounted for by the fact that DC appliances are used. The same can be said for the calculated peak demand as a significant fraction of these energy savings result from the lowering of each of the individual appliance's power rating [21]. Thus the currently calculated demand will be used for the final models, having incorporated a safety margin in this unconventional way.

3.2.3. Limiting Peak Demand

As can be seen in Table 3.2, the peak demand is still high at almost 9 kW, but now more comparable to a common household [19]. This peak power is only reached if all appliances are used simultaneously. Realistically this power demand will seldom be reached, and it would thus be costly and power inefficient to size the whole system on this peak demand.
RQ-M.DCG.4 states that all users must be able to use all needed appliances in their homes, so the power limit can only be set for power usage, which does not limit the use of the mentioned appliances. Looking at the used appliances, the most significant power saving is obtained by limiting the induction stove. Furthermore, the boiler can be limited by only turning it on during moments where the demand

is relatively low. In case all appliances are on, the stove can still be used to its average demand, while the hot water which is available in the boiler can be used for the shower and water tap. By using this method to limit the peak demand, the requirement RQ-M.DCG.4 is met.
Subsequently, the peak demand is limited to a maximum of 4746.68 W. In case the power demand risks exceeding this limit, the stove will be used as a buffer by limiting its power demand - in the most extreme case - to 1500 W. If this does not suffice, the same can be done for the boiler until it is completely off. The rest of the average demand, as well as daily, monthly, and yearly energy usage remains the same.

Now that the peak demand has been established, the system should be sized such that both the microgrid and nanogrid are able to supply their respective maximum demand in order to meet RQ-M.DCG.2 and RQ-M.DCG.3. Only after the design validation in Chapter 6 can it be determined whether these requirements are met.

3.2.4. Final Demand Estimation Results

As the final demand of a tiny house and the common usage have been established, the total demand of the community can be calculated. The total demand corresponds to the estimated demand of one tiny house, scaled to 12 households, plus the common demand of tunect. The resulting usage is shown in Table 3.3.

Table 3.3: Total sustainable usage of the whole community, including usage of 1 tiny house, 12 houses and common usage.

Category	**Peak power** [W]	**Wh/day**	**kWh/month**	**kWh/year**
1 house	4746.68	4562.48	138.78	1665.31
12 houses	56960.16	38324.84	1165.71	13988.57
Common usage	4142.00	2731.23	83.07	996.90
Total usage	61102.16	57481.00	1748.38	20980.56

3.3. Tiny House Demand Models

The total peak demand, average demand as well as the energy usage per day, month, and year presented in Section 3.2 are an estimation based on the usage of certain appliances. By using data from general household usage in the Netherlands, as well as an actual tiny house community, two behaviour models are constructed. The first model estimates the energy use of a tiny house during one day. The second approximates the energy use of one tiny house throughout the year. Results of these models will be presented next.

3.3.1. Model of One Day & Results

For the single-day model, smart meter data from the Distribution System Operator (DSO) Liander has been used [23]. This data includes smart meter measurements of energy usage for every 15 minutes for the year 2013. Since then, more efficient products, heating, and isolation have been introduced [24], however the behaviour of the residents of these houses in 2013 is estimated to be equal to current household behaviour. This data set contains the smart meter values in Wh for 78 houses over the course of one year, measured with intervals of 15 minutes.
From this data, a daily average energy demand of one tiny house can be constructed using the fractions of energy usage from the houses measured by the smart meters. The summed data values of all houses are divided by the measured 78 houses to get a daily average per house. By dividing the value of each 15-minute interval by the total Wh usage of a day, the fraction of energy used in that interval can be calculated. Multiplying this fraction with the calculated average daily usage of a tiny house results in 15-minute interval energy usage. Summing these intervals for every hour results in the hourly Wh usage for a tiny house. The resulting graph of this usage model is shown in Figure 3.1. The graph shows the estimated energy usage of one tiny house throughout an average day. The energy demand of an average smart metered house is shown as well.
As there is no power consumption data available, an option to still gather data for power consumption is to divide the energy usage in Wh by the measured time, hence dividing by 0.25 hours. These values are thus a multiplication of 4 of the energy demand. These values are much lower than the peak demand,

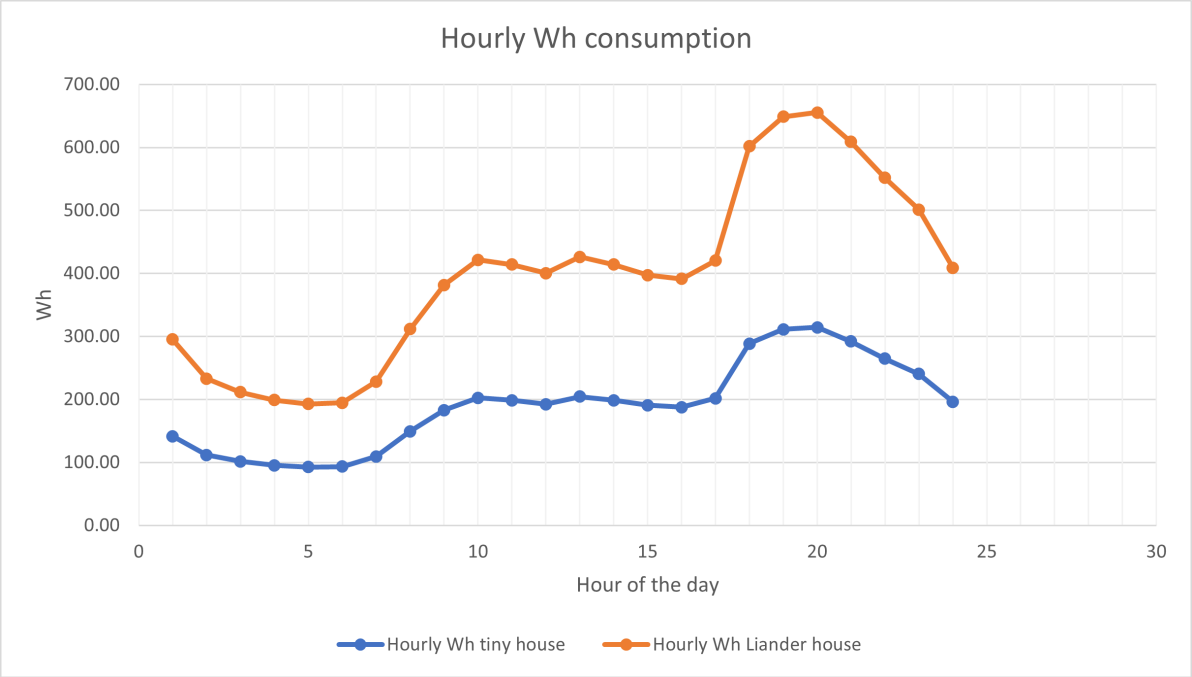

Figure 3.1: Average hourly energy usage in Wh over a day.

however they will be saved for possible later usage. In Appendix B.5.2 a short explanation and graph is provided for the Wh per hour or average hourly power demand over a day.

3.3.2. Model of One Year & Results

The daily average model is valuable for estimating demand throughout an average day, however inconsistencies arise when comparing lower usage in summer versus higher usage in winter. In these cold months, extra heating is required and the total appliance use increases as well as people tending to stay inside more. In the summer, almost no heating is required, and people are outside a lot more, hence a decrease in usage is expected.
To get an insight into the usage during colder months, data is used of a tiny house community located near Den Bosch in the Netherlands, called 'Minitopia'. From the available data, 5 houses were selected which had continuous data values for each month in the same year. A fraction can be calculated from the average monthly usage of these houses and can be multiplied by our yearly usage. This results in the average yearly usage being divided over 12 months. In Appendix B.6, a short explanation and graph containing the monthly usage in kWh resulting from the yearly model is provided. The values for each month, together with the percentual decrease of our estimated usage versus average Minitopia usage is shown in Table B.12.

To get the daily average in these months and to be able to compare it to our estimated average daily demand, the monthly usage is then divided by the number of days in each month. This results in the average daily usage for each month for both the Minitopia houses as well as our estimated demand for a tiny house, shown in Figure 3.2.
In Table 3.4, the values of daily energy demand in Wh for each month have been presented. As it is the scaled behaviour of the Minitopia usage, the difference is the same for each month. The usage of a tiny house is 60% of the usage of an average Minitopia house. The month with the highest daily average energy usage for our estimation is December, with an energy usage of $5712.30Wh$ for one house over one day. The month with the lowest daily average usage can be seen to be September, with an energy usage of $3062.18Wh$ for one house over one day. This difference is due to the different temperatures, possibly bad isolation, and the PV panels producing less in winter. As the largest daily usage needs to be accounted for in the sizing of the storage and supply units, December will be used for the storage selection while keeping in mind that generation will be low at that time of the year.

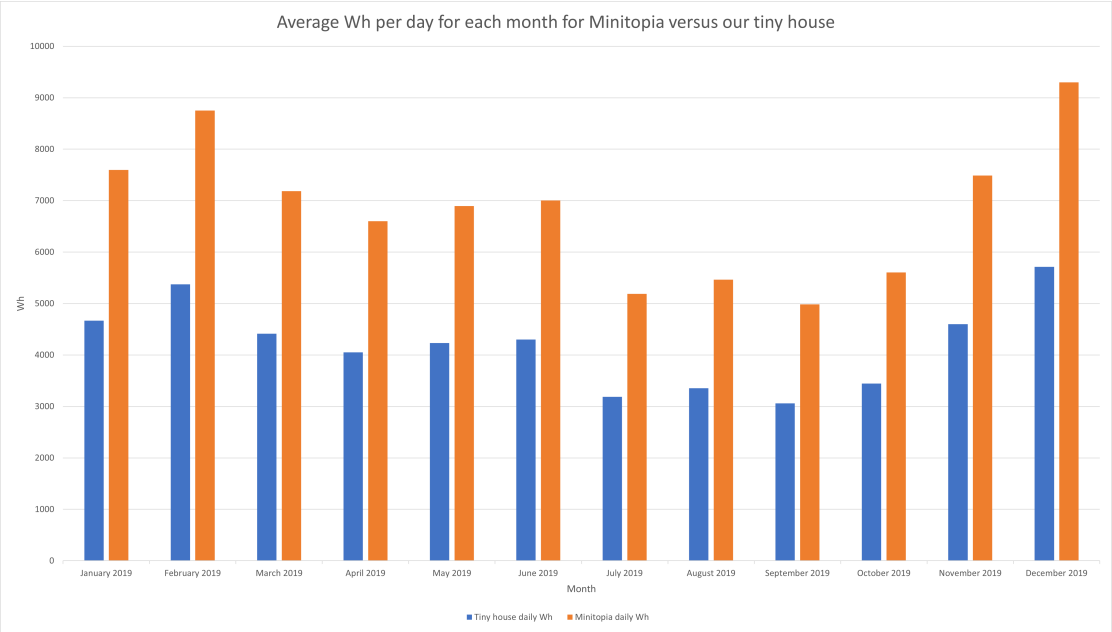

Figure 3.2: Daily usage in Wh per month for the estimated demand of one versus minitopia tiny house usage, based on a monthly average.

Table 3.4: Daily usage of minitopia tiny house vs tunus in Wh.

Month	Minitopia usage [Wh]	Tiny house usage [Wh]
January	8232.90	4665.17
February	9255.00	5374.38
March	8096.13	4411.83
April	7049.33	4053.23
May	6796.77	4234.87
June	7716.67	4300.36
July	5349.03	3186.95
August	6225.81	3354.51
September	5373.33	3062.18
October	6625.81	3443.35
November	7573.33	4597.78
December	10967.74	5712.30

4

Supply & Storage Design

In Chapter 3, the estimation of the average daily demand of a tiny house has been established, as well as the variations in daily energy demand throughout the year. In Section 4.1, the needed energy generation in the form of RESs is determined to supply the whole community using the estimated monthly demand. The RESs will consist of feasible options on a roof in Rotterdam: solar and wind energy generation. The considered methods to harbor these forms of energy are PV panels, PVT panels, and VAWTs or Horizontal Axis Wind Turbine (HAWT)s. As explained in Section 3.1.1, the heating of the tiny houses will be done using the heat grid developed in [5]. A short analysis will be provided on the heating method and an adjusted version will be elaborated.
After RES selection, an initial model is created to determine the required energy generation in order to supply 90% of the estimated energy demand throughout the year. This initial model will produce a rough estimate on the needed generation, as the ESS is not accounted for. In Section 4.2, a comparison of available ESS methods is made and a suitable ESS option is chose. Subsequently, to fulfill the 90% availability required by RQ-M.DCG.5, a second model is made which incorporates a finite and lossy ESS. This second model estimates the amount of time the microgrid uses energy from the main grid and enables establishing the correct sizing of the ESS based on the PoR. Using this second model, two types of storage systems are examined; a distributed and a centralised storage system. For both scenarios, costs, sizing, and availability will be deliberated. Lastly, a comparison between technical, economic, and social advantages and disadvantages will be made.

4.1. Renewable Energy Sources

The first step in establishing the energy generation system for the community is to identify the proper methods of sustainable energy generation. RQ-M.DCG.8 states that the generation of the grid should be solely based on more than one RES. Subsequently, the considered sustainable methods will consist of the most feasible options on a roof in Rotterdam: solar and wind energy generation. The products for the methods of RESs need to be selected. For this selection, the technical performance, costs, and environmental aspects are taken into account. After the products have been selected, their performance is analyzed and modeled. Using this model, the number of modules of each of the selected RESs is determined based on how much generation is needed to supply the estimated demand.

4.1.1. The Heat Grid

As mentioned in Chapter 3, a major factor in energy usage is heating. Demand rises in the winter while solar generation decreases due to fewer sun hours and weaker irradiation. To resolve this problem, a heat grid was designed in [5]. RQ-M.DCG.12 states that the design must include a heating grid based on the heat grid designed in [5]. To develop a better understanding of how the heat grid operates and what should be adjusted to fit the current grid design, a revision of the heat grid from [5] is done. Based on this analysis, some adjustments are made after the discovery of a discrepancy in the initial design in [5]. The complete analysis of the heat grid and the adjustments can be found in Appendix C.1. The heat grid can be considered as follows.
19 PVT panels are put on the roof of a separate construction which contains a heat battery and a large

heat pump. The heat of the sun can be captured by the PVT panels and stored in the heat battery. The heat pump ensures heat circulation to and from the houses and is power by the electricity generated by the PVTs. The heat grid is thus considered as a separate system, disconnected from the microgrid. Nevertheless, the system now does include a version of the heat grid designed in [5], meaning RQ-M.DCG.12 is met.

4.1.2. PV

As the energy generated by the PVTs will only be used for the heat grid, additional energy sources are needed to supply the demand of the community. Between 2005 and 2012, the production of solar panels has increased by a factor of sixteen, and the market is still growing. Among other factors, higher efficiencies, decreasing costs of poly-silicon, and large investments in this growing industry have resulted in an annual price reduction of 21% [25]. Moreover, solar energy is the most abundant and inexhaustible of all renewable energy resources [26]. It has been found that many tiny houses supply a significant fraction of their own demand using PV panels. For these reasons, PV panels are chosen to be one of the main methods of energy generation in this design.

Panel Selection

Both the roof of the tuni themselves and the high-rise on which the tuni are built are relatively small. Usable space is thus a limiting factor in this design, so high-efficiency panels are a fitting choice for the current design. Product research on mainly high-end, high-efficiency solar panels is carried out, resulting in a comparison shown in Table 4.1.

As can be seen, several factors are compared in order to establish which panel would be the best fit for the current design. Except for the Trinasolar Vertex, all panels are top of the range, explaining why most specifications are fairly similar. The power rating of solar panels is given at Standard Test Conditions (STC), which entails radiation of $1000W/m^2$ at a cell temperature of 25 °C, which is obtained at an ambient temperature of approximately 0 °C. These circumstances are not very realistic which is why the performance at Nominal Operating Cell Temperature has been considered as well. Other considerations are the temperature coefficient which indicates the attenuation of the cell efficiency for higher temperatures and the power tolerance. The power tolerance indicates the initial deviation of the rated power as each solar panel has slightly different behaviour. Except for FuturaSun, all companies ensure a positive power tolerance meaning the power rating will only be similar or higher than advertised. Besides the rated efficiency, it is found that it is essential to look at how this efficiency is sustained throughout the years. All companies give a guarantee of how much of the initial power rating is still put out after one year and after 25 years. As the community is meant to operate for a long time, the efficiency and its degradation are considered to be of great importance. Finally, two crucial factors were the price per panel and the product warranty each company is willing to give.
Having considered these factors, the LG Neon R panel is chosen to be used in the design. This decision is mainly based on the fact that it has the second-highest efficiency for the second-lowest price while coming with 25 years of product warranty. Moreover, the temperature coefficient and degradation factor are considered to be very decent. It has to be noted that the TrinaSolar is by far the cheapest solar panel while having a very decent efficiency. However, making the design future-proof, its product warranty and degradation factor are deemed insufficient for this design.

PV Panel Performance

To assume that a solar panel constantly puts out its rated power would be very optimistic and unrealistic. Besides the obvious fact that PVs will not generate energy at night, there are many other factors that influence the performance of solar panels. The daily received irradiance of the sun fluctuates heavily; besides clouds that can block out a significant fraction of solar energy, the length of the day and the height of the sun and thus, the strength of its radiation play a significant role. In the model described in Section 4.1.4 all of this will be accounted for by using KNMI weather data of Rotterdam over the last 20 years. Moreover, the orientation and the tilt of a panel, the temperature and degradation, and other environmental aspects affect the PVs' performance. A performance analysis is done and can be found in Appendix C.2. Based on this analysis, the overall efficiency of the panels is estimated to be 19.14%.

A model has been created to compare the demand of the community throughout the year against the

Table 4.1: Comparison table of five PV modules based on the these data sheets: LG:[27], FS:[28], TS:[29], SP:[30] RS:[31].

Panel	*LG*	*FuturaSun*	*Trinasolar*	*Sunpower*	*REC Solar*
Max power STC [W]	380	360	385	400	380
Max power NOCT [W]	286	272	290	N/A	289
Temp. Coeff Pmax [%/°C]	-0.3	-0.3	-0.34	-0.27	-0.26
Power tolerance	0∼+3 %	± 3 %	0∼+5 W	0∼+5 %	0∼+5 %
Efficiency [%]	22	21.3	20	22.6	21.7
Degradation [%/year]	0.3	0.4	0.55	0.25	0.25
1 year guarantee [%]	98	99	98	98	98
25 year guarantee [%]	90.8	89	84.3	92	92
Price [€/module]	289	N/A	149	369	330
Product warranty [yrs]	25	15	12	25	20

amount of energy that can be generated by the chosen RESs. Utilizing this model, it can be estimated how much generation is needed throughout the year, which will be discussed in Section 4.1.4. Since the demand in the winters is high, while solar irradiance is low, another RES is needed, which in this case will be wind turbines.

4.1.3. Wind Turbines

In the colder seasons, the wind is a fairly present factor in the Netherlands, especially at heights [32]. As the community will be built on the roof of a high-rise building, the wind can be a great resource to generate clean energy.

In order to accomplish this, a wind turbine is to be selected. In [5], the decision was made to use four turbines of the same type: the Aeolos-V 1kW VAWT. Market research on Aeolos and its competitors has been carried out to verify whether a suitable turbine has been selected.
As for the turbine type, the use of VAWTs compared to HAWTs is found to be a fitting choice for several reasons. Usually, one of the most significant drawbacks of VAWTs is the fact that the modules harness less wind because of their location close to the ground due to their short base. This is not an issue on the roof of a high-rise building. Furthermore, a VAWT is smaller and thus less obtrusive for the inhabitants of the community and usually needs less maintenance [33]. The biggest advantage of the VAWT is its ability to generate power in turbulent winds, regardless of wind direction and duration of the wind gust. According to the Institution of Mechanical Engineers, turbulence can even improve efficiency, meaning modules can be built near each other and other constructions without affecting their performance [34]. Irregular winds are prevalent in urban areas, which is why VAWTs are the better choice compared to HAWT.
A disadvantage of wind turbines is that turbulence could cause vibrations which results in noise. However, the smaller Aeolos models are rated for 45 dB max, which is within RIVM guidelines for noise in residential areas [35].
As for the product itself, it has been found that Aeolos is one of the leading products in this market and is considered an excellent choice for the current design. However, it has been decided that the 2 kW model is a better fit as the wind turbines will be much needed in the winter when demand is higher and solar irradiance is lower. Choosing one larger turbine with a higher power output has been considered as well. However, these are louder and exceed noise limits. Furthermore, smaller wind turbines can start to generate power at a much lower wind speed, ensuring the turbines can generate throughout the seasons. In [5] the turbines were considered to be merely additional support to the generation via PV and PVT. In this design, the wind turbines will prove to be of utmost importance for achieving 90% availability. This will be shown and discussed in Section 4.1.4.
Now that the generation methods are chosen to be several RESs, RQ-M.DCG.8 is met.

4.1.4. Supply Models & Results

As the proper PV panels, wind turbines, and PVT panels have been selected, the model to analyse the needed amount of each of these sources can be determined. As explained in Section 4.1.1, the PVT panels will not be used in the estimation of required energy generation, hence only the PV panels and

wind turbines will be considered. This model will use the daily demand of each month for the whole community, which is determined in Table 3.4 and explained in Section 3.3, to determine the needed daily generation.
As the total usage for the community for each month has been defined, the RESs need to be quantified. The PoR states that 90% of the time, the community's demand needs to be supplied by the microgrid itself. The needed production was set to be at least 90% as well.
For this purpose, weather data from the Delft University of Technology from the KNMI station in Rotterdam has been downloaded [36]. From this data, the solar irradiation, as well as the wind speed, have been used to determine the hourly energy generation of a VAWT and a square meter of PV panel. The weather data, as well as its usage for the PV panels and VAWTs, are explained in Appendix C.3
As the power output for each hour is now known for both the PV panels as well as the VAWTs using the weather data and the previously explained inefficiencies, the amount of both RES methods had to be determined to supply 90% of the energy demand. The availability is determined using a supply model which uses the following assumptions:

- The energy generated by the RESs can always be used for the demand.
- The energy generated by the RESs is stored in an infinitely sized battery with no losses.
- Cable and converter losses have been ignored as they have not been selected yet.

From the model, using 6 VAWTs and 61.2 m^2 of PV panels (36 modules of 1.7 m^2, 3 per house), the average availability throughout the year turns out to be 95.2%. This is larger than the previously required 90%. However, this model only compares the energy demand instead of the required 90% in operating time; hence a safety margin of around 5% is considered for the result. The daily generation versus demand for all months is presented in Figure 4.1. In Table 4.2, the numbers of generation and demand are presented, as well as the relative overshoot or undershoot and the energy availability for each month, where the yearly average resulted in 95.2% availability. This shows that July is the best month and November the worst month in terms of available energy. In Appendix C.4, how much of either RES is needed if the other would not be implemented is elaborated and shown. Hourly generation versus demand is also shown for the highest demand in December versus lowest demand in July. This hourly generation will be used in Section 4.2.

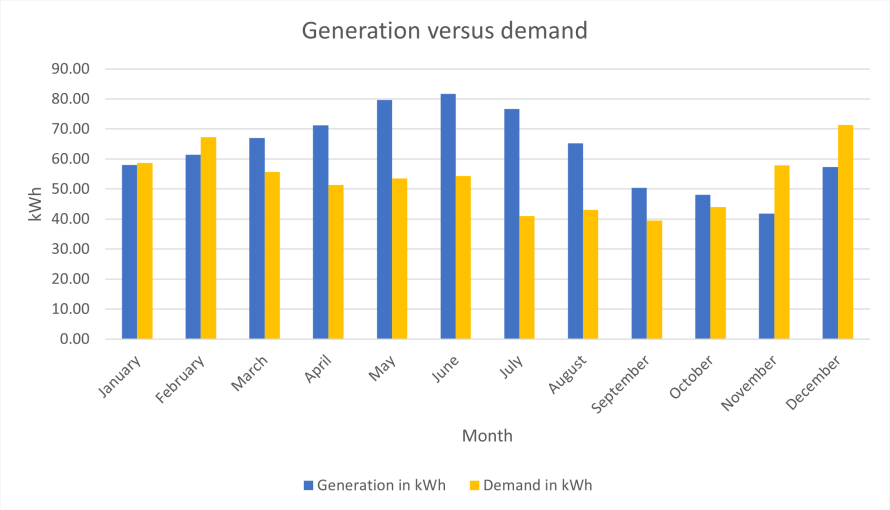

Figure 4.1: Daily energy generation versus demand for each month.

The PoR requirement is still not met due to only looking at the daily energy balance of the system instead of the time which it can supply without being connected to the main grid. For this purpose, hourly generation will be assessed and combined with an ESS method.

Table 4.2: Daily generation versus demand and comparison for each month.

Month	Generation [kWh]	Demand [kWh]	Difference [kWh]	Difference [%]	Available [%]
January	58.00	58.71	-0.72	-1.22	98.78
February	61.39	67.22	-5.84	-8.68	91.32
March	67.00	55.67	11.33	20.35	100.00
April	71.14	51.37	19.77	38.49	100.00
May	79.64	53.55	26.09	48.72	100.00
June	81.72	54.34	27.39	50.41	100.00
July	76.62	40.97	35.64	86.99	100.00
August	65.18	42.99	22.19	51.63	100.00
September	50.45	39.48	10.97	27.79	100.00
October	48.12	44.05	4.07	9.24	100.00
November	41.87	57.90	-16.04	-27.69	72.31
December	57.27	71.28	-14.01	-19.66	80.34

4.2. The Energy Storage System

One of the major challenges of using RESs only is that generation and demand do not correlate. An example is that a lot of solar energy is generated when most users will be at work, and demand is thus low. An ESS is needed to store this overproduction, so the users can use this energy at a time of overconsumption, such as dinner time, as shown in Chapter 3. In the following section, several ESSs are compared in order to select the appropriate storage method.
With the selected ESS, a model is made which also incorporates hourly generation and demand to estimate the availability for the PoR. Both an aggregated or centralised model and distributed model will be made to analyse both scenarios. A comparison will be done between cost, availability and sizing. Lastly, the scenarios will be analysed in technical, economic, and social aspects.

4.2.1. ESS choice

As both demand and the generation methods have been established, research is done on several types of storage systems to identify the appropriate storage method. Table C.2 summarizes the main advantages and disadvantages of each ESS mainly based on information found in [37], [38] and [39].
An ESS based on lithium-ion batteries have been selected because of their high energy density, relatively low price, adequate efficiency, and sufficiently high power output. A hybrid storage system consisting of batteries and a supercapacitor, or batteries and a flywheel, has also been considered. However, data of real-time power demand is needed to draw conclusions on how effective these solutions will be in reality. A recommendation for such a hybrid system is done in Section 7.2.
When sizing the battery system, it is essential to look at power rating as RQ-M.DCG.9 states that the chosen ESS should be able to handle peak power demand. Two systems with lithium-ion batteries will be considered: an aggregated or central battery system and a partly distributed battery system are both considered to be valid options. An aggregated system would mean the entire community has only one central battery system. This would mean all excess energy that is not directly supplied to the loads will flow to one central point to be stored and used at a later point. The partly distributed system would consist of both a central battery to store all excess energy generated by the turbines and a home battery for each of the tuni. Assuming that in this scenario, each house has its own PV system, all excess energy supplied by the residential PV system can first be stored in the home battery. In case the home battery is full, excess energy can be stored in the central battery. In case of overconsumption in the household, the home battery would supply first so that the central battery is mainly used for backup and supplying peaks in power. This system would minimize long pathways and thus losses.
A more detailed comparison is made on the advantages and disadvantages of either system, resulting in the table shown in Table C.3. Before deciding on which of the two systems to choose, both have been modeled to determine sizing and feasibility.

For each system, products have been researched to meet the following requirements:

- At least one day of energy demand (exact sizing will be done by experimenting with models, in

case of distributed, main and home combined should supply at least one day's worth)

- Should be able to supply at least peak demand (in case of distributed, main and home combined should at least supply peak demand)
- Round Trip Efficiency (RTE) of at least 90 %
- Depth of Discharge (DoD) of at least 70%
- Should not suffer from hysteresis effect
- Should be in the 300-500V output/input voltage range
- Should have enough cycles for at least 10-15 years

For the main battery, the battery modules of 'BYD' are selected [40]. These batteries consist of 2.76 kWh battery modules that can be connected in series up to 22.1 kWh. If required, large battery units can subsequently be connected in parallel for higher power output. One unit of either 19.3 kWh or 21.1 kWh has a power rating of 17.9 kW. These units meet all other requirements easily as its RTE equals 96%, DoD equals 90% and are rated for at least 20 years lifetime. The 'Simpliphy 2.6' is chosen for the home battery, which also meets these requirements. The specifications of both lithium-ion batteries are much better than the initial research on ESSs indicated in Table C.2, showing how fast this technology is evolving over the last few years.

4.2.2. Centralised ESS Model & Results

In order to properly size the energy storage of the ESS, a model has to be created which takes the demand, supply, and storage into account. The first scenario which will be considered is a centralised ESS model. A short explanation of the model and the selected battery has already been provided in Section 4.2.1. An in-depth explanation of the system is elaborated in Appendix C.6 which also contains a dedicated flow chart for the centralised model.
In order to supply the maximum power demand of the community, as well as being able to roughly store the daily demand in most months, while also having an availability of at least 90%, the model resulted in 4 batteries. Using 4 batteries and the previously determined demand and generation, the following results were obtained, which fulfill almost all the requirements mentioned in Section 4.2.1.

- Availability = 93.73 %
- Capacity = 4 · 19.3 kWh = 77.2 kWh
- Effective capacity = 0.9 · 77.2 kWh = 69.48 kWh
- Peak power = 4 · 17.9 kW = 71.6 kW
- RTE = 96 %

The requirement that at least one day of average estimated demand should be available is fulfilled when looking at the total capacity and using the values in Table 4.2. When looking at the usable capacity, it can be seen that only the month of December cannot be supplied for an average day due to a shortage of a few kWh. This requirement is thus roughly met, and as the other requirements are met with a sufficient margin, 4 batteries will be used for the design. In conclusion, for the centralised model, 4 of the BYD HVM 19.3 [40] batteries have been chosen. The figures of the State of Charge (SoC) being tracked hourly for each month can be found in Appendix C.8. The MATLAB code for the centralised model can be found in Appendix F.1.

4.2.3. Distributed ESS Model & Results

The second scenario that is considered is the distributed model for the storage system. A general explanation for this model is presented in Section 4.2.1. A detailed explanation of the distributed model, as well as dedicated flowcharts, can be found in Appendix C.7.
Using 2 home batteries for each house, as well as 2 of the larger batteries used in the centralised model for the central storage, the following results are obtained from the model, with calculations included for the ESS requirements.

- Availability = 93.33 %
- Capacity = 2 · 19.3 kWh + 12 houses · 2 · 2.6 kWh = 101 kWh
- Effective capacity = 0.9 · 2 · 19.3 kWh + 1 · 12 houses · 2 · 2.6 kWh = 97.14 kWh
- Peak power = 12 houses · 2 · 1.275 kW + 2 · 17.9 kW = 66.4 kW
- Effective efficiency = 0.96 * (2 · 0.9 · 19.3 kWh / 97.14 kWh) + 0.98 * (12 houses · 2 · 2.6 kWh / 97.14 kWh) = 97.28 %

As can be seen from the calculations, the distributed model storage system fulfills all requirements with exceptional capacity. In order to be able to supply the peak demand, 2 batteries per household needed to be selected (where each household has the same amount of batteries for equal power generation per house), causing the capacity of the system to be oversized by $\frac{97.14-71.28)}{71.28} = 36.28\%$ in the best case and $\frac{97.14-39.48)}{39.48} = 146.05\%$ in the worst case (by taking the highest and lowest demand in Table 4.2, respectively). In the comparison, this excess capacity will be deliberated against the higher cost and lower transportation losses which would be minimised in the distributed model. In conclusion, for the distributed model, 2 home batteries per tiny house, resulting in 24 of the simpliPhi PHI 2.6 [41] batteries were chosen. For the central storage, 2 of the BYD HVM 19.3 [40] batteries have been chosen. The figures of the SoC being tracked for each month can be found in **??**. The MATLAB code can be found in Appendix F.2.

4.2.4. System Comparison & Selection

Having established that both the centralised and partly distributed system enable the system to have an availability of more than 90%, the requirement RQ-M.DCG.5 is met regardless of which system is chosen.

Now, a decision has to be made on which of the systems will be used. As the topology design heavily depends on which of these systems is used, this decision must be made before starting on topology design. In order to make a complete analysis, technical, economic, and social advantages and disadvantages of both systems have been analysed and presented in Table C.3. From this analysis, it is found that the distributed model has the potential to be more flexible and efficient with the energy supply to the community. It is however a lot more complex and expensive in capital, maintenance, and software. On the other hand, the centralised system favors simplicity and lower costs, however low flexibility and higher maintenance costs in case of battery failure. On the social side, both systems are considered equally advantageous, as the centralised model favors low danger due to central storage, while the distributed system favors the individuals who want to use their PV panels for themselves. To meet the requirements, and to minimize costs and complexity, the centralised system is preferred and thus chosen. This means 4 of the BYD HVM 19.3 [40] batteries, with a combined power rating of 71.6 kW, will be used for this design, meaning RQ-M.DCG.9 is met as well. The centralised system uses the least amount of DC-DC and AC-DC converters and hence fulfills RQ-S.DCG.3. This requirement states that the amount of any type of converter should be kept as low as possible in order to minimize costs and optimize efficiency. In order to compromise for some of the design trade-offs made by this decision, the following will be accounted for in the topology design.

Each house will have its own PV modules installed, implying that the solar panels on a house will primarily supply the demand of the individual house directly, without the use of a home battery. This means the social disadvantage of centralised can be remedied while still keeping fire hazards in houses low. Furthermore, it is decided that in the topology design, flexibility should be a primary objective to fulfill the PoR requirement RQ-S.DCG.4 of independent operation of a tiny house in case of an adjacent failure.

5

Topology Design

In the last chapters, the demand, supply, and storage of the tiny house community have been established. Now, the last part of the design phase will be discussed: creating the optimal topology. In Section 5.1, the topology of the microgrid is discussed which connects the VAWTs, ESS, Point of Common Coupling (PCC), the tiny houses and the common usage tunect together. This topology includes the voltage bus topology, the microgrid layout, the converters and control/optimization algorithms, and lastly, the used wiring. In Section 5.2, the smaller nanogrid will be considered, which connects the demand of a tiny house and the PV panels to the microgrid. For the nanogrid, the voltage bus topology, converters, and control/optimization algorithms, as well as the used wiring, are discussed. In Section 5.4, safety considerations concerning the voltage bus polarity, grounding of both microgrid and nanogrid, fault handling and voltage stability, and proposed solutions are elaborated. In Section 5.4, the safety of the microgrid and nanogrids for the residents is discussed and standards for these types of grids as well as human interaction with these grids is elaborated upon. Lastly, in Section 5.5 a cost analysis is done on the hardware required for the complete grid design.

5.1. Microgrid Topology

This section will cover the design of the microgrid and the considered aspects of that design. These aspects are summarised as the topology of the voltage bus, the required converters and proposed control/optimization algorithms, the wiring used in the system to operate. Moreover, the physical layout design of the microgrid, which fits on the roof of the considered high-rise, is presented and discussed.

5.1.1. Bus Topology

The voltage bus is the voltage line that interconnects the ESS, the RESs, the houses, and lastly, the main grid. It is essential to choose the appropriate voltage level of this bus, as well as the topology of the bus itself. As RQ-M.DCG.1 states, the microgrid should operate on DC and thus only DC bus voltages are considered.

Voltage choice

The voltage levels which are commonly used in residential grid applications, discussed in [42], vary a lot. The voltages mentioned range from 12 VDC to 400 VDC, however their usage is quite different. In [43], it is mentioned that the most standardised choice for DC microgrids is 380 VDC or 400 VDC due to the high amount of applications in the data center area. Another advantage of this higher voltage is that losses are lower. As the primary energy source of this grid consists of RESs, and their energy is being supplied by the ESS, the losses in the cables need to be minimised in order to use the generated energy most efficiently. A secondary benefit is that the cables themselves are less expensive for a lower current rating. Hence, in order to minimize the losses and costs, the highest voltage was chosen. This resulted in 400 VDC being chosen as the operating voltage of the voltage bus, implying RQ-M.DCG.1 is met.

Topology choice
After choosing the operating voltage of the DC microgrid, the topology of the microgrid itself can be chosen. The main topologies for a DC microgrid are radial, ring and other combinations of these basic forms. Also, the primary forms of bus topology itself are considered, being single-bus, multi-bus, and reconfigurable. Their basic structure, as well as their respective advantages and disadvantages, are discussed in Appendix D.1.

For this microgrid, based on RQ-S.DCG.4, the nanogrids should be able to operate under a fault occurrence somewhere else (except the possible faulted nanogrid). The best option for this requirement is to use a ring topology, which enables bi-directional power flow, power-sharing, and fault isolation. A series multi-bus ring-based voltage bus topology has been chosen, where each bus connects a specific part of the microgrid (ESS, RES etc.). This chosen topology thus enables fault isolation and continued operation of non-faulted locations, which fulfills RQ-S.DCG.4. As power sharing is also enabled, RQ-C.DCG.3, which states that the tiny houses could share power with each other, is also met. The grid is designed to be able to operate in ring topology, however due to the normally open switch between the two sets of batteries, the grid effectively operates in radial as shown in Figure 5.1. This is to reduce complexity and for easier identification of faults. The more complex reconfigurable multi-bus system can be considered for later research, as data on the fault rate of tiny houses is not researched in this thesis and is unknown up to this point.
A disadvantage of the used series multi-bus ring topology is the possible significant losses in voltage and power due to the bidirectionality of the system and the long distances power can travel. This will be analyzed during the wiring analysis as well as in Chapter 6.

5.1.2. Microgrid Layout

In Figure 5.1 a schematic overview of the physical grid layout is shown. An electric overview of the interconnection of all buses, including the nanogrid, can be found in Figure 5.3 in Section 5.3.3. As can be seen in the figure, the loads, generators, and batteries are connected to the main ring bus, which uses a series-connected multi-bus configuration as shown in Figure 5.3. As soon as the faulty area has been identified, the area can be isolated from the ring and the switch between the batteries will be closed to ensure power flow to all other areas. These potential faults will be discussed in Section 5.3.3. The batteries are connected via bidirectional converters on either side of this open ring bus. This way, most of the demand and generation on the left side of the roof will flow to and from the left set of batteries and idem for the correct battery and the right side of the roof.
The green lines indicate the connection between the AC-DC converters of the VAWTs and the ring. Each converter is placed near its designated turbine to ensure power flow at 400 VDC, decreasing currents and thus losses. This is especially important for the VAWT connection as they are purposely placed as far from the community as possible to minimize disturbances caused by the turbines. The power generated by the turbines can be used to either supply the loads of the houses, recharge the battery system, or supply back to the main grid via the pink line.
Tunect has two DC-DC converters connected to the main ring. One buck converter is used for power sockets with 48 VDC output. These sockets can be used for the printer, outdoor lighting, and the controllers required by the control group. The other converter has an output of 400 VDC to supply the washing machines. This converter is used to ensure that the loads of the washing machines do not cause significant bus voltage fluctuations and is thus used for stabilization purposes. The maximum allowable bus voltage fluctuations will be discussed in Section 5.3.
The purple lines indicate the connection between the nanogrid of each of the tiny houses and the main ring. This nanogrid will be extensively discussed in Section 5.2 which explains that this connection can both supply to the loads of the homes and supply back to the microgrid as each house has its own PV panel system. This connection enables power-sharing between the houses, recharging the battery system, and supplying back to the main grid via the PCC.
All wires will be routed either underground, meaning inside the roof of the high-rise itself, or through insulated ducts. Both options will have to be researched on-site in order to choose the suitable method. As seen in the figure, most lines will be routed via a similar path so that in case of a line fault, all lines can be accessed at the same location.
Finally, in this layout, it has been assumed that the bottom left corner of the roof is facing south. This way, all sloped roofs and the PVTs of the heat grid face south to ensure optimal solar generation.

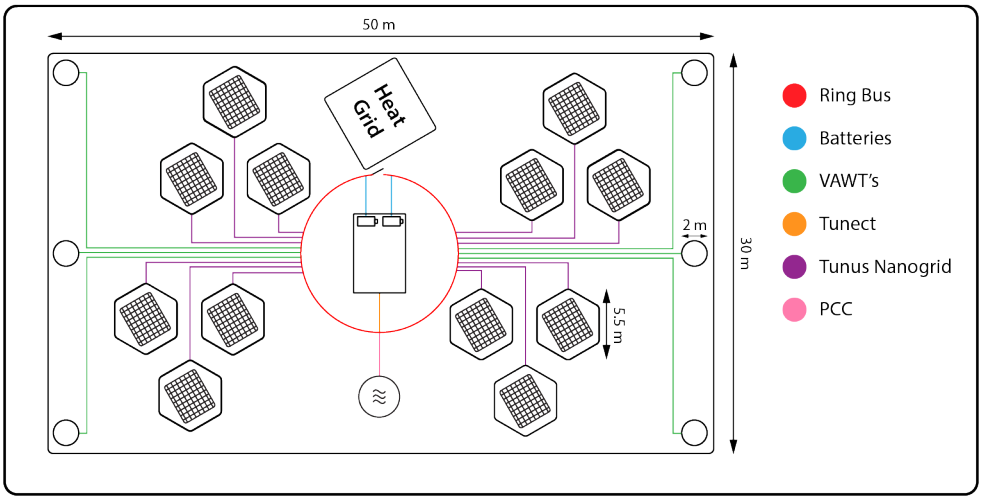

Figure 5.1: Schematic overview of the overall microgrid layout and wiring on the rooftop of a high-rise building.

5.1.3. Converters & Control

Until now, the general topology of the microgrid has been designed, with its designated operating voltage. Next, the converters which connect the loads, generation, and storage to the grid have to be designed. RQ-M.DCG.11 states that all converters used in the system should be able to handle the maximum rated input and output power of their respective connection points. As the actual design of converters and control algorithms falls outside the scope of this thesis, the main design requirements will be considered and recommendations on hardware will be made. Also, a control algorithm and, if applicable, an optimization algorithm will be presented as well. RQ-S.DCG.5 states that each of the RES converters should use a control algorithm for optimal power extraction. Based on this requirement, the converters for the VAWTs and PV panels will use a form of Maximum Power Point Tracking (MPPT). The general requirements for the converters are mentioned below. Each of the converters should have these properties.

- Protected against overvoltage and overcurrent
- Galvanically isolated.
- Able to disconnect from the microgrid in case of faults in the lines, generation, demand, or converter itself.
- Able to handle large power fluctuations.

In Table 5.1, the needed converters together with their respective requirements and optimization algorithms are shown. The chosen optimization algorithms for the VAWTs and ESS are explained in Appendix D.2.

Table 5.1: Microgrid converter requirements and recommended optimization methods.

Microgrid locations	*Wind turbine*	*Battery*	*Main grid*
Converter type	AC-DC	DC-DC	AC-DC
Direction	Unidirectional	Bidirectional	Bidirectional
Vin	48 VAC	280-420 VDC	230 VAC
Vout	400 VDC	400 VDC	400 VDC
Power rating	>2600 W	>31 kW	>62 kW
Current rating	>6.5 A	>76.37 A	>152.73 A
Optimization algorithm	MPPT: Perturb & Observe	Dual phase shift control + neural network	Custom autonomous control

VAWT
The unidirectional AC-DC converter for the wind turbines will be placed at the base of each wind turbine. The general requirements of the wind turbine converter are shown in Table 5.1.
The manufacturer of the wind turbine indicates compatibility with the 'CTC-3K' [44]. This is a grid-tie controller where the output can be set to 400V to ensure bus stability. As this controller can be set to the required DC output voltage, no additional converter is needed. The proposed MPPT algorithm is a form of Perturb & Observe algorithm, which is discussed in more detail in Appendix D.2.

Batteries
The bidirectional DC-DC converter for the battery will be used twice, following two parallel connections of two batteries each. The converters must comply with the general requirements as well as the requirements mentioned in Table 5.1. Furthermore, in charging mode, the converter must regulate the grid voltage to the current battery voltage. In discharging mode, the converter regulates the variable voltage of the battery to that of the DC grid and keeps the grid voltage stable. A recommendation is made to contact [45] which can supply the needed converter and after deliberation, our proposed control system explained in Appendix D.2 could be implemented.

PCC
RQ-M.DCG.6 states that, in case of overconsumption or faults, the microgrid should be able to connect to the AC main grid in order to supply the shortage of energy. RQ-M.DCG.7 states that, in case of overproduction, the microgrid should be able to supply back to the main grid via a connection.
This connection to the main grid needs to be facilitated by a bidirectional AC-DC converter. This converter needs to comply with the general requirements as well as the requirements mentioned in Table 5.1. The proposed control method in [46] will be used to regulate the DC microgrid voltage as well as minimise circulating current. The design proposed in [47] can be used for further optimal design of the PCC converter. The product shown in [48] is a great candidate for our power needs as well as bidirectionality. Using the proposed technologies for the PCC AC-DC converter, both RQ-M.DCG.6 and RQ-M.DCG.7 are met.

5.1.4. Wiring
In order to connect all selected modules without creating substantial losses, the wiring should be selected carefully. As Figure 5.1 is drawn on-scale, decent estimations of wire lengths can be made. Based on the maximum power that will flow through each wire connection, the maximum current is calculated to establish the required wire cross-section. RQ-M.DCG.10 states that the power lines must be able to handle the maximum voltage and current assigned to each wire section at all times. Thus the selection of the cross-section is primarily based on the datasheet of the selected wires [49] as there is an indication of a maximum allowable current per cross-section. The thickness of the wires was kept to a minimum to minimize costs. After the initial selection, maximum voltage drops were calculated for the longest possible path of each wire section using the equation shown in Appendix D.3. Some adjustments were made by choosing thicker wires for certain sections when the voltage drop was higher than 5 %. Table D.1 shows the final selection of all wires and their specifications. Based on the total length of wire needed for each section and the prices found on [50], the costs were calculated.

5.2. Nanogrid Topology
Now that the main microgrid has been designed, the connection of the nanogrid to the tiny houses themselves, as well as their connection with the PV panels, needs to be discussed. As concluded in Section 4.2.4, the PV panels are connected to the nanogrid instead of the microgrid in order for the PV panels to primarily supply the demand of the tiny house it is installed on. The same subdivision of aspects as for the microgrid is used to discuss the design.

5.2.1. Bus topology & Nanogrid Layout
In Figure 5.2 a schematic overview of the residential nanogrid layout is shown. The design of the tiny houses ensures some space under the living room area in which all converters and the boiler can be stored. As seen in the figure, there are three DC-DC converters in each house, all of which are unidirectional and connected to the 400 VDC bus. It is decided to install 48 VDC sockets in the house

for all basic appliances. This is a standardised DC voltage, which is safer for the users compared to the 400 VDC bus [42]. The left module converts the 400 VDC to 48 VDC, which is then distributed throughout the house for the lighting and the power sockets. These power sockets can be used for all residential appliances except for the boiler, oven, and stove. The distribution of the power sockets is designed to handle a total of 1000 W at once, which is sufficient for supplying all selected appliances simultaneously and, for example, some additional laptops. The three PV panel modules on the roof are connected in series, which results in a maximum voltage of 128.7 VDC, which is then converted by the module in the middle to 400 VDC to supply to primarily supply the residential loads or the microgrid to be redirected to other houses or the battery system. The suitable converter is only used to ensure that the bus remains at a stable 400 VDC. This module supplies to the boiler, oven, and stove, which have the highest power ratings. The decision has been made to connect these appliances to a dedicated high voltage power socket as supplying these on 48 VDC would require excessive currents resulting in significant inefficiencies and losses. As these appliances can cause very sudden changes in the residential loads, the converter is thus added for stability purposes. Furthermore, these three appliances are conveniently close to the space under the living area so that the high voltage sockets can be safely put in this space out of reach of the tiny house residents as these sockets are not meant to be unplugged because of safety reasons.

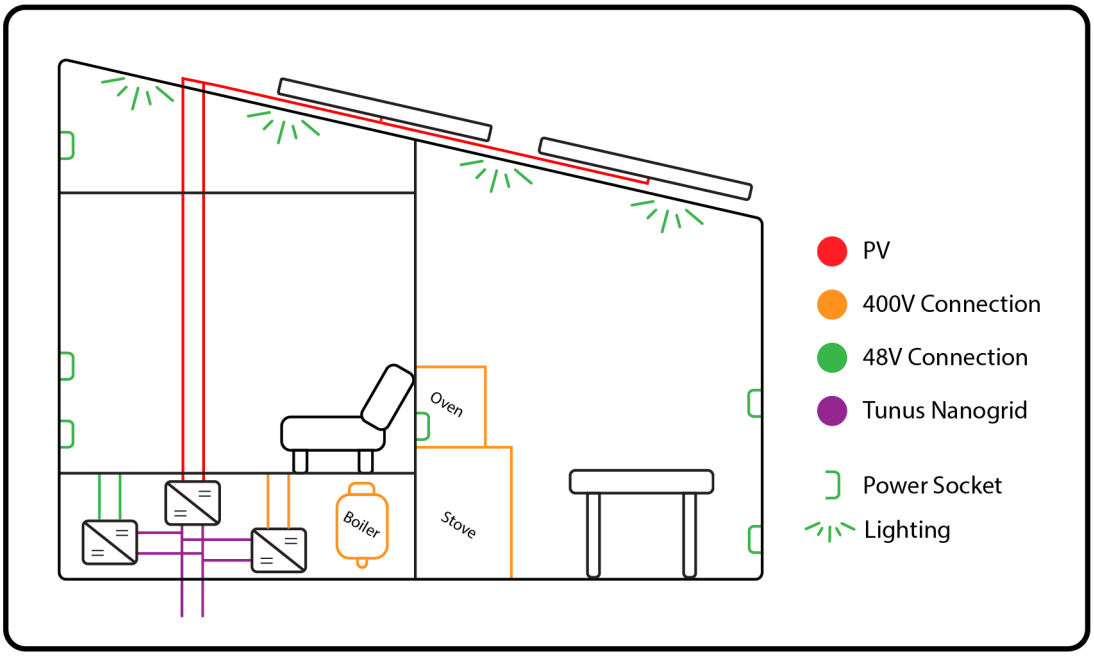

Figure 5.2: Schematic overview of the overall nanogrid layout and residential wiring of a tunus.

5.2.2. Converters & Control

The nanogrid of the house is designed to connect to the main grid using a low-power connection, a high-power connection, and a PV panel connection. The high-power socket of 400 VDC will connect the high-power appliances, which would draw too much current from the low-power 48 VDC connection. Lastly, the PV panel connection will ensure the correct conversion of the PV panels to the microgrid. Again, the design of these converters falls outside the scope of this design, hence only the design requirements will be discussed and recommendations are made. The general requirements of the converters are equal to those mentioned in Section 5.1.3. The requirements for these converters are shown in Table 5.2, where Proportional Integral Derivative (PID) control is given as a standard option for the 48 VDC and $400VDC$ sockets. The chosen optimization and/or control algorithms of the 48 VDC sockets, 400 VDC sockets and PV panels are also elaborated in Appendix D.2.

48V Sockets

The first converter which will be looked at is the unidirectional low-power converter. The low-power connection of 48 VDC will facilitate most of the idle usage and other low-power appliances mentioned

Table 5.2: Nanogrid converter requirements and recommended optimization algorithms.

Nanogrid locations	*low-power demand*	*high-power demand*	*Solar panel*
Converter type	DC-DC	DC-DC	DC-DC
Direction	Unidirectional	Unidirectional	Unidirectional
Vin	400 VDC	400 VDC	128.7 VDC
Vout	48 VDC	400 VDC	400 VDC
Power rating	>1 kW	>5 kW	>1900
Current rating	>20.83	>11.87	>10.19
Algorithm	PID	PID	MPPT: Biologically inspired

in Chapter 3. This converter should comply with the general requirements mentioned in Section 5.1.3, as well as the requirements mentioned in Table 5.2. A recommendation is made to contact De Wit Elektronica [51], which is a company that designs DC-DC converters up to 1 kW. They can be contacted to design and supply a converter that fulfills the requirements. A simple control algorithm using PID is recommended.

400V Sockets
The high-power converter will have similar requirements as the low-power converter, however a higher output voltage, as well as more power, needs to be converted. This converter should comply with the general requirements mentioned in Section 5.1.3, as well as the requirements mentioned in Table 5.2. A recommendation is made to contact Tame Power [45], which is a company that supplies high-power DC-DC converters. They can be contacted to supply the converter which fulfills the requirements. Again, a simple control algorithm using PID is recommended.

PV System
The nanogrid of each house is connected to the previously mentioned high-power and low-power sockets through their respective converters. The last converter that needs to be designed is the DC-DC converter for each set of solar panel modules on the houses. These sets contain 3 solar panel modules, each connected in series. This converter should comply with the general requirements mentioned in Section 5.1.3, as well as the requirements mentioned in Table 5.2. Furthermore, a form of MPPT should be implemented to extract the maximum amount of power from the PV panels under varying irradiance. The chosen algorithm is a form of the biologically inspired MPPT algorithm. Further elaboration can be found in Appendix D.2.
The DC-DC converter listed in [52] is considered as a possible product for the PV panels. It is capable of handling the output of the PV panels, as well as implementing extra safety measures for faults in the grid, PV panels, or the converter itself.
Using the proposed technologies and algorithms presented in the previous sections and ensuring that all proposed specifications can be implemented, RQ-M.DCG.11 is met. How this is done precisely is a matter for further research as this is out of scope according to the PoR.
As the converters for both the VAWTs and PV panels use a form of MPPT algorithm, requirement RQ-S.DCG.5 is met.

5.2.3. Wiring
The selected nanogrid wiring and its specifications can be found in the same Table D.1 in Appendix Appendix D.3. Notable is that the wiring of the 48 VDC socket potentially has the most significant losses. This is due to the relatively high current at a lower voltage. The absolute voltage drop is not significant, however the relative voltage drop is fairly high. Nevertheless, these losses can be considered low still, especially considering these types of currents will never occur as the full power would have to be drawn by the furthest load, which in this case is one of the sockets used for lighting. Now that all wires for the system have been selected, based on current carrying capability, and are only upsised to decrease losses, it can be said that RQ-M.DCG.10 is met.

5.3. Stability

The stability of the grid is essential for the correct operation of the RESs, ESS and appliances. The converters connected to the grid have a specific operating voltage range that needs to be ensured during regular operation. The primary stability issue consists of faults in the microgrid, which require certain grounding, fault detection and isolation, and lastly, fault reparation. The main methods to ensure voltage stability are the previously discussed control algorithms for the converters, especially the bidirectional converters, which connect the microgrid to the battery and the main grid.

5.3.1. Polarity of the voltage bus

One of the voltage bus aspects which has not yet been mentioned is the polarity of the voltage bus. The polarity has two main variants; unipolar and bipolar.
Unipolar voltage indicates the use of two wires to form the dc voltage bus. The voltages are +VDC and -VDC for the positive and negative wire, respectively. When connecting to a unipolar voltage bus, the resulting voltage is thus equal to $+VDC - (-VDC) = 2VDC$. The advantages of a unipolar connection are simplicity and power transmission at one voltage level for the voltage bus. The disadvantages can be summarised as low redundancy, as a line fault in a unipolar voltage bus causes the entire line to fail.
A bipolar voltage bus indicates the use of three wires, +VDC, neutral, and -VDC. As three wires are available, +VDC, -VDC, and 2VDC are available as voltage levels. The main advantages are that the grid is able to use three voltage levels for conversion instead of one. Redundancy is in place as well; if one line fails, the other two can ensure the continuation of power flow.
According to [53], for voltage levels above 200 VDC, a bipolar bus needs to be implemented in order to provide safety margins comparable to that of a standard microgrid. However, the PLC group has designed their communication to operate at a unipolar bus configuration for our DC grid. This limits the design to use a unipolar bus implementation, limiting the safety of the microgrid and parts of the nanogrid that operate at 400 VDC. To still ensure safety for the users, several measures will be discussed in Section 5.4.
Following that design limitation, a unipolar voltage bus will be used in this grid. In order to obtain the required 400 VDC, $+VDC = 200$ and $-VDC = -200VDC$ for the positive and negative wire, respectively.

5.3.2. Grounding

Now that the polarity of the system has been determined, the appropriate grounding method can be selected. In a general microgrid, two types of faults can occur: Line to Line (LL) and Line to Ground (LG). The former occurs less often and is limited by the resistance of all the other modules in the system. The most significant problem in a microgrid is thus the latter type of fault, LG. This fault can pull the voltage of the affected line down to zero, increase the voltage of the other line with respect to ground, and lastly can cause an arc which is dangerous for people [54].
For unipolar voltage buses, the only grounding possible is grounding one of the two lines, with a preference for the positive line. Several grounding devices are available, which alter the characteristics of the grounding method. A limitation is set to the grounding of the microgrid, as the voltage is larger than 48 VDC. This means that the microgrid can not be ungrounded, while the nanogrid can be.
Based on RQ-S.DCG.4 about service continuity, as well as being able to implement protection and provide safety, this results in the following aspects of grounding needed to be optimised:

- Low LG fault current
- Easy Relay protection
- Enable Service Continuity
- Provide System Reliability
- Enhance Safety

From the conclusion drawn in [54], the unipolar parallel resistance grounding method is the optimal choice for our microgrid. As the entire system uses isolated converters, these converters isolate certain sections from the rest of the grid. Each of these isolated sections should have at least one grounding

point. For the nanogrid, the low-power sockets will be parallel grounded to keep fault detection and resolvement methods the same. Parallel resistance grounding provides the aforementioned aspects, while some disadvantages occur as well: the common-mode voltage is high, which causes the converters having to filter out the common-mode voltage. The transient overvoltage is high as well, meaning the converters need overvoltage protection. Lastly, power losses occur due to the grounding, as the current is always able to flow to ground. In Figure D.1, the parallel resistance grounding is shown.
As mentioned previously, for safety reasons, the high voltage levels of the microgrid and partly the nanogrid should use a bipolar configuration. The recommended bipolar grounding option would be to use bipolar resistance grounded systems, which have the same advantages as unipolar parallel resistance grounding. This is a similar configuration as the unipolar parallel resistance grounding; however, the neutral wire is now grounded with a resistance instead of the positive or negative wire. The implementation is shown in Figure D.2.

5.3.3. Fault Detection & Protection

The occurrence of faults in the grid is not uncommon and should be accounted for in the final design. Faults can cause instability in the system and may very well damage components. Large faults and the resulting damaged components can also pose a threat to its users, which is why a protection scheme must be implemented.
There are many different methods and devices that can be used to build these schemes. Selecting an optimal design needs extensive research and depends on many factors like topology, primary control, component ratings, converter stability, and restoration control schemes. As a large fraction of these aspects is too in-depth for this design, a protection scheme is proposed, which is shown in Figure 5.3 and based on [53] and [55].

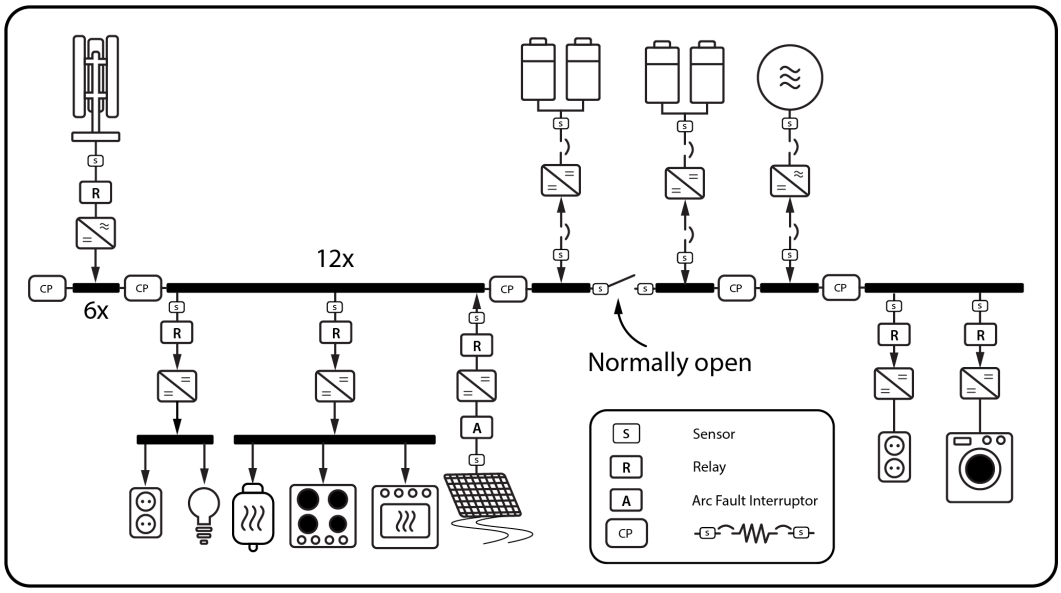

Figure 5.3: Interconnection of all buses, including the proposed protection scheme.

The measured voltage and current are the only two parameters available to detect faults in a DC microgrid [53]. These measurements are performed by sensors connected to the transmission lines at designated points as shown in Figure 5.3. As stated in RQ-M.DCG.14, hourly measurements of power usage must be available for the communication to the control software group. The proposed sensor locations ensure that all power flows for control can be measured. The results of these measurements can be sent via the transmission line communication and thus RQ-M.DCG.14 is met. These sensors can also provide real-time power usage measurements, which can be displayed on an interface for the users to see their power usage, fulfilling RQ-S.DCG.2. This requirement states that each tiny house and common usage should have an interface to view their energy usage.
All buses connected to the main ring are connected to one another with a circuit indicated by 'CP' or

central protection. This circuit consists of the transmission line connecting each of the buses with two sensors and two solid-state DC breakers at each end of the line. These sensors and breakers can share information with a central protection control system. It is decided to use solid-state DC breakers as this technology comes with many advantages. These breakers ensure fast switching time, low conduction losses, no risks of arcing or mechanical wear, high current carrying capability, and full controllability. Furthermore, these breakers can operate bidirectionally and can be opened and closed manually. All this makes them an excellent choice to function both as switches and protection at the most crucial interface. Due to the central control, the systems can quickly identify the fault's location and isolate the faulty bus or line. To ensure that the rest of the grid stays operational, the switch between the sets of batteries can be closed to make the grid operate in ring configuration in such fault situations.
A protection scheme using centrally controlled solid-state DC breakers is not only highly reliable but also bidirectional. This is why the connection between the batteries and the ring is also protected by this scheme on both sides of the DC-DC converters. This is done because the batteries and their converters are expensive and of utmost importance for the grid to function correctly. For the same reasons, both sides of the AC-DC converter of the PCC are protected with the same scheme.
All other modules are protected with a simpler, cheaper local protection scheme. All PV systems are protected by a technology called 'combination arc-fault circuit interrupter'. These can detect and protect against series arc-fault, overload, and short circuit faults. As can be seen in Figure 5.3 all other components are protected by relays. It is recommended to use digital protective relays with a microprocessor as those can identify and protect against several fault conditions. These relays work with a delay time to check whether the detected fault is short-term or long-term and can reclose on their own. This autonomous behaviour makes for relatively reliable local protection while minimizing complexity and costs. Finally, if any faults are missed by the primary protection, the backup protection within the circuitry of the converters will add an extra line of defense against faults.

5.3.4. Voltage stability

RQ-M.DCG.13 states that the voltage buses of the microgrid and nanogrid must remain at a constant optimally chosen voltage with a minimum and maximum fluctuation of a to be determined percentage. In case of overconsumption, the available power can drop in the grid, causing the voltage to drop as well. On the other hand, in case of overproduction, or production that is sufficiently higher than the current demand, the available power in the microgrid can increase, causing the voltage to increase as well. These two voltage fluctuations can cause issues in the operation of the converters. As the converters which are now selected will not be used in the final design, the standard voltage fluctuation for systems ranging from 120 VAC to 600 VAC from the ANSI C84.1 standard is taken as reference [56]. In this standard, two voltage ranges are mentioned: range A (95% to 100% of the operating voltage) and range B (91.7% to 105.8% of the operating voltage). Range A is the safest of these options and ensures correct operation, hence this stricter range is chosen as maximum voltage fluctuation range.
The proposed control algorithms in case of islanded or grid-connected mode, hence for the bidirectional DC-DC converter to/from the battery as well as the bidirectional DC-AC converter to/from the grid, have been designed to stabilize this voltage fluctuation. However, for our current design, these control algorithms have not been implemented. During the design validation, the voltage fluctuation will be checked to see if RQ-M.DCG.13 can be met.

5.4. Safety

Now that the grid's stability has been ensured to a certain degree, the actual safety for the residents of the tiny houses needs to be guaranteed. This will be done by looking at standards that provide standardised implementations of DC microgrids and can thus provide another degree of safety. Also, the possible interaction of residents with the microgrid or nanogrid will be considered.

5.4.1. Standards

RQ-S.DCG.6 states that the entire microgrid should comply with the safety regulations of the EU in association with Dutch regulations and safety and connection standards for DC grids. In order to fulfill this requirement, safety regulations for DC microgrids in the EU and standardised connections are researched in current standard development. The current developments in standards for DC microgrids are discussed in [53]. In addition, a small list of the most noteworthy standards will be provided in

Appendix D.4.2. As these standards are quite expensive and far above our budget for all subgroups, a small summary is provided. For practical implementation, these standards should be bought to ensure the grid design is done in a standardised way, minimizing dangers and faulty connections. The mentioned standards include safety considerations that have been considered in the protection circuitry, while the most prominent part considers standardised implementation for operation, maintenance, and design of DC microgrids in city, rural and remote areas. The application of the mentioned standards would thus ensure that RQ-S.DCG.6 is met.

5.4.2. Human interaction

The microgrid and the nanogrids of each house are relatively small, making human interaction possible with the electrical appliances and components. As discussed in Section 5.3.1, a unipolar bus design is not able to provide the same level of safety as a standard grid for voltage levels higher than 200 VDC. As a bipolar implementation is not possible due to the communication, several measures are taken to prevent accidental human interactions with the higher voltage levels. These measures consist of isolating the high-power connections with the induction cooker and the electric boiler. This also means the inhabitants themselves will not be able to access these sockets easily, and except for maintenance, the high-power sockets will only be used for these two appliances. For tunect, the high-power usage sockets of the washing machines will be isolated in the same way. The batteries and their converters will not be accessible without a particular key and can only be accessed by maintenance or residents with the necessary experience. Lastly, the wind turbines will be inaccessible through fences and will be accessible to maintenance.
In case of maintenance, the previously mentioned isolation methods will be accessible to the appropriate personnel. For the high voltage levels in the grid, the multi-bus structure can isolate the defected part of the grid. Then, the protection schemes will make sure that the cables, converters, and other components will be safe for human interaction.

5.5. Cost Analysis

Throughout the design process, specific products for many of the system's main components have been selected. RQ-S.DCG.1 states that the balance between costs of the entire DC grid and its functionality should be optimised. While deciding on what components to select, costs have been taken into account on several occasions. Some examples are the decision to select the cheaper battery composition, minimizing the number of converters needed, trying to minimize the wiring prices, and choosing the cheaper local protection for some of the modules.
Now that all those design choices have been made, a cost analysis can be performed. Even though appliances have been selected for the demand estimation, the cost analysis does not include them. This is because DC appliances are not on the market yet. Furthermore, appliances are not necessarily considered to be part of the grid. This cost analysis only considers the costs of the main components of the grid and can be found in Appendix D.5. As shown there, the total price of this grid design will be around €166,000.
This price, however, is mainly based on prices found online. Most of these prices include 21% VAT and are offered by a retailer. Considering that such a microgrid design is most likely to be used by a contractor, it is assumed that when the components are bought in bulk and directly from the supplier, these prices decrease by approximately 40%, also subtracting taxes. This results in a total price of around €100,000. This can be considered a fairly reasonable price as the most significant components are selected to operate for at least 20 years, and the costs are shared by 12 households.

6

Design Validation

The design choices in the design phases of demand, supply, storage, and topology have been discussed but not yet verified. RQ-M.DCG.15 states that this should be done using power analysis simulation software, which needs to be carefully selected. RQ-M.DCG.15 is only met after certain demand cases show functional results. The resulting program was chosen to be Simulink [57], which is a transient analysis program based on MatLab, with a specialised power component library called Simspace. The loads, RESs, ESS and main grid need to be modeled and subsequently connected to the microgrid and nanogrids.

6.1. Models of each subsystem

In order to correctly model the designed grid, each subsystem consisting of either demand, supply, or storage needs to be modeled correctly. Even though the circuits are simplified due to the top-level design and limited by the Simulink transient analysis, the electrical analysis can give some relevant results. These results will be discussed for each subsystem.

6.1.1. Demand

The demand will be modeled with two constant power load blocks from Simscape, where the high power and low power loads of the 400 V and 48 V sockets, respectively, are connected in parallel. No converter losses are included as this has been taken into account with the 30% safety margin explained in Chapter 3. The appropriate wire length is then added for each house and is connected to the microgrid voltage bus. This circuit is explained and shown in Appendix E.1.1.

6.1.2. PV panel module

In Simscape, there is a solar cell block available, which can take the short circuit current and the solar irradiation used for this current as input. The short circuit current is filled in from the datasheet [27], being 10.84 A at 1000 W/m^2, while the open-circuit voltage needs to be equal to 3 times the open-circuit voltage of a single module (as 3 modules have been connected in series for each house), which is equal to $3 \cdot 42.9VDC = 128.7VDC$. By giving 206 series cells as input, this gives 128.7 VDC as open-circuit voltage. After connecting 20 of these solar cells in parallel, a short circuit current of $10.67A$ was reached. This configuration gave the closest short circuit current to the desired value of $10.87A$. Lastly, a DC-DC converter that boosts the voltage to 400 VDC is implemented. This circuit is explained and shown in Appendix E.1.2.

Due to the top-level design and simple subsystems, connecting the PV panel subsystem to the loads, while the battery and wind turbine models with their respective converters were active, was not possible due to limitations in Simulink. This limitation having to do with insufficient matching of load and demand for the DC-DC or DC-AC converters. To remedy this, an equivalent model was constructed. Since the PV panels are connected directly to the loads, it was chosen to model their contribution by lowering the power demand of the loads by 25%. This percentage is chosen as the maximum output power of the PV panels is equal to 13.68 kW, which is roughly 25% of the total peak demand of 62.1 kW.

6.1.3. Wind turbine

The second RES method are the VAWTs. In Simscape, there are several wind turbine blocks available, however these only work with torque as output and a complex connection circuit needs to be created in order to deliver the electrical power output for a certain wind speed. It was thus chosen to implement an load flow source, which is able to supply a certain amount of active power, which was set at 2 kW. As the wind turbine is rated at 48 VAC [58], a rectifier rated at 48 VAC and a fixed power loss of 4% is implemented (as a loss > 0% had to be implemented in the Simulink block). Then a DC-DC converter of 400 VDC reference voltage was used to connect to the main grid. This circuit is explained shown in Appendix E.1.3.

As with the PV panel model, calculations of an AC power source with a rectifier and DC-DC converter are not possible if other DC-DC converters are connected. This lead to the choice of modeling the wind turbine as a battery of 48 VDC with a DC-DC converter to 400 VDC and connected to its own set of wiring. As each wind turbine is now modeled as a battery, the three turbines are taken as one single battery, which caused the resistance to be decreased by a factor of 3 due to parallel connection. The contribution of the PV panels was modeled as a 25% decrease in demand, while the wind turbines, which have a peak output power of 15.6 kW, will supply the 75% of the remaining demand together with the batteries.

6.1.4. Battery / PCC

The ESS was quite simple to model, as Simscape has a battery block that incorporates most parameters mentioned in the [40]. After filling in a nominal voltage of 358 VDC, as well as the capacity of 2 times 19.3 kWh multiplied with the RTE, the battery was complete. Another DC-DC converter was placed to boost the voltage to 400 VDC. The model is explained and shown in Appendix E.1.4. The PCC was also modeled as a battery with a DC-DC converter to 400 VDC with its own section wiring.

6.1.5. Wiring

The wiring for the microgrid and connections to the nanogrid are simple to model. As every wire operates at DC, the only modeled parameter of a cable is thus the resistance. The values for the resistance are based on the wiring calculations given in Appendix D.3, and the wiring resistances in [49]. After calculating the total resistance for each type of cable, the average lengths for each connection (ESS, RESs or loads) are used to calculate the actual resistor values. The results of these calculations are explained and shown in Appendix E.1.5.

6.1.6. Grounding and protection

As no analysis of the fault rate of the system has been done and no fault detection or resolving methods are implemented, faults and grounding methods will not be analyzed in the simulation.

6.1.7. Grid layout

In order to model the entire community, the subsystems have to be connected in a certain way. In general, the layout as presented in Chapter 5, with a normally open switch disconnecting the two batteries, will be considered. This means that the general connection of subsystems to the microgrid will consist of 2 batteries on either side, 2 equivalent wind turbines, 12 tiny houses, 12 sets of equivalent PV panel production, and lastly, tunect. Each of these subsystems will be connected to the positive polarity wire of the voltage bus using resistors with the value of the respective section resistance, while the negative polarity of the bus will work as a ground connection for all of the systems. The schematic of the microgrid with all the possible subsystems connected (RESs, ESS, loads and PCC) is shown in Figure E.5.

6.2. Simulation scenarios

Now that each subsystem has been modeled, certain cases can be created to test if the ESS and RESs can supply the demand while still operating in the ±5% voltage fluctuation range. The six cases which have been considered are shown below. 150% of demand is also tested based on RQ-C.DCG.4, which states that design validation could be done for excessive scenarios of maximum power demand. Each of the cases indicates whether the aforementioned subsystems are included and which subsystem circuits are connected to the microgrid. In case of no batteries, the batteries are disconnected from the

microgrid. In case of no generation, the wind turbines are disconnected, and the load is set to 100%. In the case of main grid connection, the main grid is connected to the microgrid at tunect.

- **Case 1:** Maximum demand, all batteries, no generation
- **Case 2:** Maximum demand, all batteries, full generation
- **Case 3:** Low power demand, all batteries, no generation
- **Case 4:** Maximum demand, no batteries, only main grid
- **Case 5:** 150% of demand, all batteries, no generation
- **Case 6:** 150% of demand, all batteries, full generation

6.3. Case analysis

For each of the cases, the voltage at the loads was measured, as well as the current through the wire leading to the load. By calculating the difference in voltage of the grid and the loads and multiplying this with the current through the wire, both the voltage and power drops could be calculated. For each case, the minimum and maximum voltage in V and their percentual decrease with respect to the 400 VDC grid voltage are shown. The power losses in W due to the wiring are shown as well as the percentage of this loss with respect to the drawn power of each of houses / tunect. These results are summarised in Table 6.1.

Table 6.1: Voltage drop in V and % and power loss in W and % for each of the cases.

Case	Voltage drop [V] Min - Max	Voltage drop [%] Min - Max	Power drop [W] Min - Max	Power drop [%] Min - Max
1	2.81 - 7.39	0.70 - 1.85	31.49 - 89.38	0.71 - 1.88
2	2.05 - 5.46	0.51- 1.36	18.34 - 49.25	0.52 - 1.38
3	0.32 - 1.28	0.08 - 0.32	0.11 - 2.72	0.08 - 0.32
4	1.76 - 6.31	0.44 - 1.58	18.27 - 76.06	0.44 - 1.60
5	4.23 - 11.19	1.06 - 2.80	71.54 - 204.92	1.07 - 2.88
6	2.71 - 9.12	0.68 - 2.28	27.19 - 138.5	0.68 - 2.33

As can be seen in case 1, which is the worst common case, the maximum voltage drop is 7.39 VDC, which is equivalent to 1.85 % of the grid voltage. This voltage drop is thus still well within the ±5 % allowed voltage fluctuation limit [56]. The power loss is maximally 1.88 %, which in comparison with the losses predicted in Table D.1, is as expected. This is due to each wire section contributing to the losses, and hence the addition of the losses in Table D.1 is expected. The main grid connection performs better than the battery connection. This can be explained due to the lower connection resistance of the main grid, as well as only a single wire is used, instead of the two connection wires needed for the two sets of batteries.

When looking at the cases where generation is able to support the batteries, it can be seen that the voltage drop is lowered due to local generation of PV panels, as well as intermittent generation by the VAWTs. Between cases 1 and 2, the generation is able to provide 0.29 % less voltage drop and 0.4 % less power loss.

The cases of 150 % power demand, with and without generation, are both hypothetical as the batteries are physically not able to deliver this power demand, and the grid is not designed for higher demand than 100%. Still, it shows that the voltage drop is in the acceptable range being maximally 2.80 % without generation and 2.28 % with generation. The generation provides 0.52% less voltage drop and 0.55 % less power loss. As 150% of demand still shows functional results and is hence validated for this grid design, RQ-C.DCG.4 is met. If even better cables are used which could handle this current, the losses would be even lower.

Now that the design has been successfully validated using Simulink, showing acceptable voltage fluctuations and functional results in several demand cases, both RQ-M.DCG.13 and RQ-M.DCG.15 are met. Furthermore, it can finally be concluded that both the microgrid and nanogrid are able to supply the limited peak demand of the community and one tiny house respectively and thus RQ-M.DCG.2 and RQ-M.DCG.3 are met as well.

7

Conclusions and Recommendations

The complete design and validation of an electricity grid for a community of tiny houses have now been completed. The design phases consisted of estimating the energy demand, determining the required supply and storage for this demand, and optimizing the topology for the microgrid and nanogrid. The validation phase consisted of simulating several demand and generation cases in Simulink, which resulted in the required functional results.

7.1. Conclusions

The first design phase resulted in an hourly, daily, and monthly estimation of the community's energy demand. The average daily usage of the community was estimated to be 57.48 kWh/day. Using a model of generation, RESs in the form of 61.2 m^2 PV panels and 6 VAWTs are chosen to supply this estimated demand. To store and supply energy of the varying energy generation of the RESs, different ESS options are considered, and 4 of the selected Li-Ion batteries are chosen with a total capacity of 77.2 kWh, and power output of 64.6 kW. In the last design phase, the topology of the community is designed, which resulted in a ring topology operating in a unipolar series-connected multi-bus configuration, operating at 400 VDC. In order to easily identify faults and reduce complexity, this topology effectively operates in radial (by using a normally open switch). This topology also includes proposals for the required converters and control/optimization algorithms, the appropriate wiring for each connection, the selected grounding, fault detection and protection, and other safety considerations. A cost analysis is made of the grid of the entire community with all selected components, resulting in an estimated total cost of around €100,000. Lastly, design verification is performed on the proposed design, which resulted in functional results during maximum demand with a maximum voltage drop of 1.85 % and power loss of 1.88 %. For 150% demand, the results still showed functional results with a maximum voltage drop of 2.80 % and power loss of 2.88 %.

Throughout the thesis, all requirements presented in Chapter 2 have been discussed. The primary requirements (must haves), and secondary requirements (should haves) have provided guidance in most design choices, while some tertiary requirements (could haves) helped to improve the design. The design meets all the primary requirements, which is discussed and concluded throughout the design phases and design validation. Furthermore, all of the secondary requirements have been accounted for as discussed throughout the thesis. Though not all can be considered successfully met, as terms like 'optimize' make these requirements hard to fully comply with as there is always room for improvement. Another obstacle was a pay-wall for information on standardization of safety, stability, and connections. Some of the tertiary requirements have been implemented as well, and if not, they will be discussed in Section 7.2. Finally, the top-level system requirements have not been discussed explicitly, as all requirements relevant to the DCG subgroup have been converted into relevant subgroup requirements.

7.2. Discussion & Recommendations for Future Work

The current design presented in this thesis is a top-level design, and on many aspects, further research is needed to realise and optimise the design. Discussion on the current results as well as some recommendations based on the research and results of each chapter are made below.

Energy Demand Estimation
To improve the accuracy of the demand estimation, more data from existing communities can be researched. The data from the two researched communities was very insightful, however it did also show how big the difference between tiny house communities can be. Real-time power data would drastically improve the accuracy of the estimation of peak power, as well as the timing of the peak power. Additional market research on DC appliances would help determine the feasibility and time scale of realising this design.

Supply & Storage Design
The current design is developed to operate in Rotterdam, enabling the microgrid to use the main grid as backup and to supply back to the city. For now, it has been decided to supply back to the main grid. RQ-C.DCG.6 states that in case of overproduction, supplying excessive energy back to the main grid could be minimised in order to minimize grid connection. In order to fulfill this requirement as well as making the design more scalable, the overproduction could be diverted through turning off the PV system when needed, or further research could be done on finding different ways.
RQ-C.DCG.1 states that the microgrid could operate completely islanded. As the availability of the current design is already substantial and to fulfill this requirement, it would be interesting to research what would be needed to enable complete off-grid operation.
To improve the reliability and efficiency of the current design, an entirely distributed battery system could be an option as less expensive home batteries become available. Further research is needed on connecting the energy demand and supply of the heat grid to the microgrid to enable power sharing between the system resulting in more efficient use of energy.
And finally, employing aerodynamics research, optimal locations for the VAWTs could be found. Currently, these are simply put as far away as possible. As discussed in Section 4.2.1, no real-time power data is available from either demand or generation. This meant that RESs and ESS methods could only be selected using an energy balance instead of a power balance. Research could be done for high power density ESS methods, such as a high-speed flywheel. A hydrogen-based storage and generation system could also be considered, such as proposed in [59].

Topology Design
As discussed earlier, the use of a bipolar bus would be a better option for this design, not only to improve safety but also reliability. In case a line is faulty, half of the bus is still operational due to the third line. To further increase the system's safety, it is recommended to research the European and Dutch safety standards more in-depth. Subsequently, a detailed protection and safety system can be designed. Custom converter design should be done in order to implement all recommended optimization control algorithms. RQ-C.DCG.5 states that primary control methods could be defined and compared for this implementation. To fulfill this requirement, research could be done on the primary control of the system.

Design Validation
In Chapter 6, Simulink with its specialised library Simspace was used to validate the designed grid. If more time would have been available, the proposed converters could have been designed in Simulink and implemented. Furthermore, basic versions of our proposed control/optimization algorithms could have been designed in Simulink as well.
However, this software was not optimal, as it is a transient-based analysis software with no proper blocks for power flow analysis. The most appropriate software for a power flow analysis of a top-level design would be libraries like MATPOWER (in MATLAB) or PandaPower (in Python). However, even these programs specialize in large regional AC grids of several MW, whereas our grid operates on DC and consumes less than 0.1 MW. A DC power flow is possible in these programs, but this approximates an AC power using fixed voltage levels but varying voltage angles (hence reactive power is still present). Programming a modified DC power flow based on this software which only utilises real voltages and currents and only active power flow is out of the scope of this thesis but could be researched to validate the top-level grid design properly.
Furthermore, in Simulink, no proper RES or ESS blocks were available for power flow analysis or simulations of several hours. Hence, the previously used energy balance analysis was not possible, and only power demand could be compared. This meant rough equivalent models had to be designed.

Acronyms

AC Alternating current.

CNS Control & Software.

DC Direct Current.

DCG DC Grid.

DoD Depth of Discharge.

DSO Distribution System Operator.

EMI Electro-Magnetic Interference.

ESS Energy Storage System.

HAWT Horizontal Axis Wind Turbine.

IEA International Energy Agency.

MPPT Maximum Power Point Tracking.

PCC Point of Common Coupling.

PID Proportional Integral Derivative.

PLC Power Line Communication.

Poc Proof of Concept.

PoR Program of Requirements.

PV Photo-Voltaic.

PVT Photo-Voltaic Thermal.

RES Renewable Energy Source.

RTE Round Trip Efficiency.

SoC State of Charge.

VAWT Vertical Axis Wind Turbine.

A

System PoR

This section covers the top-level system requirements of the Bachelor Graduation Project 'Distribution of the electricity grid of a tiny house community'. The system requirements relevant to the DCG subgroup have been rephrased and put into the requirements of the subgroup as shown in Chapter 2.

A.0.1. Functional Requirements

Must have

- **RQ-M.SYS.1:** The system must use the designed DCG, where information will be sent to the Control & Software (CNS) subsystem using the designed Power Line Communication (PLC).
- **RQ-M.SYS.2:** The system must be able to supply the 12 tiny houses and the common usage of the community.
- **RQ-M.SYS.3:** The system must use renewable energy sources as supply units only.
- **RQ-M.SYS.4:** The system should have an availability of at least 90%.
- **RQ-M.SYS.5:** The system must be able to do forecasting of factors influencing the system based on the users' behaviour and the weather.
- **RQ-M.SYS.6:** The system must be able to communicate grid information over the power lines using a power line communication system.

Should have

- **RQ-S.SYS.1:** The system should be designed such that the costs are minimised for the given functional requirements.
- **RQ-S.SYS.2:** The system should be designed such that the efficiency is optimised.

Could have

- **RQ-C.SYS.1:** The system could be designed to operate in islanded mode all of the time.
- **RQ-C.SYS.2:** The system could be designed to be scalable, i.e., both the number of tiny houses per community and the number of communities can be easily increased.

A.0.2. Non-Functional Requirements

Below, all non-functional requirements of the top-level system will be given. They describe how the system should operate.

- **RQ-NF.SYS.1:** The minimum speed of the power line communication system should be such that it can sustain a transfer that is fast enough such that all data can be delivered to the devices within a timely manner.

B

Demand

In the following sections, the individual appliance selection is made, and usage calculation is done for the initial estimation, as well as the sustainable modifications made. Lastly, the notes from the interview with a tiny house community in Delft called 'Pionierskwartier' are shown.

B.1. Appliance selection

In the next lists, the used appliances with their respective usages are shown for all appliance categories. Care has been taken to select low power usage versions for all appliances and, if possible, the best possible energy efficiency grading.

Base Load

The baseload consists of essential appliances which are almost always turned on, where the selected appliances are shown below.

- Ventilation: `https://www.ventilatieland.nl/artikel/17345/badkamer-ventilator-energiezuinig-stil-en-met-timer-diameter-100-mm-wit-100ts.html`
- Lights: `https://www.lighting.philips.nl/consumer/p/led-spot/8719514314030`
- WiFi Router: `https://www.trendnet.com/products/wireless-ac-router/ac1200-dual-band-wifi-router-TEW-831DR`
- Fridge/Freezer Combination: `https://www.bemmelenkroon.nl/merken/frilec/berlin1651a_plus__plus__plus_-fril/`

Kitchen Appliances

The chosen kitchen appliances are shown below.

- Blender: `https://www.amazon.nl/Russell-Hobbs-Geluidsreductiesysteem-Ruimtebesparend-25290-56/dp/B07NDH6L3W`
- Induction Stove: `https://www.bcc.nl/keuken/fornuis-en-kookplaat/inbouw-inductie-kookplaat/aeg-inductie-kookplaat-hk604200cb/254912?channable=006f3669640030303030303030303030303030323534393132b4&utm_medium=vergelijkingssites&utm_source=beslist&utm_campaign=keuken_fornuis-en-kookplaat_inbouw-inductie-kookplaat&utm_content=000000000000254912&bl3nlclid=814e82ec-b569-40ab-80da-b81ce151cd7a&utm_term=BESLI814e82ec-b569-40ab-80da-b81ce151cd7a`
- Oven/Microwave Combination: `https://www.magnetronoven.nl/inventum/mn256c/`

- Coffee Machine: https://www.bcc.nl/keuken/koffiezetapparaat/nespresso-machine/nespresso-magimix-koffieapparaat-pixie-m112-aluminium/57585?channable=006f3669640030303030303030303030303030303035373538350a&utm_medium=vergelijkingssites&utm_source=beslist&utm_campaign=keuken_koffiezetapparaat_nespresso-machine&utm_content=0000000000000057585&bl3nlclid=0584d9d6-d3d7-4adc-b5c9-a7fc6caf9354&utm_term=BESLI0584d9d6-d3d7-4adc-b5c9-a7fc6caf9354
- Kettle: https://www.bol.com/nl/p/russell-hobbs-textures-plus-waterkoker-zwart-snelkookfunctie-extra-zuinig-gemakkelijk-reinigbaar-2-400-watt/9300000031652517/?Referrer=ADVNLGBL000&utm_source=google&utm_medium=cpc&utm_campaign=beslist-SDA&utm_term=BESLI0ea7189c-b948-4862-883a-0147441dc53d~9300000031652517&bl3nlclid=0ea7189c-b948-4862-883a-0147441dc53d
- Kitchen Machine https://www.coolblue.nl/en/product/140640/magimix-cuisine-systeme-5200-xl-matte-chrome.html

Heat Regulation
The appliances which contribute to the heat regulation of a tiny house are shown below.

- Boiler: https://www.techniq.nl/eldom-favourite-elektrische-boiler-50-liter.html?utm_source=Google+Merchant+Center&utm_medium=referral&utm_term=111166944&utm_campaign=easyads&gclid=Cj0KCQjwk4yGBhDQARIsACGfAeuC8EYKXLO-bl3sTNKUDnRWaBUHN9ZJM-ICcccJFvA7vVVjCVRBjGwaAnh_EALw_wcB
- Water Pump: https://www.waterpump.co.uk/dab-evosta-2-40-70-180-circulation-pump-central-heating-pump?sqr=dab
- Shower: https://www.mijnupfallshower.nl/prijzenupfallshower.html
- Air Conditioning: https://www.totalhomesupply.com/p/frigidaire-ffra051wa1-5-000-btu-window-unit-room-air-conditioner-manual-control

Remaining Appliances
The remaining appliances which are considered are shown below.

- Phone Charger: https://www.apple.com/shop/product/MD810LL/A/apple-5w-usb-power-adapter
- Computer Charger: https://www.hp.com/us-en/shop/pdp/hp-zbook-studio-g5-mobile-workstation
- Vacuum Cleaner: https://www.cnet.com/products/dyson-dc40-origin-upright-vacuum-cleaner/
- Handheld Vacuum: https://www.coolblue.nl/product/234250/philips-fc6149.html#product-specifications
- Hair Dryer: https://www.agstore.nl/philips-bhd027-00-energiezuinige-foehn-111143707.html
- LED Television: https://www.mediamarkt.nl/nl/product/_philips-32phs5525-12-1662224.html

Tunect Appliances
For the common usage, extra care must be taken for low power usage and high efficiency as a dryer and washing machine use a lot of energy throughout the year. These appliances, as well as the printer, outdoor lights, and control unit are shown below.

- Washing Machine: https://www.coolblue.nl/product/869937/haier-hw80-b14636n.htm
- Dryer:https://www.coolblue.nl/product/867486/siemens-wt7u4600nl.html#product-specifications
- Printer: https://www.freeprintersupport.com/laser-printer-vs-inkjet-printer-power-consumption
- Outdoor Lights: https://www.lighting.philips.com/main/prof/outdoor-luminaires/road-and-urban-lighting/road-and-urban-luminaires/luma-gen2/910925867324_EU/product
- Control Unit: https://www.sossolutions.nl/raspberry-pi-4-model-b-4gb?gclid=Cj0KCQjwk4yGBhDQARIsACGfAevGqgRmVmj9JlobiJgr4Xczf4yvITPGWHhDD7t4Q05cn_mM26cuA1UaAjlTEALw_wcB

B.2. Initial power and time usage tables

In this section, the initial demand estimation consisting of the peak and average power demand, time usage, and daily, monthly, and yearly energy usage is shown for each of the categories, using the selected appliances in Appendix B.1 and the time usage in [17] and [18]. The initial baseload is shown in Table B.1, the kitchen appliances in Table B.2, the heating regulation appliances in Table B.3 and lastly the common usage in Table B.5.

B.2.1. Base load

Table B.1: Initial usage estimation of the base load.

Appliance	Peak power [W]	Average power [W]	Time used [h/day]	Energ usage [Wh/day]	kWh/month	kWh/year
Ventilation	8.00	8.00	6.00	48.00	1.46	17.52
Lights	12.00	12.00	8.00	96.00	2.92	35.04
Wifi router	5.68	1.42	24.00	34.08	1.04	12.44
Fridge + freezer	55.00	10.73	24.00	257.53	7.83	94.00
Total	80.68	32.15		435.61	13.25	159.00

B.2.2. Kitchen appliances

Table B.2: Initial usage estimation of the kitchen appliances.

Appliance	Peak power [W]	Average power [W]	Time used [min/day]	Energ usage [Wh/day]	kWh/month	kWh/year
Blender	400.00	400.00	4.00	26.67	0.81	9.73
Induction cooker	3650.00	1500.00	33.33	833.25	25.34	304.14
Oven	2400.00	2000.00	30.00	1000.00	30.42	365.00
Microwave	900.00	550.00	20.00	183.33	5.58	66.92
Coffee machine	1260.00	1260.00	15.00	315.00	9.58	114.98
Kettle	2400.00	2400.00	12.50	500.00	15.21	182.50
Kitchen machine	1100.00	1100.00	10.00	183.33	5.58	66.92
Total	12110.00	9210.00		3041.58	92.51	1110.18

B.2.3. Heating

Table B.3: Initial usage estimation of the heat regulation.

Appliance	Peak power [W]	Average power [W]	Time used [h/day]	Energ usage [Wh/day]	kWh/month	kWh/year
Boiler	2000.00	2000.00	0.85	1700.00	51.71	620.50
Water pump	44.00	44.00	8.40	369.60	11.24	134.90
Shower	150.00	150.00	0.20	30.00	0.91	10.95
Air conditioning	450.00	450.00	1.00	450.00	13.69	164.25
Total	2644.00	2644.00		2549.60	77.55	930.60

B.2.4. Other appliances

Table B.4: Initial usage estimation of all remaining appliances.

Appliance	Peak power [W]	Average power [W]	Time used [min/day]	Energy usage [Wh/day]	kWh/month	kWh/year
Phone charger	10.00	5.00	240.00	20.00	0.61	7.30
Computer charger	150.00	150.00	38.24	95.60	2.91	34.89
Vacuum cleaner	850.00	850.00	8.33	118.06	3.59	43.09
Hair dryer	1600.00	1600.00	9.00	240.00	7.30	87.60
LED Television	24.00	24.00	233.33	93.33	2.84	34.07
Total	2634.00	2629.00		566.99	17.25	206.95

B.2.5. Tunect usage

Table B.5: Initial usage estimation of tunect.

Appliance	Peak power [W]	Average power [W]	Time used [min/day]	Energ usage [Wh/day]	kWh/month	kWh/year
Washing machine	2000.00	2000.00	45.37	1512.33	46.00	552.00
Dryer	1000.00	1000.00	349.15	5819.18	177.00	2124.00
Printer	12.00	0.79	1440.00	18.90	0.57	6.90
Street lights	120.00	120.00	480	960.00	29.20	350.40
Control module	10	10	1440	240.00	7.30	87.60
Total	3142.00	3130.79		8550.41	260.07	3120.90

B.3. Interview notes

- Estimatjon of energy usage
  - Appliances
    - Estimated average base load of 40 Watts: ventilation, lights, smart computer, fridge, wifi etc.
    - Kitchen appliances: Coffee machine, phone charger, external monitor and laptop
  - Energy usage using fossil fuel sources (pellet heating, gas furnace, gas boiler etc.): 2 kWh per day
  - Estimated energy usage using mostly electric per day:
    - 1.8 kWh of cooking
    - 1.6-1.8 kWh of heating usage (shower/heating)
    - Total: around 3-4 kWh
  - Yearly energy estimation of 1000 kWh: 200 kWh of heating and 800 kWh of cooking.
- Heating:
  - Singular heating system: could be done using PV system, sun collectors, and a heat pump. This can also function as a heat pump in case of overproduction.
  - Using a common heating system is difficult due to heat losses in storage and transportation. If done properly could be very useful, but only if the whole community uses the heating system.
  - Heating system requires very well isolated houses (passive house standard) to theoretically function. In the winter, a heat grid might not be enough, hence a backup heating system could be used like a hydrogen battery that feeds an electric generator or a salt water extraction battery.
  - Isolation requires a trade-off, as larger isolation causes less space to be available, which might lead to the houses becoming bigger to compensate.
- Electricity connection:
  - Most used option is the VICTRON transformer, which keeps the connection to the main grid stable and regulates the power usage.
  - With current products, AC outlets would still be required, however DC might be an option if researched. The current grid for a tiny house should be AC due to safety and easy connections with common appliances.
- Generation
  - Easy solar controller which makes sure the battery, solar panels, and demand of a tiny house are regulated. This means each house must have its own battery in order for it to function.
  - Estimation of 90% availability if excellent solar panels are used as well as a battery. More realistic if other sources like wind or hydrogen are used.
  - Using a VICTRON connection, net 0 energy can be used from the grid as power can be delivered back.
- Storage:
  - Use a lithium-ion battery, the best performance for your community.
  - Supercapacitor not needed as peak power demand will seldom occur, especially not in a few seconds. Maximum power also not comparable to fast EV charging.
  - Hydrogen could be an option, but right now quite expensive and not quite there in terms of capacity.

B.4. Tables after modifications

In this section, the peak and average power demand, time usage, and daily, monthly, and yearly energy usage of the remaining appliances after modifications are shown for all categories. In Table B.6 the base load is shown, the kitchen appliances are shown in Table B.7, the heating regulation appliances in Table B.8 and lastly Table B.10 shows the common usage.

B.4.1. Idle appliances

Table B.6: The sustainable usage estimation of the base load, which has remained the same as the initial estimation.

Appliance	Peak power [W]	Average power [W]	Time used [h/day]	Energ usage [Wh/day]	kWh/month	kWh/year
Ventilation	8.00	8.00	6.00	48.00	1.46	17.52
Lights	12.00	12.00	8.00	96.00	2.92	35.04
Wifi router	5.68	1.42	24.00	34.08	1.04	12.44
Fridge + freezer	55.00	10.73	24.00	257.53	7.83	94.00
Total	80.68	32.15		435.61	13.25	159.00

B.4.2. Kitchen appliances

Table B.7: The sustainable usage estimation of the selected kitchen appliances. The microwave has 0 peak as the oven and microwave can only run separately.

Appliance	Peak power [W]	Average power [W]	Time used [min/day]	Energ usage [Wh/day]	kWh/month	kWh/year
Blender	400.00	400.00	4.00	26.67	0.81	9.73
Induction cooker	3650.00	1500.00	45.00	1125.00	34.22	410.63
Oven	2400.00	2000.00	20.00	666.67	20.28	243.33
Microwave		550.00	10.00	91.67	2.79	33.46
Total	6450.00	4450.00		1910.00	58.10	697.15

B.4.3. Heating

Table B.8: The sustainable usage estimation of the selected heat regulation.

Appliance	Peak power [W]	Average power [W]	Time used [min/day]	Energ usage [Wh/day]	kWh/month	kWh/year
Boiler	2000.00	2000.00	0.85	1700.00	51.71	620.50
Water pump	44.00	44.00	8.40	369.60	11.24	134.90
Shower	150.00	150.00	0.20	30.00	0.91	10.95
Total	2194.00	2194.00		2099.60	63.86	766.35

B.4.4. Other appliances

Table B.9: The sustainable usage estimation of the selected remaining appliances.

Appliance	Peak power [W]	Average power [W]	Time used [min/day]	Energ usage [Wh/day]	kWh/month	kWh/year
Phone charger	10.00	5.00	240.00	20.00	0.61	7.30
Computer charger	150.00	150.00	38.24	95.60	2.91	34.89
Vacuum cleaner	12.00	12.00	8.33	1.67	0.05	0.61
Total	172.00	167.00	286.57	117.27	3.57	42.80

B.4.5. Tunect usage

Table B.10: The sustainable usage estimation of tunect.

Appliance	Peak power [W]	Average power [W]	Time used [min/day]	Energ usage [Wh/day]	kWh/month	kWh/year
Washing machine	4000.00	252.05	360.00	1512.33	46.00	552.00
Printer	12.00	0.79	1440.00	18.90	0.57	6.90
Street lights	120.00	120.00	480	960.00	29.20	350.40
Control module	10	10	1440	240.00	7.30	87.60
Total	4142.00	382.84		2731.23	83.07	996.90

B.5. Daily model

In this section, the data used for the daily model, as well as extra results of both the daily and monthly model.

B.5.1. Liander Data

The daily model is constructed based on real-life data made available by Liander [23]. Following the link in the bibliography, the used data can be found in the middle of the page under the 'slimme meter' or smart meter section.

B.5.2. Graphs from daily data

Using the energy usage behaviour of the Liander data [23] and scaling with the estimated usage of a tiny house, the daily Wh usage for every 15 minutes for a tiny house can be calculated and is shown below in Figure B.1. The data values are shown in Table B.11.

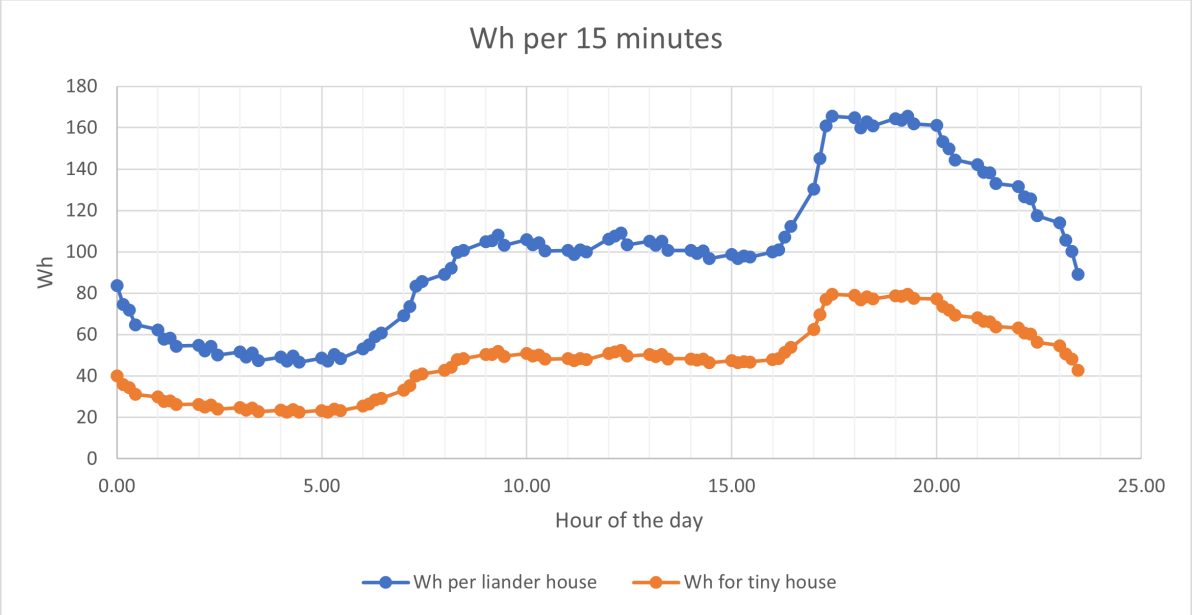

Figure B.1: Average energy usage of one tiny house (orange) and one average household (blue) in Wh over a day in 15 minute intervals.

Table B.11: Daily usage for a tiny house versus average liander household.

Hour	Tiny house usage [Wh]	Liander usage [Wh]
0	141.56	295.08
1	111.79	233.02
2	101.48	211.54
3	95.52	199.11
4	92.46	192.73
5	93.35	194.58
6	109.43	228.11
7	149.51	311.65
8	183.16	381.81
9	202.31	421.72
10	198.71	414.21
11	192.09	400.41
12	204.47	426.23
13	198.72	414.23
14	190.61	397.33
15	187.77	391.42
16	201.69	420.42
17	288.77	601.94
18	311.18	648.65
19	314.52	655.62
20	292.06	608.81
21	264.65	551.65
22	240.47	501.26
23	196.19	408.96

B.6. Monthly model

The monthly model uses the behaviour of an average of 5 houses of the 'Minitopia' tiny house community and scaling this with our yearly usage results in a monthly energy consumption distribution. The monthly energy usage in kWh of a tiny house for all months is shown in Figure B.2. The orange data shows the average monthly usage in kWh for a house in Minitopia, whereas the blue data is the scaled version of our estimated tiny house demand. As can be seen from the figure, the monthly demand of minitopia is always higher, in table Table B.12, the values can be found. The tiny house usage is 60% of the Minitopia usage.

Table B.12: Minitopia vs tiny house monthly usage in kWh.

Month	**Minitopia usage** [kWh]	**Tiny house usage** [kWh]
January	235.49	144.62
February	245.03	150.48
March	222.70	136.77
April	198.00	121.60
May	213.77	131.28
June	210.07	129.01
July	160.87	98.80
August	169.33	103.99
September	149.59	91.87
October	173.81	106.74
November	224.60	137.93
December	288.34	177.08

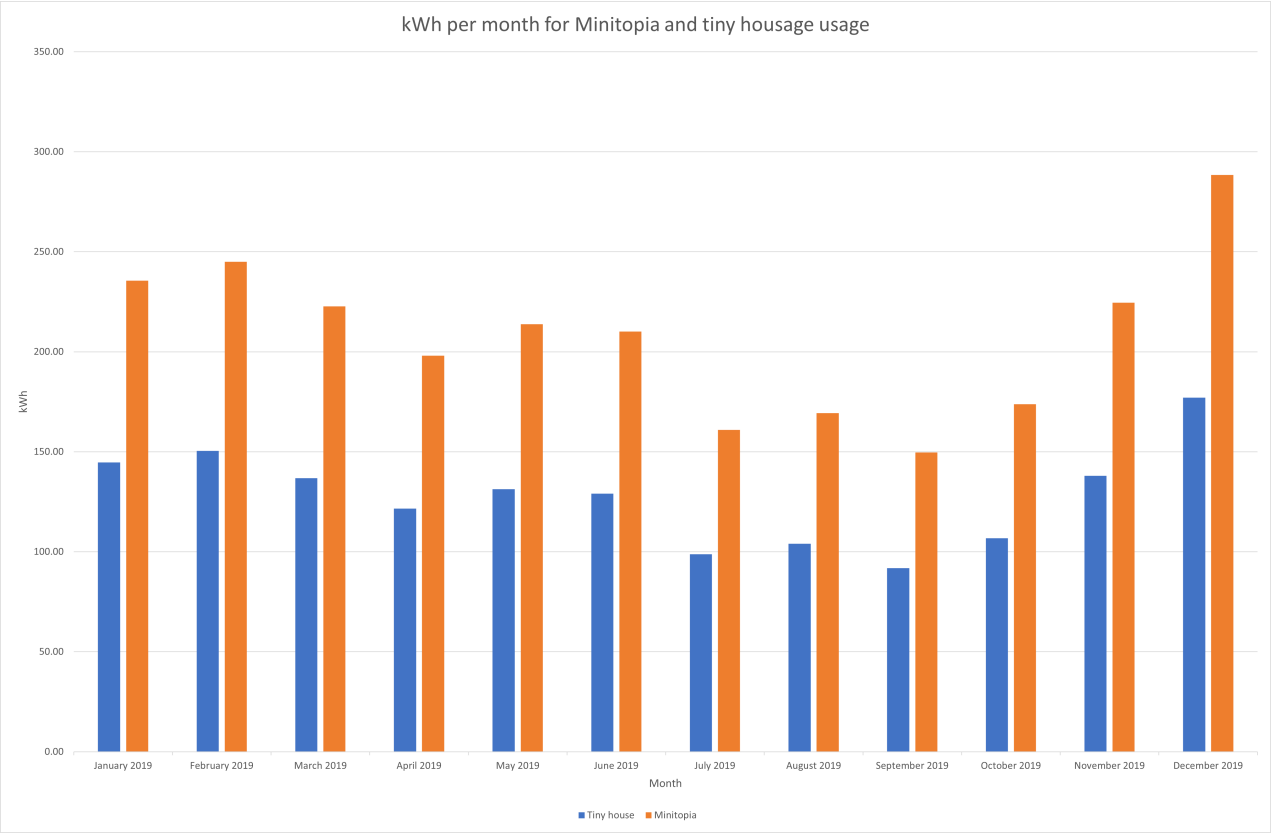

Figure B.2: Average monthly energy usage in kWh per month.

C

Supply and Storage

C.1. Heat Grid Analysis

In Figure C.1 a schematic overview of the heat grid is given. The heat grid consists of three main components: the heat generation by PVT panels, the seasonal heat storage by the heat battery, and the residential heating system.

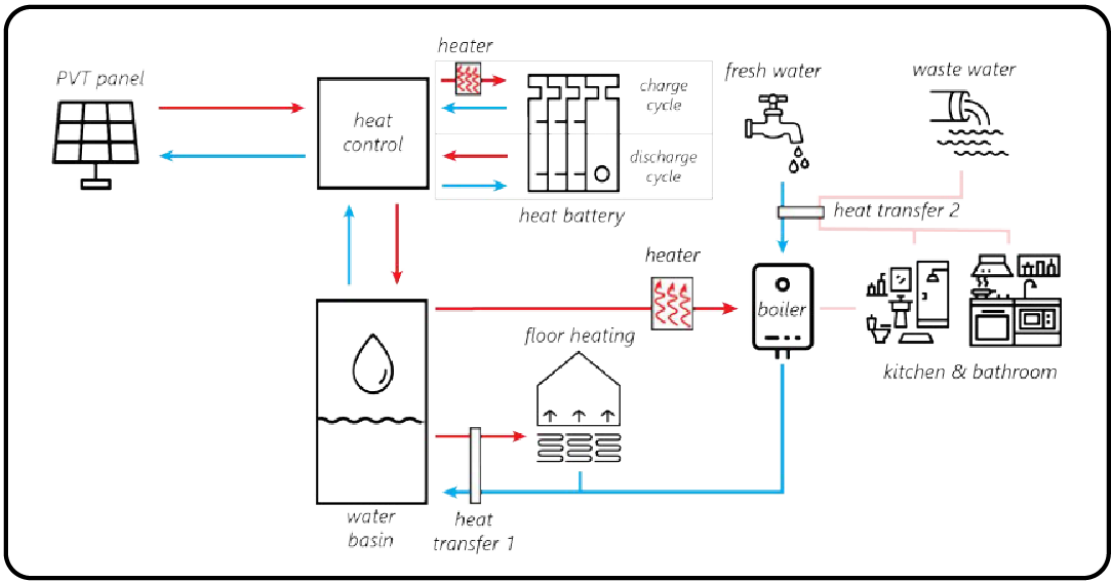

Figure C.1: Schematic overview of the heat grid designed in [5].

PVT panels make use of solar energy in two different ways at the same time by combining PV technology with that of a sun boiler. Similar to a standard PV the PVT panels convert solar irradiance into electrical energy through the photovoltaic effect, which is both a physical and chemical phenomenon using photons to create a flow of electrons. Additionally, PVT's are able to capture the heat of the sun by transferring it into the fluid that runs through the panel. This process has three advantages over the use of PV's in combination with electric heating. The first advantage being that one panel can generate both electricity and capture heat while taking up a similar amount of space as a standard PV. Secondly, capturing and storing energy in heat for heating purposes is a much more efficient process compared to generating electrical energy with PV's to store it in a battery to convert it into heat by an electrical boiler subsequently. Finally, the fluid in the panel is heated by extracting the heat out of the panel itself, cooling the panel, which is advantageous for the efficiency of the photovoltaic system as this decreases when the temperature rises.
When the fluid -in this case water- has extracted the heat, the warm water is transferred through copper insulated pipes to either the heat battery or the residential heating system. The chosen heat battery is

being developed by TNO for residential purposes and is planned to become available on the market in 2022 [60]. The use of such a heat battery enables the system to cover seasonal fluctuations in temperature. This way, the PVT panels can capture a lot of solar heat in the summer and store it in the heat battery until it is needed in the colder winter months.
When heat is needed inside, either the PVT's, or the heat battery can deliver warm water to the residential heating system within each of the tuni. Each system has its own basin. The water of this basin can be used for either floor heating or warm tap water. As the water in the basin is already warm, it can be used for floor heating directly. Tap water must be at least 60 °C, so an electrical boiler is used to provide the required additional energy to heat the tap water. This supplementary energy accounted for $1700kWh$ per day on average in the demand calculations in Section 3.1. Finally, the residential heating system also contains a wastewater heat recovery system which reuses heat of old tap water to heat new water coming into the boiler, resulting in fewer losses. This heat grid is assumed to be operating on one large heat pump, which is powered by the PVT panels' electrical energy, which will be further explained now.

When reviewing the system, a major discrepancy has been found in the calculations of the energy demand in [5]. An initial calculation was done in order to establish the needed PVT panel area per house based on the heat needed per residence, which was calculated to be $3.08m^2$ per tunus. Then, a second calculation was done, which established that $3.2m^2$ of PVT panel area per tunus was required to power the heat pump of the system. The decision was then made to use two $2m^2$ PVT panels per tunus which would suffice for both heat demand and energy demand for the circulation system. However, in further calculations, all electricity generated by these panels was considered to be available for other energy purposes even though the more significant fraction ought to be used for the heat pump. To avert this duplicate of energy use without redesigning the heat grid, as this is out of scope, the following is considered. A total of 19 PVT panels of $2m^2$ will be used $(12 * 3.08m^2 = 36.96m^2)$ and are assumed to be sufficient for generating both heat for all 12 tuni and the energy needed for the heat grid to function correctly. The PVT's can be placed in a central area near the heat battery and the entire heat grid is considered as an isolated system, disconnected from the electricity grid. A basic schematic of the heat grid construction that will be implemented in this design is shown in Figure C.2.

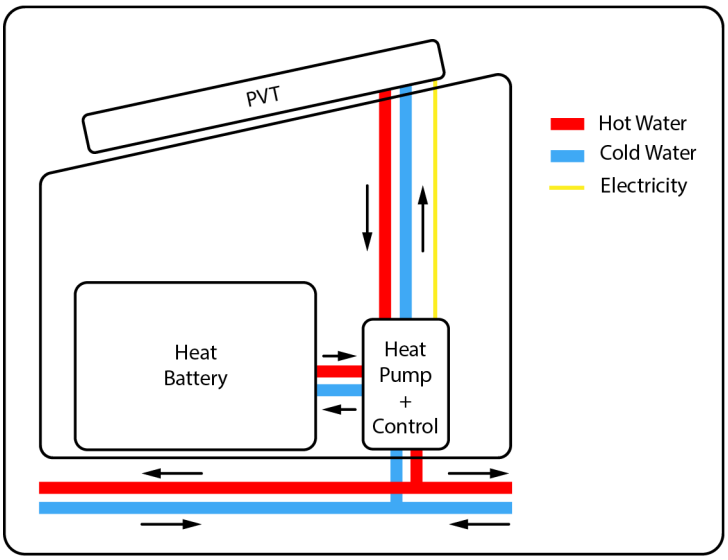

Figure C.2: Schematic overview of the heat grid construction implemented in current design.

C.2. PV Panel Performance Analysis

In the Netherlands, the optimal orientation is towards the south at a tilt of $37°$ [61]. In [62] it is found that as long as the panels are oriented within $20°$ towards the south at a tilt of $30°$ to $40°$ orientation losses are easily kept under 5%. The roofs of the tuni have a slope of $30°$ on which all panels can be placed towards the south relatively well, and thus a maximum loss of 4% throughout the year is

assumed as the panels will remain stationary and do not follow the sun's orbit. As briefly discussed before, the temperature of the solar cells influences the efficiency as well. Most solar cells function best at a temperature of approximately 25°C and decrease in efficiency when the temperature increases. The panel's temperature not only depends on ambient temperature, but also on factors like radiation strength, wind, and precipitation. In [63] research is done on the influence of temperature on solar panel efficiency throughout the year. Results indicate a loss of 6.4% and 7.2% in German residences, however sloped residences in hotter countries like Italy indicate a loss of 5.5%. Based on the fact that the Dutch climate is colder and the solar panels will be put on inclined roofs, a loss of 5% is assumed. A major cause of inefficiencies for solar panels in an urban environment is losses due to shadows of surrounding buildings. However, as the community is built on the roof of a high-rise building, this is less of a problem. The assumption is made that the high rise is high enough that no other buildings can block out the sun, and so the shadow losses are assumed to be zero in this case. Besides zero shadow losses, it has been decided to disregard losses due to snow and dust as well as both have little influence on a high rise in a Dutch city.
Finally, the attenuation of the power output over time plays an important role in the panels' efficiency throughout the years. In [27] the attenuation after one year and the degradation factor for the following 24 years can be found. From this, the losses by degradation are calculated to be

$$\frac{2\% + (98\% - 90.8\%)}{2} = 4.6\% \tag{C.1}$$

The total additional losses of the PV system are thus as follows.

Orientation/Tilt Loss	4%
Temperature Loss	5%
Degradation Loss	4.6%
Resulting Efficiency	87%

C.3. KNMI weather data usage

The data set from the KNMI weather station in Rotterdam [36] contains hourly measurements of the following weather aspects:

- Irradiance: average global horizontal irradiance (GHI) $[W/m^2]$.
- T_ambient: average ambient temperature measured at 1.5 m above the ground.
- T_ground: the average ground temperature at 10 cm above the ground.
- Wind: average wind speed at 10 m above the ground.
- Cloud: cloud coverage in eighths of the visible sky area where 0 is clear-sky, and 8 is a completely obscured sky.
- Pressure: air pressure at the measurement station in Pascal.
- Rainfall: rainfall at the measurement station in mm/hr.

As a selection was already made for the losses of the PV panels and the wind turbine in Section 4.1.2 and **??**, the only data which was used for the model was the irradiance in $[W/m^2]$ and the average wind speed in m/s. The values for these two weather aspects are measured every hour over a whole year. The measurements are also averaged over the last 30 years, starting from January 1991 until April 2021 (when the file was downloaded).

To correctly gather hourly data, the hourly measurements of each day are averaged for each month, resulting in an average hourly model for a day in each month. This model thus contains average hourly irradiation and wind speed over a day for each month. For the PV panel, the energy generation per square meter is calculated by multiplying the irradiation per square meter with the module efficiency of the PV panels mentioned in the datasheet [27] as well as the losses elaborated in Section 4.1.2.

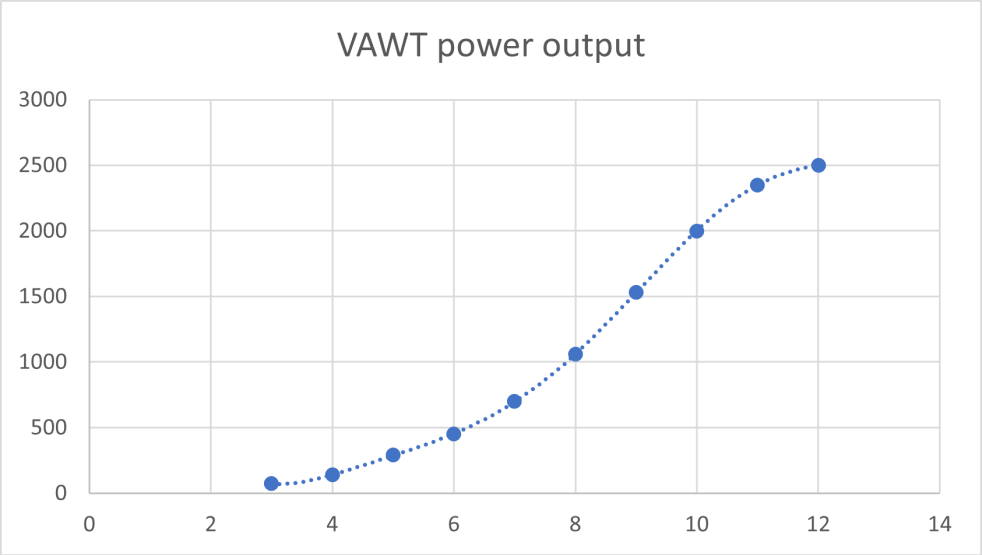

Figure C.3: The power output of the Aeolos-V 2 kW wind turbine for the windspeed.

For the VAWT's, no losses were available in the datasheet and only the power curve in the datasheet is used shown in the datasheet [58]. There are only 12 integer wind speeds shown, hence a polynomial approximation had to be made. Using the highest order approximation available in Excel (6th order), a formula was created to calculate the output power for every wind speed. This formula is shown in Equation (C.2), where P is the output power in W and v the average wind speed in m/s. The power curve is shown in Figure C.3 for wind speeds up to 12 m/s.

$$P = 0.0725 * v^6 - 3.3441 * v^5 + 60.575 * v^4 - 551.26 * v^3 + 2689.8 * v^2 - 6598.3 * v + 6399 \quad \text{(C.2)}$$

C.4. Other supply model results

The model of the s in combination with the daily demand for each month resulted in 6 VAWTs and 3 modules of the selected PV panel, resulting in a total of 36 modules, or 61.2 m^2 PV panel. The monthly generation and demand have also been shown for the selected amount of each RES. Another analysis was done to see whether the generation could have been done with only one form of the two selected forms of RES, hence checking if only generation using VAWT's or PV panels would have been possible. As can be seen from Table C.1, the amount of VAWT's needed in the summer months and the amount of PV panels in the winter months is extremely large and not suited for the community on the roof of a high-rise building in Rotterdam. Furthermore, the hourly generation in December and July, which are the highest and lowest demand respectively, are shown in Figure C.4 and Figure C.5.

Table C.1: Amount of VAWT's and PV panels needed in case of only one RES method.

Month	**Only VAWT**	**Only PV** $[m^2]$
January	8	448.37
February	9	261.60
March	9	117.99
April	14	66.28
May	16	55.70
June	17	53.27
July	15	41.74
August	18	51.96
September	16	69.62
October	10	135.67
November	11	379.67
December	9	738.88

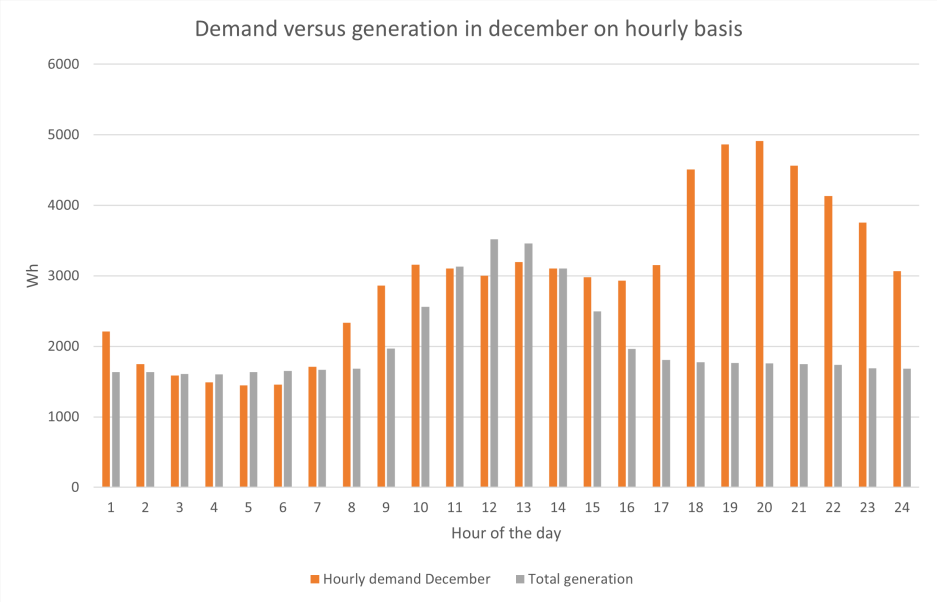

Figure C.4: Hourly generation versus demand in the month december.

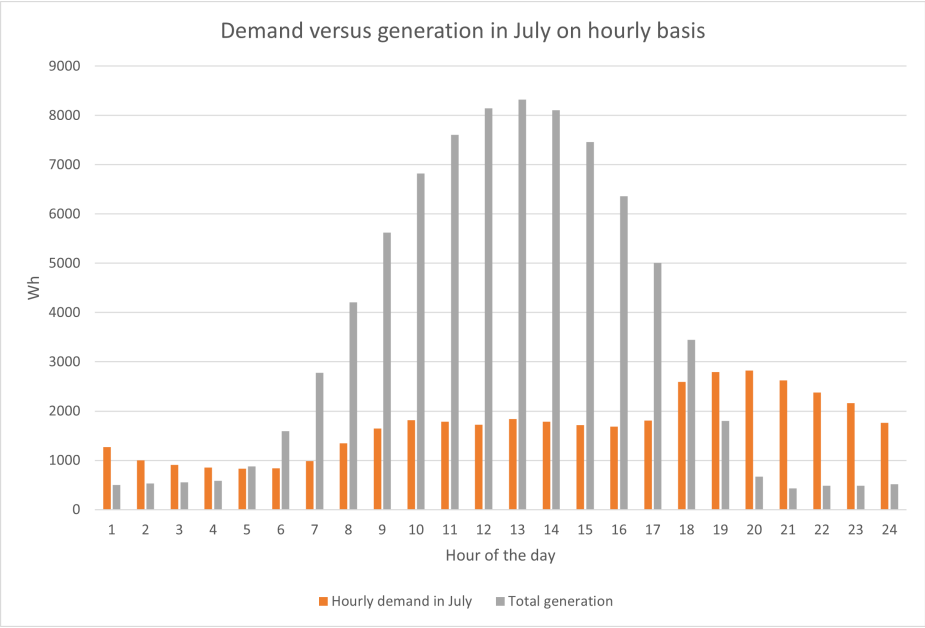

Figure C.5: Hourly generation versus demand in the month july.

C.5. ESS Comparison

In Table C.2, the compared criteria and results for each of the considered ESSs are shown.

Table C.2: Comparison table of several types of ESS.

Type	Energy [$/kWh]	Power [$/kW]	Response Time	System RTE [%]	Life Cycle [yrs]	Advantages	Disadvantages
Lead Acid Battery	559	2194	1 sec	72	3-10	- High energy density -Decent power density -Decent response time -Cheap	- Medium efficiency - Very DoD sensitive - Very environment sensitive - Short life cycle - High charge time
Li-ion Battery	469	1867	1 sec	86	10-15	- High energy density -Decent power density -Efficient -Decent response time -Cheap -Low discharge rate (5%/mount)	- DoD sensitive - Relatively short life cycle
Supercapacitors	72000	300	16 ms	92	16	- High peak power output - High power density - Fast response - Efficient - Reliable - Do not heat up	- Low energy density - Expensive - Bulky/heavy - High discharge rate (40%/day)
High speed Flywheel	11520	2880	250 ms	86	>20	- Relatively high power output - High power density - Fast response - Efficient - Reliable - Low maintenance	-High initial costs - High discharge rate (20%/hour) - Idling losses (<2%)
Hydrogen FC	25	1100-2600	250 sec	21-46	4.6	- High energy density by weight - Relatively cheap - High flexibility (large storage, relatively easy transport)	- Very inefficient - Storage needs to be pressurised or cooled or both or put into metal hydrides

C.6. Centralised model setup and flowchart

The centralised storage model uses the hourly demand and generation to keep track of an energy balance, where the battery will fill in the surpluses and deficits. By adding a number of the previously selected ESS, the effect of the efficiency of the battery and limited capacity can be modeled for the energy balance to determine the availability. Below, the method to obtain the hourly usage for each month is explained, as well as the hourly generation for each month.

The hourly usage of a tiny house for each month is calculated by scaling the previously determined average hourly demand in Table B.11 with the daily energy usage of each month as shown in Table 3.4. This results in an hourly usage of the tiny house community for an average day of each month. For the generation, an hourly model for each month is made by averaging the wind speeds and solar irradiation for every hour for the whole month, creating an hourly solar and wind generation for an average day for each month.

The battery is modelled with an integer multiple of the capacity of the selected battery, $19.3kWh$, with an RTE of 96% and a minimum SoC of 10% based on [40]. As only hourly data is available, an energy balance is kept between the generation and storage, where a positive difference between generation and demand leads to the battery being charged. A negative difference will thus cause the battery to be discharged. Using this energy balance, the SoC of the battery can be calculated and tracked throughout a whole year. A flowchart of this model is shown in Figure C.6.

Using the SoC calculation, the time when the battery is charged by the RES's can be determined. The availability is calculated as the hours of not needing energy supply from the main grid divided by the total hours. First, the difference between the hours in which the battery and generation can deliver the demand and the hours in which the battery is charged by the RESs and the demand is drawn from the main grid is calculated. This difference is then divided by the number of hours in a year, resulting in the total availability.

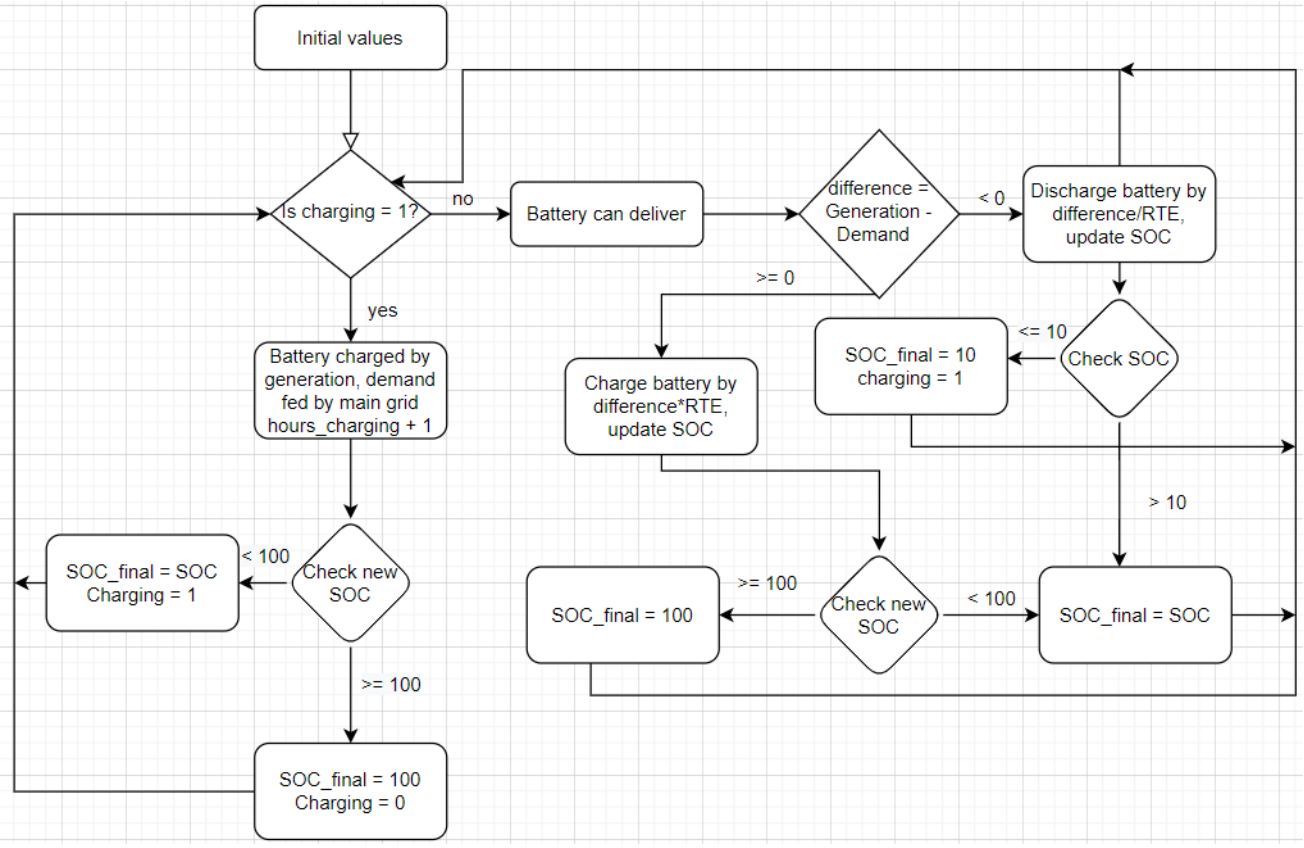

Figure C.6: Flowchart of the centralised storage model.

The flowchart shows how the model works precisely and how the SoC and charging time of the battery are calculated. In general, a surplus in generation will charge the battery multiplied with the RTE. If the battery is already full, the excess energy will be delivered back to the main grid. If there is a deficit of energy, the battery will supply this deficit divided by the RTE. If the SoC reaches 10%, the battery will go into charging mode. The generation will be directed solely to the battery in charging mode, and the main grid will supply the demand. When the SoC of the battery is at 100% again, the charging mode is turned off, and the battery, together with the generation, can once again supply the demand. In case of overproduction, the excess energy will be delivered to the main grid. The design choice to solely use the RES's for charging the battery is made to limit the power flow in the design. An advantage to let the main grid charge the battery is that the availability would be a lot higher, defeating the purpose of designing an optimal amount of generation and storage.

C.7. Distributed model setup and flowchart

The distributed storage model uses the hourly demand and generation to keep track of an energy balance, where the surpluses and deficits will be filled in by either the home or central battery. This model is more distributed than the centralised version, as both a central battery and a home battery are used. The home battery is connected to the PV panels and will primarily supply the demand of a tiny house. The central battery is connected to the VAWT's and tunect, primarily supplying TUNECT. By adding a number of either battery, the effect of the efficiency of the batteries as well as limited capacity can be modeled for the energy balance in order to determine the availability. The hourly demand and generation have been obtained in the same way as explained in Appendix C.6.

The central battery is modelled with an integer multiple of the capacity of the selected battery, $19.3kWh$, with an RTE of 96% and a minimum SoC of 10%. The home battery is an integer multiple of $3kWh$ capacity, with an RTE of 98% and a minimum SoC of 0%. The same number of home batteries will be installed in each house to have the same local output power in each house. As there are two SoCs which need to be tracked, two flowcharts have been made. The first flowchart shown in Figure C.7 shows the calculation of the SoC for the central batteries. The second flowchart shown in Figure C.8 shows the calculation of the SoC for the home batteries of one tiny house. As each house consumes the same average demand each month, the SoC of a set of home batteries in one house represents the SoC of the home batteries in all of the houses.

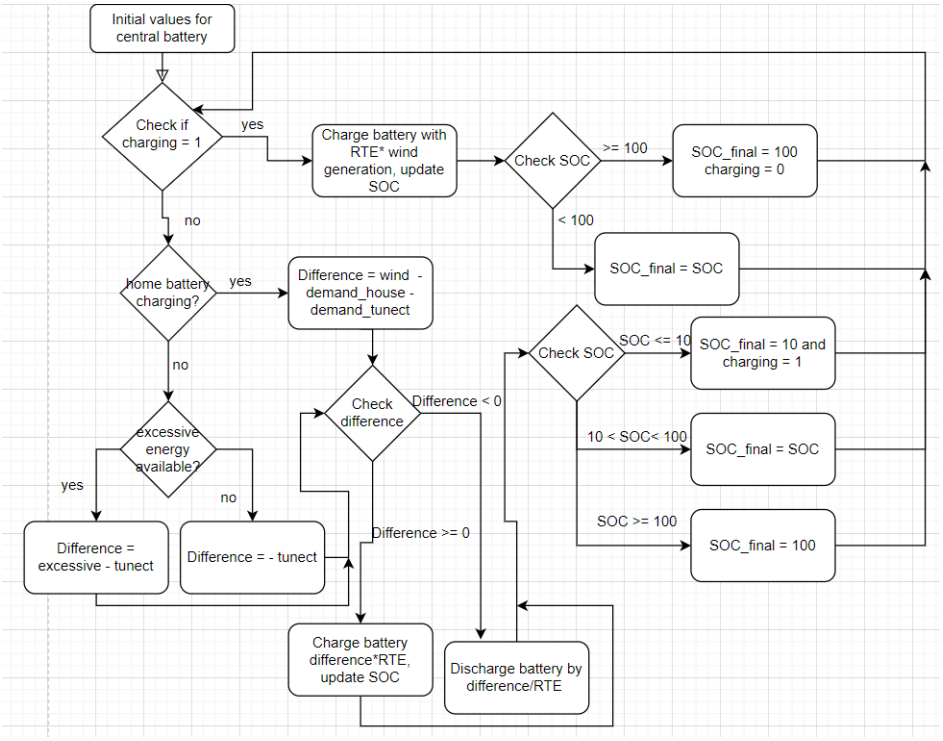

Figure C.7: Flowchart of the central batteries for the distributed storage model.

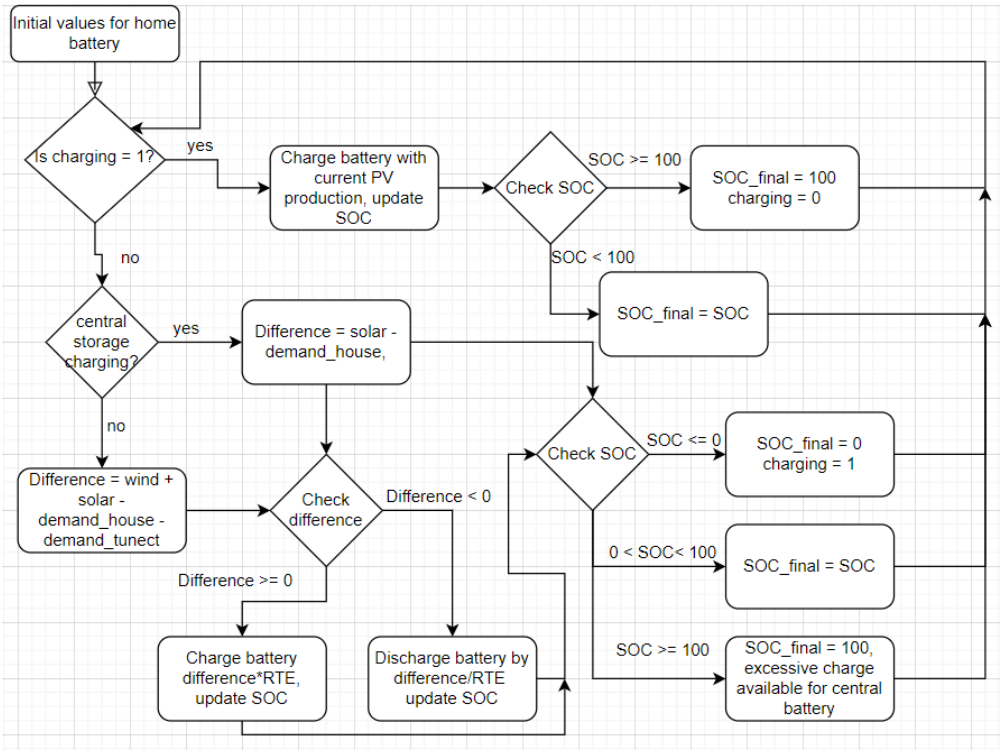

Figure C.8: Flowchart of a home battery for the distributed storage model.

The flowcharts show how the model works and the SoC is calculated, and also how the batteries interact with each other. In general, the home battery and PV panel supply the tiny house demand, and the wind turbine and central battery supply the tunect usage while being available for backup energy for the houses. If the home battery is full, the excess energy of the PV panels will charge the central battery. If the home battery is empty, it is charged with the PV panel production. The house demand is then supplied by the VAWT production as well as the central battery. If the central battery is full, excess wind energy can supply the demand of the tiny houses and charge the home battery. If the central battery is charging, all the generation of the VAWT will be directed to the central battery. If both batteries are charging, the production of the RES's will charge the batteries, while the main grid supplies the demand of the community. If both batteries are full, excess energy will be delivered back to the main grid. The design choice to solely use the RES's for charging the battery is made to limit the power flow in the design. An advantage to let the main grid charge the battery is that the availability would be a lot higher, defeating the purpose of designing an optimal amount of generation and storage.

C.8. Centralised model graphs

In the following graphs, the SoC is shown for February, using 4 of the selected central batteries, as well as the determined demand and generation. The other months follow either a similar pattern or a repetitive saw-tooth pattern, which will not be shown here.

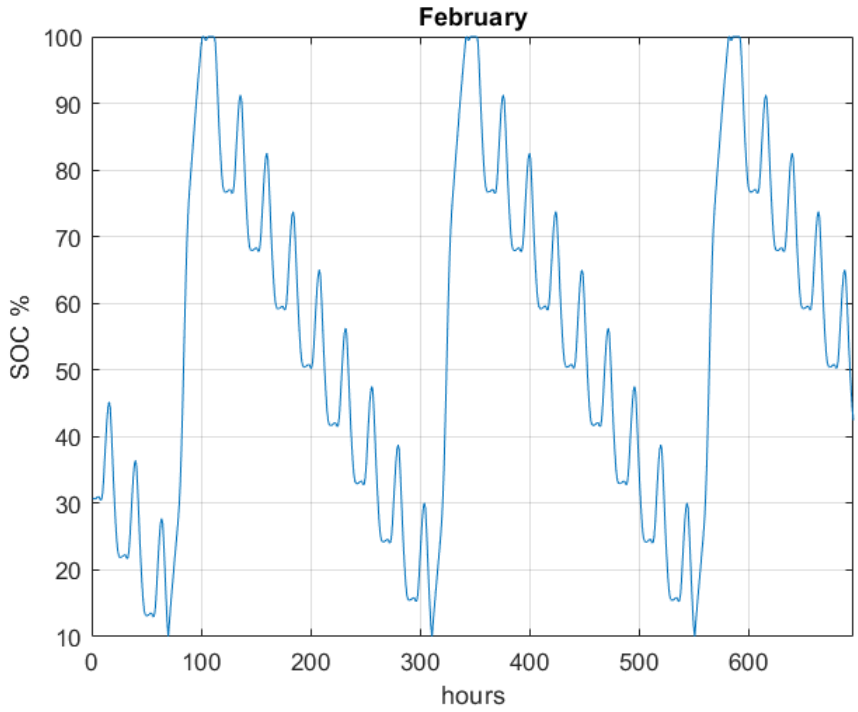

Figure C.9: SOC throughout the month February.

C.9. Distributed model graphs

In the following graphs, the SoC is shown for February, using 2 of the selected central batteries and 2 of the selected home batteries per house (hence 24 in total), as well as the determined demand and generation. The other months follow either a similar pattern or a repetitive saw-tooth pattern, which will not be shown here.

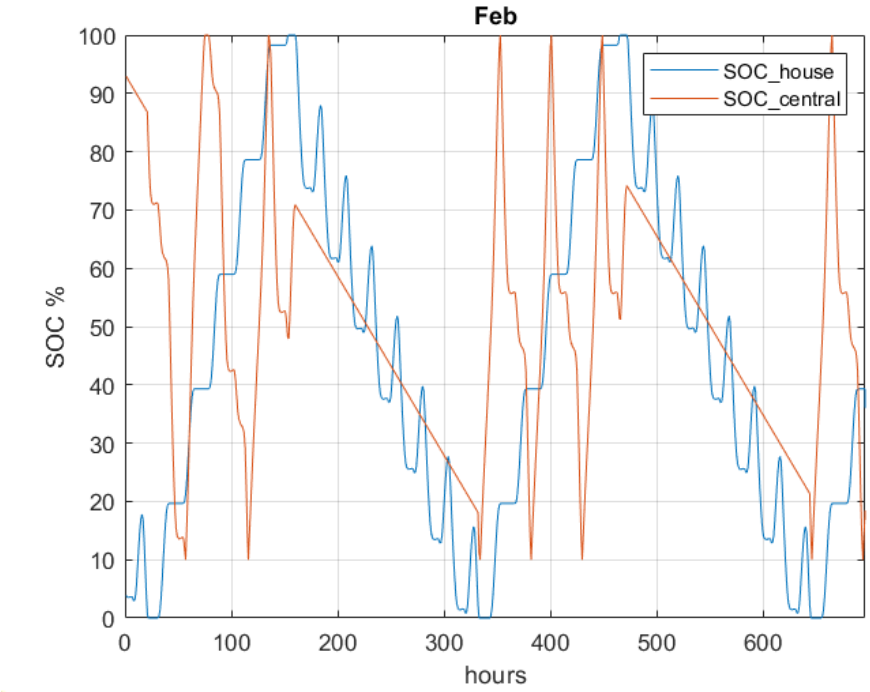

Figure C.10: SOC of both the home and central batteries for February.

C.10. Battery System Comparison

In Table C.3, the technical, social and economical aspects of both the centralised and distributed model are compared.

Table C.3: Analysis on several aspects on both battery systems.

Comparison	Central	Partly distributed
T1: design traits	Simplicity, central SOC tracking and one-way power flow	Complex design, tracking of SOC of both central and home batteries. More converters needed, which is against RQS.DCG.3 Flexibility due to bidirectional power flow, but unnecessary oversize in capacity.
T2: efficiency	Battery efficiency 2% lower and cable losses are roughly estimated to be 4 times higher due to longer distances	Less cable losses, limiting solar supply efficiency due to home battery losses.
T3: reliability	If the central connection fails, whole network down.	Can rely on home battery and solar production in case of central fault.
S1: safety	Batteries are in a central place, limiting fire/explosion danger for the houses. Large batteries are present and compact, damage to other nearby sources/storages may be larger.	Batteries in homes of users, presenting a chance of fire hazard in homes.
S2: Own usage	Users may be dissatisfied if power production on their own house is used elsewhere.	The usage in a home will be supplied by its own battery and solar panel, this could make the users investment more satisfying.
E1: capital	4 central batteries are relatively cheap for the whole community. As a central system is simpler, the initial cost in control, converters and wiring will be lower.	Looking at only batteries and the necessary converters, a combination of central and home batteries will be three times more expensive. More wiring, converters, battery management and general control software and hardware is needed.
E2: maintenance	Damage of the larger batteries will result in higher replacement costs of the batteries and potentially nearby electronics.	Replacement of home battery will be cheaper, however much more other hardware is needed which can cause higher failure rate.
E3: operational	Due to simplicity, the operational costs will be low. How much lower is hard to estimate and for either system operational costs are expected to be low.	A more complex control system is required, this leads to higher operational costs due to more complex software updates. The more complex control can make the whole system more efficient, making the energy costs lower. However this efficiency increase is not guaranteed, hence operational costs can vary.

D

Topology

D.1. Microgrid Topology Analysis

Physical Topology

The radial topology consists of a central generation point with power lines connecting to the demand. In case of main grid connection, the power flow is unidirectional towards the loads, while the battery is charging. The advantages can be summarised to be a simple design, enabling power sharing from one load to the other and its common application for LVDC (< 1500 VDC) loads. The disadvantages are that one fault can affect all of the users and the grid is not flexible to handle the fault [55].
The ring topology uses a ring shaped voltage bus, where all the loads, storage and generation methods are connected to this ring. In case of main grid connection, the operation remains the same as power flow can still be bidirectional. The main advantages are bidirectional power flow throughout the ring, fault isolation with continuity of service (except the faulty location) and thus ensuring higher reliability. The main disadvantage is that two faults are able to completely isolate the loads from power, as their separate isolation can cause the other loads to become disconnected as well [55].

Bus Topology

A single-bus voltage bus uses one large node where all of the loads, generation and storage are connected to. The main advantage is that the microgrid voltage can easily be regulated and an increase in flexibility of the system as it can easily be expanded. The disadvantages consist of uncontrollable voltage of the grid as the SoC of the battery determines this voltage, as well as unregulated battery charging. As all of the converters are operating in parallel, the current can start to circulate and loads can be unevenly balanced in their demand. [53]
A multi-bus voltage bus uses parallel or series connected microgrids, and in our case sometimes nanogrids. This configuration facilitates the isolation of faults independent of the rest of the system, as well as enabling power sharing between the micro- or nanogrids [53].
Reconfigurable bus topology consists of more complex multi-bus topologies, enables even greater amounts of power sharing and interconnectivity. However, the control and operation of such a complex bus is quite difficult [53].

D.2. Converter Control Analysis

VAWT

The control strategy proposed in [64] will be considered. As the exact wind turbine parameters are as of yet unknown, the generic Perturb and Observe MPPT algorithm will be used, which is able to handle large wind speed variations and is able to handle the voltage level of our microgrid. In further research, the exact turbine parameters from the VAWT [58] could be retrieved from contact with Aeolos. This could enable the implementation of the more complex control algorithms with possibly more efficient and accurate MPPT.

Batteries
The control methods presented in [65] provide great insight into the available control methods for the bidirectional DC-DC converter for the batteries. As with the solar MPPT algorithms, a distinction can be made between classical control algorithms (PID and phase shift) and more supervisory control algorithms (Model predictive, artificial neural network, fuzzy logic). In [65], a summary is also given for each of the control methods. For the microgrid, large fluctuations in power can occur as RESs are per definition unreliable and have large fluctuations in power generation. Another requirement is that the efficiency should be as high as possible, to optimally use the generated energy of the RESs. This leads to dual phase-shift to be the best control algorithm, as it incorporates high efficiency as well as high dynamics. A suggestion made by the article is to use such a classical control algorithm such as Proportional Integral (PI) inside a supervisory loop. A possible control algorithm could thus be a neural network in combination with dual phase shift. As a control system is designed by the CNS subgroup, it could be possible to implement a second neural network on their control unit. The main disadvantage of large amounts of computations can be mitigated as the computational power is available. However training data will be more difficult to obtain.

48V Sockets
For this converter, no extra control algorithm is needed, as it only is a load, with no optimization possible. The buck conversion itself does need to be done with control, where a standard PID converter is recommended (which is included with most commercially available converters nowadays).

400V Sockets
As for the low power converter, no extra control algorithm is necessary for optimization. As this is a 1:1 converter, a buck-boost converter with PID block will be recommended in case of higher bus voltage due to generation or lower bus voltage due to demand.

PV System
In [66], the current MPPT algorithms for PV panels are discussed. The categories can be divided into conventional, artificial intelligence and biologically inspired. The conventional algorithms are quite effective during unvarying solar irradation and can thus be used when there are often either no clouds or the sky is completely clouded. In the Netherlands however, the solar irradiance can vary a lot due to cloudy weather, thus a look is taken to the more complex algorithms like artificial intelligence methods and biologically inspired ones as well. In [66], several key criteria are listed for the MPPT algorithms: tracking speed, tracking accuracy, implementation complexity, dynamic response, periodic tuning, steady state oscillations. The biologically inspired methods come out on top of all criteria except the more complex implementation in comparison to the other methods. Further research could be done to see whether the improved performance of the biologically inspired MPPT algorithm is worth the complex implementation. Thus for later research, biologically inspired methods could increase the power extraction under varying irradiance a lot.

D.3. Wiring

In this section, the calculations for losses and the resulting wiring costs are shown in Table D.1

Table D.1: Table with all wire specifications of entire system.

Type	Max P [W]	Voltage [V]	Max C [I]	Area [mm^2]	Max length [m]	Total length [m]	Max drop [V]	Max loss [%]	Costs [€]
Main ring	61092	400	152.73	50	35	35	3.78	0.94	437
Battery	30546	400	76.37	16	6	12	1.01	0.25	30
VAWT	2600	400	6.5	1.5	30	155	4.6	1.15	124
Tunect	4142	400	10.36	1.5	5	10	1.22	0.30	6
Tunus	4747	400	11.87	1.5	22	264	6.16	1.54	211
PV	1900	111.9	16.98	2.5	10	300	2.4	2.14	426
High	4747	400	11.87	1.5	4	72	1.12	0.28	58
Low	1000	48	20.83	6	15	516	1.84	3.83	1125
Total						1304			2417

Equation (D.1) is used to calculate the maximum voltage drop in Table D.1, L is taken to be the max possible length to calculate maximum voltage drop.

$$\Delta V = 2(\rho \frac{L}{A} \cos\phi + \lambda L \sin\phi) * I \tag{D.1}$$

ΔV = Voltage drop
ρ = resistivity [$\Omega * mm^2/m$] is taken to be 0.0175 for copper at 30 °C
L = wire length
A = cross-section of wire [mm^2]
$\cos\phi$ = 1 for DC
λ = reactance coefficient
$\sin\phi$ = 0 for DC
I = current [A]

The total length in Table D.1 indicates the total amount of wire needed for the specified connection.

D.4. Stability & Safety

In this section, both the proposed grounding schemes are shown, as well as the proposed standards which could be considered for further developmetn of practical implementation of the proposed grid design.

D.4.1. Grounding

In Figure D.1, the unipolar parallel resistance grounding method is shown. In Figure D.2, the bipolar resistance grounding method is shown.

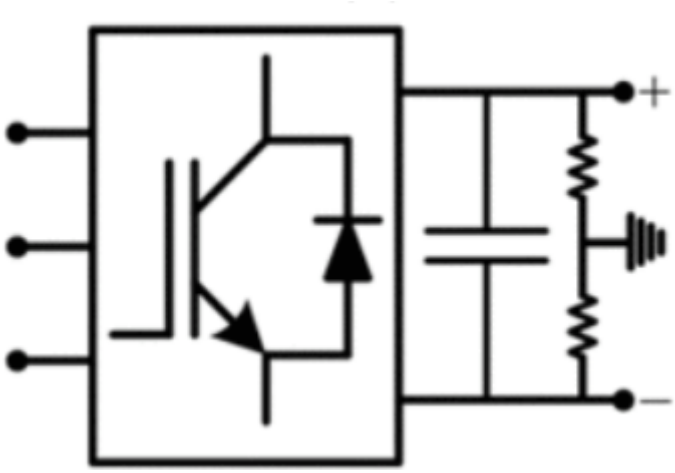

Figure D.1: Unipolar parallel resistance grounding method.

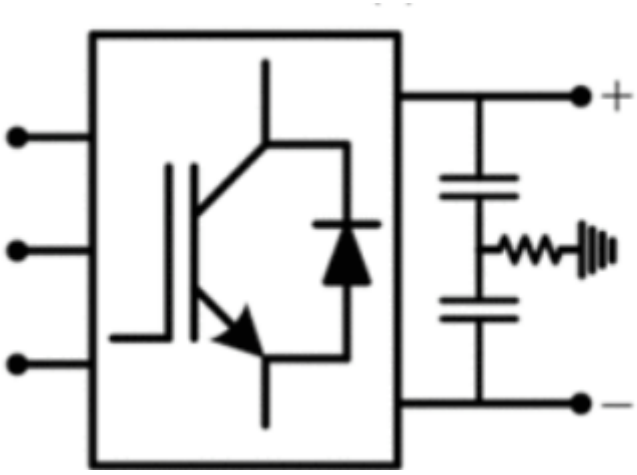

Figure D.2: Bipolar resistance grounding method.

D.4.2. Standards

- IEEE P2030.10 Standard for DC Microgrids for Rural and Remote Electricity Access Applications: Design, operations, and maintenance of a dc microgrid for rural or remote applications. Requirements for providing LVDC and AC power to off-grid loads.
- IEEE DC@home DC use in residential dwellings and a LVDC micro-grid system.
- IEEE 946-2004 Recommended Practise for the Design of DC Power Systems for Stationary Applications IEEE P946 Recommended Practise for the Design of DC Power Systems for Stationary Applications: Recommended practise include lead-acid storage batteries, static battery charg-

ers, and distribution equipment. Guidance for selecting the quantity and types of equipment, the equipment ratings, interconnections, instrumentations, control and protection is also provided.

- IEC SEG 4 Standardization Evaluation Group (SEG) - 4: Standardization of LVDC systems up to 1500V
- SEG 6 Standardization Evaluation Group (SEG) - 6: Rural and developing markets that serve potential huge market needs (notably in Asia and Africa) including networks that may be connected in the future to a traditional / interconnected grid. Facility or campus grids capable of operating in an isolated mode with respect to a large interconnected grid.
- ITU-T L.1202 (2015-04): Methodologies for evaluating the performance of an up to 400 VDC power feeding system and its environmental impact.
- IEC 62040-5-3:2016 Uninterruptible power systems (UPS) – Part 5-3: DC output UPS - Performance and test requirements: DC uninterruptible power systems (DC UPS) that deliver a DC output voltage not exceeding 1500 V.
- IEC TS 62257:2015 Recommendations for renewable energy and hybrid systems for rural electrification: Designed to be used as guidelines and are recommendations for small renewable energy and hybrid systems for rural electrification.
- Part 4-41: Protection for safety – Protection against electric shock Part 4-43: Protection for safety - Protection against overcurrent (buildings) Part 4-44: Protection for safety - Protection against voltage disturbances and electromagnetic disturbances (buildings).

D.5. Cost Analysis

For this cost analysis, product research has been done on the main components of the designed microgrid. As shown in Table D.2, for a part of the components, specific products have been selected. These are mentioned in the table and the sources of the prices are cited. Some other components are selected more generally, either because finding exact products is out of scope, unnecessary or not possible.
A detailed cost analysis on the heat grid is out of scope. Besides the PVT panels and the heat battery, the heat grid is assumed to consist of coppper piping, twelve residential heat pumps and a larger heat pump for overall circulation. For the pricing of the piping is assumed that the overall length of piping is equal to the total length of wire needed to connect the houses, which is 264 m, and pricing can be found at [50], while water pump pricing is based on [67].
The exact cost analysis of the wiring can be found in Table D.1. The price estimation of both the PV converters and the remaining converters is based on prices of relatively similar technology found at [50] and [51]. The category remaining converters consists of a combination of the 48 V socket and 400 V socket DC/DC converters needed for both the twelve tiny houses and tunect. This is a rough estimate as fitting converters could not be found. The estimation of the protection circuitry is based on similar product found at [49] and consists of sensors, protective relays and solid state DC breakers. The amount of modules needed is based on the schematic shown in Figure 5.3. The price indication should be considered a rough estimate. Finally, the PLC group provided a price indication of the required communication circuitry.

Table D.2: Cost analysis on the main hardware required for the microgrid design.

Component	**Product**	**Module amount**	**Price [€/module]**	**Total price**
PV Panel	LG Neon R [68]	36	289	10404
Wind Turbines	Aeolos V 2kW [69]	6	3380	20280
PVT Panel	TripleSolar [70]	19	2140	40660
Battery	BYD HVM 19.3 [71]	4	8290	33160
Heat Battery	TNO Salt Battery [5]	1	7300	7300
Heat Grid	N/A	-	-	18200
Wiring	Prysmian [50]	-	-	2417
PV Converters	N/A	12	400	4800
Wind Turbine Converters	CTC-3k [69]	6	561	3366
Battery Converters	Tame Power 32kW [45]	2	5000	10000
Remaining Converters	N/A	13	700	9100
Protection Circuitry	N/A	-	-	6388
Communication	N/A	-	-	800
Total				166075

E

Design Validation

E.1. Subsystem Models

In this section, the circuit models for each of the subsystems of the simulation in Simulink are explained and shown.

E.1.1. Load model

The demand of a tiny house is modeled using two constant power loads, one for the low power socket and one for the high-power socket, as shown in Figure E.1. The low-power socket uses 846.68 W for the peak demand, and the high-power socket uses 3.9 kW. A voltage meter and a current meter are used to measure the voltage drop and power loss in the wires.

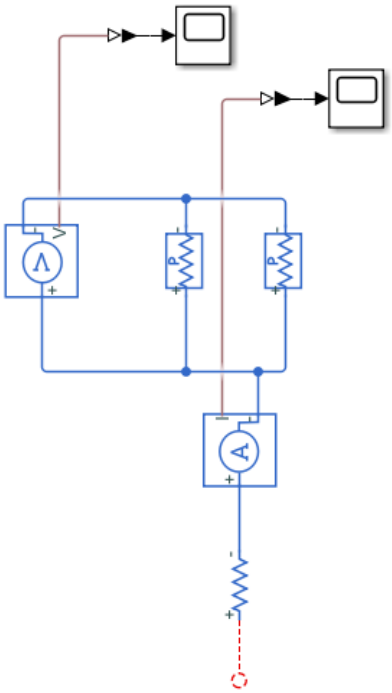

Figure E.1: Model of tiny house or common usage demand in Simulink.

E.1.2. PV panel model

In Figure E.2, the Simulink model of 3 series-connected LG Neon-R modules is shown, which resulted in $128.7VDC$ open-circuit voltage and $10.67A$ short circuit current. A voltage sensor and current sensor are implemented to measure the output over a 1 Ω resistor. The other blocks are the 400 VDC reference voltage, the 1000 W/m^2 irradiance, and lastly, the ground and equation solve block, which needs to be connected to each separate electrical network.

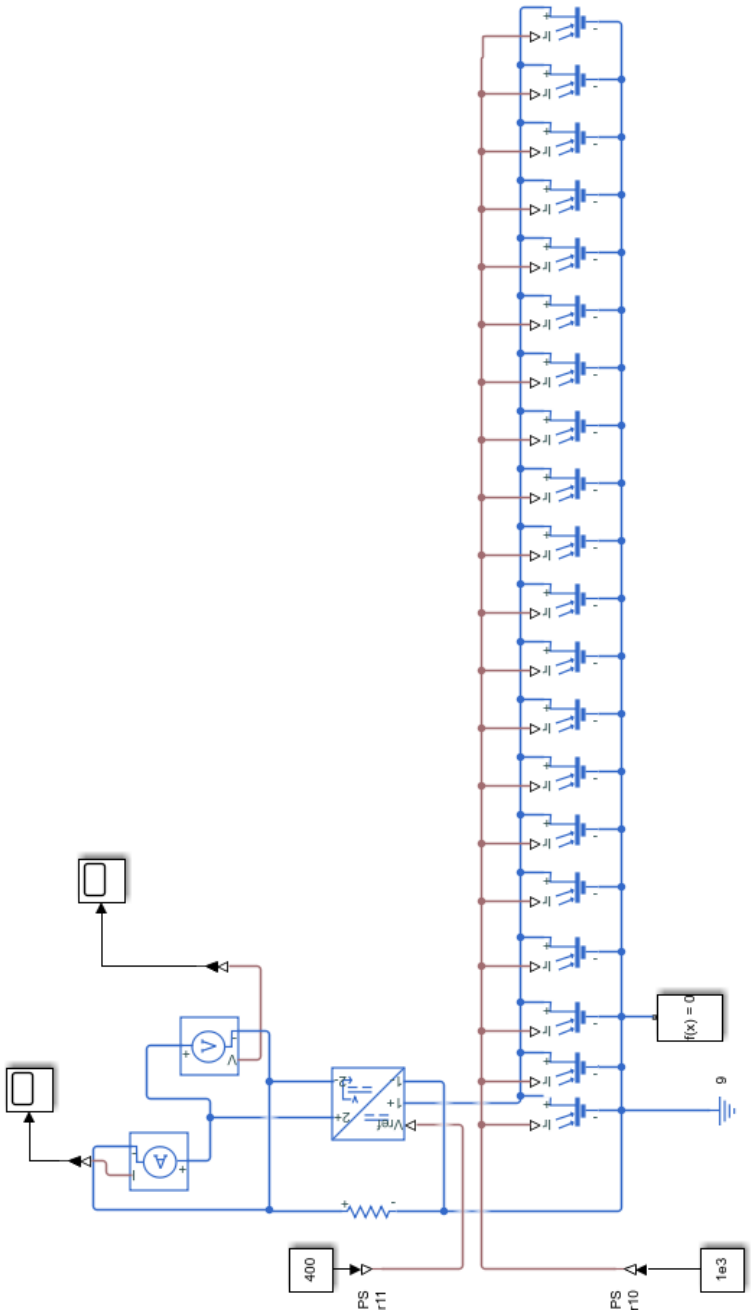

Figure E.2: Equivalent model of 3 series-connected LG Neon-R modules in Simulink.

E.1.3. VAWT model

In Figure E.3, the Simulink model of an Aeolos-V 2 kW VAWT is shown. It uses 2 kW as active power generation rated at 48 VAC. The rectifier is rated at 48 VAC as well, with a power loss of 4% as a positive power loss had to be given as input. A DC-DC converter to 400 VDC is used to connect to the microgrid. A voltage and current sensor are used to measure its output power, which resulted in the expected 2 kW output power. The other blocks are the 400 VDC reference voltage and the ground and equation solve block, which needs to be connected to each separate electrical network.

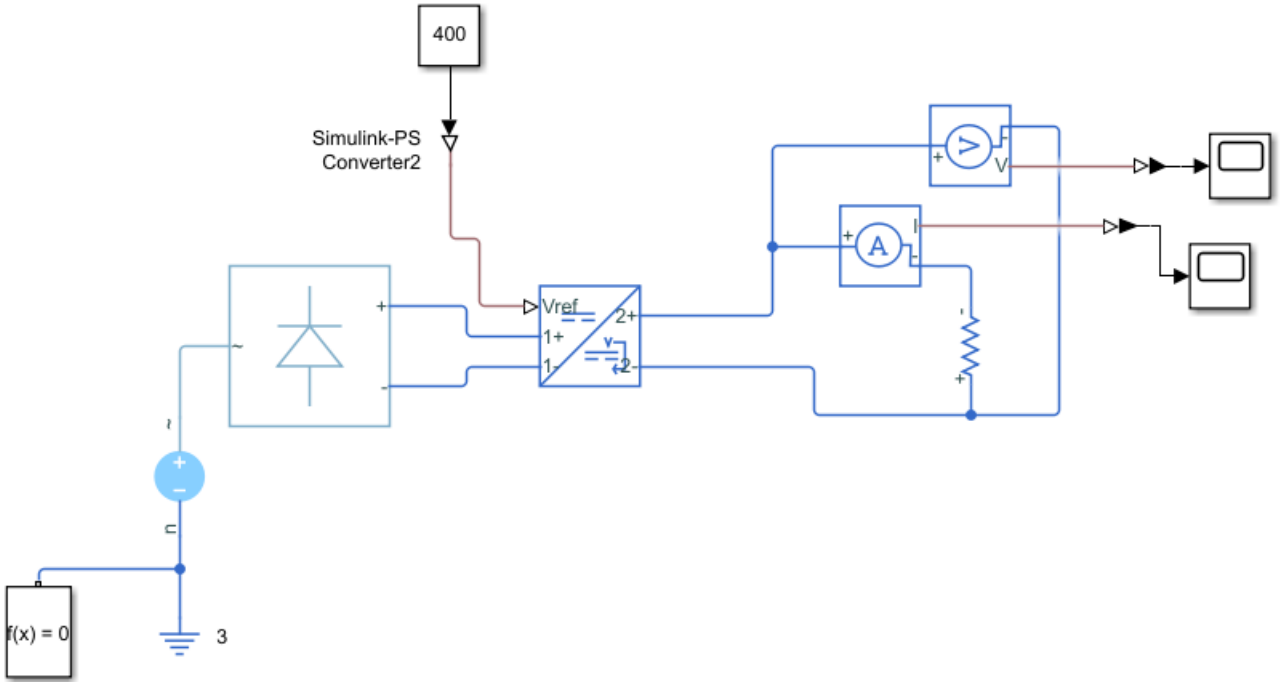

Figure E.3: Equivalent model of an Aeolos-V 2kW VAWT in Simulink.

E.1.4. ESS model

The battery model is shown in Figure E.4, which uses a battery block with the specifications given in [40] and a DC-DC converter to 400 VDC. In addition, a current and voltage sensor is implemented to measure the drawn power from the battery. The other blocks are the 400 VDC reference voltage and the ground and equation solve block, which needs to be connected to each separate electrical network.

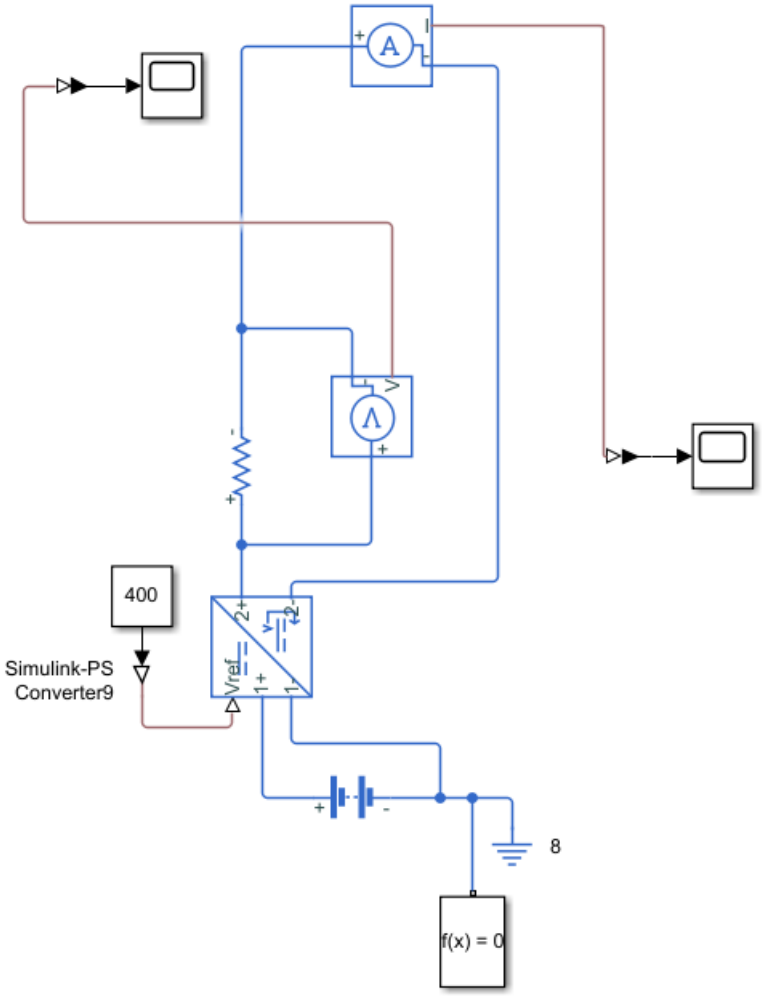

Figure E.4: Equivalent model of two parallel connected BYD HVS 19.3 batteries in Simulink.

E.1.5. Wiring model and calculations

In Table E.1, the resistances [49] and lengths based on Table D.1 are shown. The resulting total resistance, as well as the resistance per wire section, hence per resistor in Simulink, are shown. The total main grid length is 35 meters but is divided over 22 connection points (12 houses, tunect, 6 PV panels, main grid, and 2 batteries), hence each wire section will have a length of 35/22 meters. Two battery sections are used, hence each battery wire section resistance will be divided by 2. There are 6 turbines, hence each wire section will have a length of 155/6 m. Lastly, the wire section resistance is twice the cable resistance to model the resistance of each core of the wire effectively.

Table E.1: Resistor calculation for wiring in Simulink model.

Connection	Resistance per unit length	Length	Resistance	Section length	Per section
Microgrid section	0.386 $m\Omega/m$	35 m	13.51 $m\Omega$	35/22 m	1.228 $m\Omega$
Battery	1.21 $m\Omega/m$	12 m	14.52 $m\Omega$	12/2 m	14.52 $m\Omega$
Main grid	1.21 $m\Omega/m$	1 m	1.21 $m\Omega$	1 m	2.42 $m\Omega$
Wind turbine	13.3 $m\Omega/m$	155 m	2061.5	155/6 m $m\Omega$	687.17 $m\Omega$
Tiny house	13.3 $m\Omega/m$	264 m	3511.2 $m\Omega$	264/12 m	585.2 $m\Omega$
Tunect	13.3 $m\Omega/m$	5 m	$66.5m\Omega$	5 m	$133m\Omega$

E.2. Simulink grid layout

The connection of all the equivalent subsystems (load, generation, batteries, main grid and wires), being connected at the same time is shown in Figure E.5.

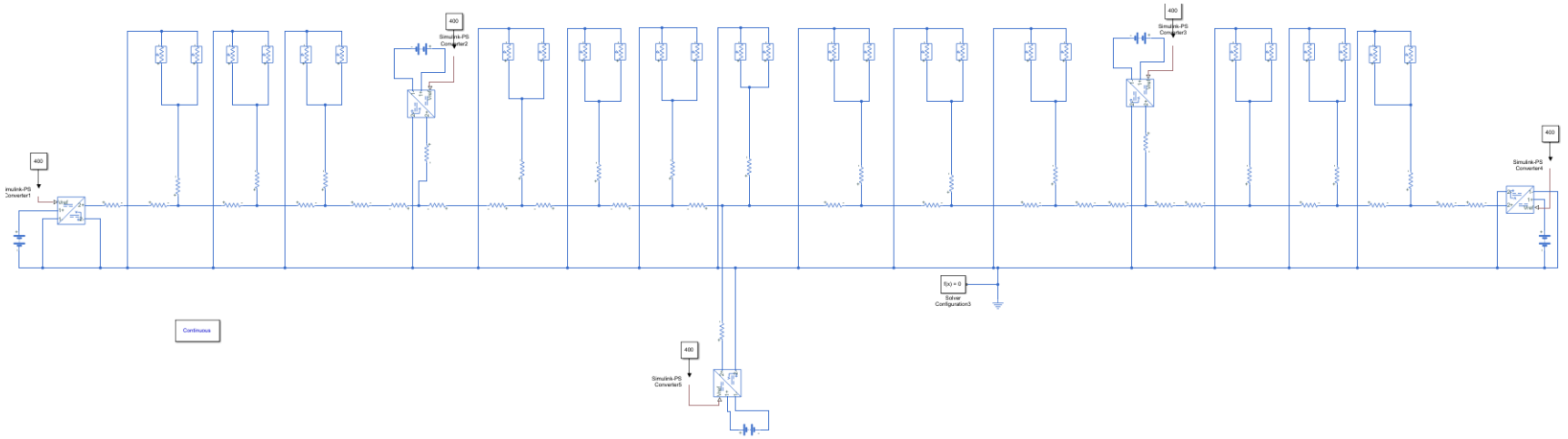

Figure E.5: Example of case layout in simulink, with batteries, generation, loads and main grid connection are shown.

F

MATLAB code

F.1. MATLAB Code Centralized Storage Model

Below, the MATLAB code can be found for the centralized storage model. An elaborate explanation is given in section C.6, as well as a flowchart representing this MATLAB code in Figure C.6. The model calculates the current SoC for each hour for a whole year, where the generation and demand are the determined hourly generation and demand for an average day for each month respectively. The final SoC of each hour is plotted for each hour for every month over the whole year, as well as the availability being calculated from the availability of each month.

```
% Authors: Paul Kluge and Jesse Richter
% Date: 18-06-2021
% Target of code: calculate SOC for a certain amount of central
% batteries with hourly demand and generation and thus availability.

clear SOC_final
clear SOC
clear charge_final
clear hours
clear demand

%Calculate the hourly demand of each month, using daily fractinos of
%liander data multiplied with monthly demand calculated from minitopia
for a = 1:12
    for b = 1:24
        demand(a,b) = daily_fractions(b)*demand_monthly(a);
    end
end

%Average hourly generation for an average day for each month is sum of
%hourly solar and wind generation of an average day that month.
gen(1,1:24) = solar_january + wind_january;
gen(2,1:24) = solar_february + wind_february;
gen(3,1:24) = solar_march + wind_march;
gen(4,1:24) = solar_april + wind_april;
gen(5,1:24) = solar_may + wind_may;
gen(6,1:24) = solar_june + wind_june;
gen(7,1:24) = solar_july + wind_july;
gen(8,1:24) = solar_august + wind_august;
gen(9,1:24) = solar_september + wind_september;
gen(10,1:24) = solar_october + wind_october;
```

```
gen(11,1:24) = solar_november + wind_november;
gen(12,1:24) = solar_december + wind_december;

% Initialise values of the model: SOC, charge, charging hours, capacity of the
% batteries, days per month and round trip efficiency (RTE).
SOC = 100;
hours_charging = 0;
hours_delivering = 0;
battery = 19.3*10^3;
batteries = 4;
lower_limit = 10;
upper_limit = 100;
total_charge = batteries*battery;
charge = (SOC/100)*total_charge;
charging = 0;
days = [31,29,31,30,31,30,31,31,30,31,30,31];
RTE = 0.96;

% calculate the SOC, charge, final values of both, and hours in which the
% batteries need to charge for the amount of days of each month for a
% whole year.
for h = 1:12
    for i = 1:31
        for j = 1:24

                if(charging == 1)
                    % if battery needs to be charged, charge battery with
                    % generation*RTE. If SOC > 100, SOC = 100. SOC_final = SOC at
                    % the end
                    hours_charging = hours_charging + 1;
                    charge = charge + RTE*gen(h,j);
                    SOC = charge*100/total_charge;
                    charge_final(j+(i-1)*24,h) = charge;
                    SOC_final(j+(i-1)*24,h) = charge_final(j+(i-1)*24,h)
                        *100/total_charge;
                    if(SOC_final(j+(i-1)*24,h) >= 100)
                        charge = total_charge;
                        SOC = charge*100/total_charge;
                        charge_final(j+(i-1)*24,h) = total_charge;
                        SOC_final(j+(i-1)*24,h) = 100;
                        charging = 0;
                    end
                else
                    % if battery can deliver, discahrge battery with current gen -
                    % demand, update SOC and charge. If SOC >= 100, SOC =
                    % 100. If SOC <= 10%, start charging battery. Else,
                    % discharge battery with difference/RTE. Lastly, update
                    % SOC_final and charge_final with SOC and charge
                    % values.
                    hours_delivering = hours_delivering + 1;
                    difference = gen(h,j) - demand(h,j);
                    if(difference >= 0)
```

```
83                          difference = RTE*difference;
84                      else
85                          difference = difference / RTE;
86                      end
87                      charge = charge + difference;
88                      SOC = charge*100/total_charge;
89                      if(SOC >= 100)
90                          charge = total_charge;
91                          SOC = 100;
92                          charge_final(j+(i-1)*24,h) = total_charge;
93                          SOC_final(j+(i-1)*24,h) = 100;
94                      elseif(SOC <= lower_limit)
95                          charge = (lower_limit/100)*total_charge;
96                          SOC = charge*100/total_charge;
97                          charge_final(j+(i-1)*24,h) = charge;
98                          SOC_final(j+(i-1)*24,h) = SOC;
99                          charging = 1;
100                     else
101                         charge_final(j+(i-1)*24,h) = charge;
102                         SOC_final(j+(i-1)*24,h) = SOC;
103                     end
104                 end
105                 disp("charge_final = " + charge_final(j+(i-1)*24,h));
106                 disp("SOC_final = " + SOC_final(j+(i-1)*24,h));
107                 disp("charging = " + charging);
108         end
109
110     end
111     %Update hours in which the battery can deliver and needs to be charged
112     %for teh current month.
113     hours_d(h) = hours_delivering;
114     hours_c(h) = hours_charging;
115     hours_delivering = 0;
116     hours_charging = 0;
117     availability(h) = hours_d(h) / (hours_d(h) + hours_c(h));
118 end
119 % Calculate total availability for a whole year
120 availability_final = mean(availability);
121
122 % Make titles for plots, plot the SOC_final for every hour for each month
123 titles = ["January", "February", "March", "April", "May", "June", "July",
        "August", "September", "October", "November", "December"];
124 for h =1:12
125     %subplot(4,3,h)
126     figure(h)
127     hours = linspace(1,24*max(days),24*max(days));
128     plot(hours,SOC_final(:,h));
129     xlabel('hours');
130     ylabel('SOC %');
131     xlim([0, 24*days(h)])
132     grid on;
133     title(titles(h))
134 end
135 disp("SOC_min = " + min(SOC_final));
```

F.2. MATLAB Code Distributed Storage Model

Below, the MATLAB code can be found for the distributed storage model. An elaborate explanation is given in section C.7, as well as a flowchart representing this MATLAB code in Figure C.7 and Figure C.8 for both the SoC of the central batteries as well as the home batteries. In the code itself, comments are placed for elaboration of the variables and what happens per seciton of code. In total, the model calculates the SoC for both batteries for each hour for a whole year, where the generation (split into wind and solar) and demand (split into the demand of a single house and tunect) are the determined hourly generation and demand for an average day for each month respectively. The final SoC of both the central batteries and one set of 2 home batteries is plotted for each hour for every month over the whole year, as well as the availability being calculated from the total amount of hours in which both batteries were charging.

```
% Authors: Paul Kluge and Jesse Richter
% Date: 18-06-2021
% Target of code: calculate SOC for a certain amount of central and home
% batteries with hourly demand and generation and thus availability.

clear SOC
clear excessive_central
clear SOC_house
clear SOC_central
clear SOC_final_house
clear SOC_final_central
clear charge_final_house
clear charge_final_central
clear hours
clf

%Calculate the hourly demand of each month of the total community and a
    single house,
%using daily fractinos of liander data multiplied with daily demand or
    monthly demand
%calculated from minitopia
for a = 1:12
    for b = 1:24
        house(a,b) = daily_fractions(b)*demand_house_monthly(a);
        demand(a,b) = daily_fractions(b)*demand_monthly(a);
    end
end

%solar contais hourly generation of an average day for each month
solar(1,1:24) = solar_january;
solar(2,1:24) = solar_february;
solar(3,1:24) = solar_march;
solar(4,1:24) = solar_april;
solar(5,1:24) = solar_may;
solar(6,1:24) = solar_june;
solar(7,1:24) = solar_july;
solar(8,1:24) = solar_august;
solar(9,1:24) = solar_september;
solar(10,1:24) = solar_october;
solar(11,1:24) = solar_november;
solar(12,1:24) = solar_december;

%wind contais hourly generation of an average day for each month
```

```
wind(1,1:24) = wind_january;
wind(2,1:24) = wind_february;
wind(3,1:24) = wind_march;
wind(4,1:24) = wind_april;
wind(5,1:24) = wind_may;
wind(6,1:24) = wind_june;
wind(7,1:24) = wind_july;
wind(8,1:24) = wind_august;
wind(9,1:24) = wind_september;
wind(10,1:24) = wind_october;
wind(11,1:24) = wind_november;
wind(12,1:24) = wind_december;

%initialise variables: capacities of batteries, SOC's, hours of charging,
%lower and upper limits and RTE's
total_hours = 0;
non_available = 0;
total_central = 2*19.3*10^3;
total_house = 2*2.6*10^3;
charge_central = total_central;
charge_house = total_house;
SOC_central = 100;
SOC_house = 100;

hours_charging_central = 0;
hours_delivering_central = 0;
hours_charging_house = 0;
hours_delivering_house = 0;
lower_limit_central = 10;
lower_limit_house = 0;
upper_limit = 100;
charging_central = 0;
charging_house = 0;
days = [31,29,31,30,31,30,31,31,30,31,30,31];
RTE_central = 0.96;
RTE_house = 0.98;

% calculate the SOC, charge, final values of both, and hours in which the
% batteries need to charge for the amount of days of each month for a
% whole year.
for h = 1:12
    for i = 1:days(h)
        for j = 1:24
            if(charging_house == 1)
                %if house battery needs to charge, charge battery with
                %current solar production *RTE_house and update SOC.
                % If SOC>=100, SOC = 100. Update SOC_final with SOC.
                hours_charging_house = hours_charging_house + 1;
                charge_house = charge_house + RTE_house*solar(h,j)/12;
                SOC_house = charge_house*100/total_house;
                charge_final_house(j+(i-1)*24,h) = charge_house;
                SOC_final_house(j+(i-1)*24,h) = charge_final_house(j+(i-1)
                    *24,h)*100/total_house;
                if(SOC_final_house(j+(i-1)*24,h) >= 100)
                    charge_house= total_house;
                    SOC_house = charge_house*100/total_house;
```

```
97                  charge_final_house(j+(i-1)*24,h) = total_house;
98                  SOC_final_house(j+(i-1)*24,h) = 100;
99                  charging_house = 0;
100             end
101         else
102             % if home battery can deliver and central battery is
                    charging,
103                 % discharge home battery with current solar - demand,
104                 % update SOC and charge. If central battery is not
                        charging,
105                 % include wind generation. If the battery supplies,
                        divide by RTE
106                 % if surplus of energy, multiply with RTE.
107                 % Update SOC and charge, If SOC >= 100, SOC =
108                 % 100. If SOC <= 0%, start charging home battery.
109                 %Lastly, update SOC_final and charge_final with SOC
                        and charge
110                 % values.
111             excessive_house = 0;
112             hours_delivering_house = hours_delivering_house + 1;
113             if (charging_central == 1)
114                 difference_house = solar(h,j)/12 - house(h,j);
115             else
116                 difference_house = (wind(h,j) - demand_tunect/24)/12 +
                        solar(h,j)/12 - house(h,j);
117             end
118             if(difference_house >= 0)
119                 difference_house = RTE_house*difference_house;
120             else
121                 difference_house = difference_house / RTE_house;
122             end
123                 charge_house = charge_house + difference_house;
124                 SOC_house = charge_house*100/total_house;
125             if(SOC_house >= 100)
126                 excessive_house = charge_house - total_house;
127                 charge_house = total_house;
128                 SOC_house = 100;
129                 charge_final_house(j+(i-1)*24,h) = total_house;
130                 SOC_final_house(j+(i-1)*24,h) = 100;
131             elseif(SOC_house <= lower_limit_house)
132                 charge_house = (lower_limit_house/100)*total_house;
133                 SOC_house = charge_house*100/total_house;
134                 charge_final_house(j+(i-1)*24,h) = charge_house;
135                 SOC_final_house(j+(i-1)*24,h) = SOC_house;
136                 charging_house = 1;
137             else
138                 charge_final_house(j+(i-1)*24,h) = charge_house;
139                 SOC_final_house(j+(i-1)*24,h) = SOC_house;
140             end
141         end
142
143         %if central battery needs to charge, charge battery with
144             %current wind production *RTE_central and update SOC.
145             % If SOC>=100, SOC = 100. Update SOC_final with SOC.
146         if(charging_central == 1)
147             hours_charging_central = hours_charging_central + 1;
```

```
148                 charge_central = charge_central + RTE_central*wind(h,j);
149                 SOC_central = charge_central*100/total_central;
150                 charge_final_central(j+(i-1)*24,h) = charge_central;
151                 SOC_final_central(j+(i-1)*24,h) = charge_final_central(j+(
                        i-1)*24,h)*100/total_central;
152                 if(SOC_final_central(j+(i-1)*24,h) >= 100)
153                     charge_central = total_central;
154                     SOC_central = charge_central*100/total_central;
155                     charge_final_central(j+(i-1)*24,h) = total_central;
156                     SOC_final_central(j+(i-1)*24,h) = 100;
157                     charging_central = 0;
158                 end
159             else
160                 % if central battery can deliver and home battery is
                        charging,
161                     % discharge central  battery with current wind -
                            demand - tunect.
162                     % If home battery is not charging, check if excessive
                            energy is available.
163                     % If excessive available, charge battery with exessive
                             - tunect
164                     % If not available, discharge with demand_tunect.
165                     % If the central battery supplies, divide by RTE
166                     % if surplus of energy, multiply with RTE.
167                     % Update SOC and charge, If SOC >= 100, SOC =
168                     % 100. If SOC <= 10%, start charging central battery.
169                     %Lastly, update SOC_final and charge_final with SOC
                            and charge
170                     % values.
171                 hours_delivering_central = hours_delivering_central + 1;
172                 if(charging_house == 1)
173                     difference_central = wind(h,j) - demand_tunect/24 -
                            house(h,j)*12;
174                 else
175                     if(difference_house >= 0)
176                         difference_central = excessive_house*12 -
                                demand_tunect/24;
177                     else
178                         difference_central =  - demand_tunect/24;
179                     end
180                 end
181                 if(difference_central >= 0)
182                     difference_central = RTE_central*difference_central;
183                     charge_central = charge_central + difference_central;
184                     SOC_central = charge_central*100/total_central;
185
186                 else
187                     difference_central = difference_central / RTE_central;
188                     charge_central = charge_central + difference_central;
189                     SOC_central = charge_central*100/total_central;
190                 end
191
192                 if(SOC_central >= 100)
193                     charge_central = total_central;
194                     SOC_central = 100;
195                     charge_final_central(j+(i-1)*24,h) = total_central;
```

```
196                     SOC_final_central(j+(i-1)*24,h) = 100;
197                 elseif(SOC_central <= lower_limit_central)
198                     charge_central = (lower_limit_central/100)*
                            total_central;
199                     SOC_central = charge_central*100/total_central;
200                     charge_final_central(j+(i-1)*24,h) = charge_central;
201                     SOC_final_central(j+(i-1)*24,h) = SOC_central;
202                     charging_central = 1;
203                 else
204                     charge_final_central(j+(i-1)*24,h) = charge_central;
205                     SOC_final_central(j+(i-1)*24,h) = SOC_central;
206                 end
207             end
208             disp("charge = " + charge_house);
209             disp("SOC = " + SOC_house);
210             disp("charge_final = " + charge_final_house(j+(i-1)*24,h));
211             disp("SOC_final = " + SOC_final_house(j+(i-1)*24,h));
212             if(charging_house == 1 && charging_central == 1)
213                 non_available = non_available + 1;
214             end
215             total_hours = total_hours + 1;
216         end
217     end
218     hours_d_central(h) = hours_delivering_central;
219     hours_c_central(h) = hours_charging_central;
220     hours_delivering_central = 0;
221     hours_charging_central = 0;
222     hours_d_house(h) = hours_delivering_house;
223     hours_c_house(h) = hours_charging_house;
224     hours_delivering_house = 0;
225     hours_charging_house = 0;
226 end
227
228 availability_final = (total_hours - non_available) / total_hours;
229 titles = ["Jan", "Feb", "Mar", "Apr", "May", "Jun", "Jul", "Aug", "Sep", "
        Oct", "Nov", "Dec"];
230 i = 1;
231 for h = 1:12
232
233     figure(h)
234     %subplot(4,3,h)
235     hours = linspace(1,24*max(days),24*max(days));
236     plot(hours,SOC_final_house(:,h));
237     hold on;
238     plot(hours,SOC_final_central(:,h));
239     hold off;
240     legend("SOC\_house", "SOC\_central");
241     xlabel('hours');
242     ylabel('SOC %');
243     xlim([0, 24*days(h)])
244     grid on;
245     title(titles(h))
246     i = i + 1;
247 end
248 % figure(2)
249 % subplot(1,2,1)
```

```
250 % plot(hours,SOC_final_house(:,1))
251 % hold on;
252 % plot(hours,SOC_final_central(:,1))
253 % hold off;
254 %   legend("SOC\_house", "SOC\_central");
255 % title(titles(1));
256 % xlabel('hours');
257 % ylabel('SOC %');
258 % grid on;
259 % subplot(1,2,2)
260 % plot(hours,SOC_final_house(:,9))
261 % hold on;
262 % plot(hours,SOC_final_central(:,9))
263 % hold off;
264 %   legend("SOC\_house", "SOC\_central");
265 % title(titles(9))
266 % xlabel('hours');
267 % ylabel('SOC %');
268 % grid on;
269 % figure(2)
270 % plot(average_daily_usage(:,1),average_daily_usage(:,2),'-o');
271 % title('Average hourly Wh usage of a tiny house');
272 % xlabel('Hours');
273 % ylabel('Wh');
274 % grid on;
275 % figure(3)
276 % bar(demand_house_monthly);
277 % xticklabels(titles);
278 % title('Daily usage per month');
279 % xlabel('Month');
280 % ylabel('Wh');
```

F.3. MATLAB Code Design Validation

Below the MATLAB code for the voltage drop and power loss analysis of the resulting voltage and current measurements of the used grid in Simulink is shown. For each house and tunect, the voltage drop is calculated in V and % by calculating the difference in V or % between the grid voltage of 400 VDC. The power loss is calculated by multiplying the voltage drop in V with the measured current through the wire connecting the houses or tunect to the microgrid. The power loss is expressed in W as well as a % of the drawn power by the house / tunect. Lastly, the voltage drops in V and % and power losses in W and % are plotted in separate figures.

```
% Authors: Paul Kluge and Jesse Richter
% Date: 18-06-2021
% Target of code: analyse the results of the simulink simulation


% Average output voltage of the batteries
average_voltage = (mean(out.battery_right_voltage)+mean(out.
    battery_left_voltage))/2;
grid_voltage = 400;

% Calculating the voltage drop and power loss for house 1, counting from
% the left
voltage_drop1 = 100*(grid_voltage - mean(out.voltage1))/grid_voltage;
voltage_diff1 = grid_voltage - mean(out.voltage1);
power_drop1 = voltage_diff1*mean(out.current1);
power_drop1_percent = 100*power_drop1/(mean(out.voltage1)*mean(out.
    current1));

% Calculating the voltage drop and power loss for house 2, counting from
% the left
voltage_drop2 = 100*(grid_voltage - mean(out.voltage2))/grid_voltage;
voltage_diff2 = grid_voltage - mean(out.voltage2);
power_drop2 = voltage_diff2*mean(out.current2);
power_drop2_percent = 100*power_drop2/(mean(out.voltage2)*mean(out.
    current2));

% Calculating the voltage drop and power loss for house 3, counting from
% the left
voltage_drop3 = 100*(grid_voltage - mean(out.voltage3))/grid_voltage;
voltage_diff3 = grid_voltage - mean(out.voltage3);
power_drop3 = voltage_diff3*mean(out.current3);
power_drop3_percent = 100*power_drop3/(mean(out.voltage3)*mean(out.
    current3));

% Calculating the voltage drop and power loss for house 4, counting from
% the left
voltage_drop4 = 100*(grid_voltage - mean(out.voltage4))/grid_voltage;
voltage_diff4 = grid_voltage - mean(out.voltage4);
power_drop4 = voltage_diff4*mean(out.current4);
power_drop4_percent = 100*power_drop4/(mean(out.voltage4)*mean(out.
    current4));

% Calculating the voltage drop and power loss for house 5, counting from
% the left
voltage_drop5 = 100*(grid_voltage - mean(out.voltage5))/grid_voltage;
voltage_diff5 = grid_voltage - mean(out.voltage5);
power_drop5 = voltage_diff5*mean(out.current1);
```

```
43 power_drop5_percent = 100*power_drop5/(mean(out.voltage5)*mean(out.
       current5));
44
45 % Calculating the voltage drop and power loss for house 6, counting from
46 % the left
47 voltage_drop6 = 100*(grid_voltage - mean(out.voltage6))/grid_voltage;
48 voltage_diff6 = grid_voltage - mean(out.voltage6);
49 power_drop6 = voltage_diff6*mean(out.current6);
50 power_drop6_percent = 100*power_drop6/(mean(out.voltage6)*mean(out.
       current6));
51
52 % Calculating the voltage drop and power loss for house 7, counting from
53 % the left
54 voltage_drop7 = 100*(grid_voltage - mean(out.voltage7))/grid_voltage;
55 voltage_diff7 = mean(out.battery_right_voltage) - mean(out.voltage7);
56 power_drop7 = voltage_diff7*mean(out.current7);
57 power_drop7_percent = 100*power_drop7/(mean(out.voltage7)*mean(out.
       current7));
58
59 % Calculating the voltage drop and power loss for house 8, counting from
60 % the left
61 voltage_drop8 = 100*(grid_voltage - mean(out.voltage8))/grid_voltage;
62 voltage_diff8 = grid_voltage - mean(out.voltage8);
63 power_drop8 = voltage_diff8*mean(out.current8);
64 power_drop8_percent = 100*power_drop8/(mean(out.voltage8)*mean(out.
       current8));
65
66 % Calculating the voltage drop and power loss for house 9, counting from
67 % the left
68 voltage_drop9 = 100*(grid_voltage - mean(out.voltage9))/grid_voltage;
69 voltage_diff9 = grid_voltage - mean(out.voltage9);
70 power_drop9 = voltage_diff9*mean(out.current9);
71 power_drop9_percent = 100*power_drop9/(mean(out.voltage9)*mean(out.
       current9));
72
73 % Calculating the voltage drop and power loss for house 10, counting from
74 % the left
75 voltage_drop10 = 100*(grid_voltage - mean(out.voltage10))/grid_voltage;
76 voltage_diff10 = grid_voltage - mean(out.voltage10);
77 power_drop10 = voltage_diff10*mean(out.current10);
78 power_drop10_percent = 100*power_drop10/(mean(out.voltage10)*mean(out.
       current10));
79
80 % Calculating the voltage drop and power loss for house 11, counting from
81 % the left
82 voltage_drop11 = 100*(grid_voltage - mean(out.voltage11))/grid_voltage;
83 voltage_diff11 = grid_voltage - mean(out.voltage11);
84 power_drop11 = voltage_diff11*mean(out.current11);
85 power_drop11_percent = 100*power_drop11/(mean(out.voltage11)*mean(out.
       current11));
86
87 % Calculating the voltage drop and power loss for house 12, counting from
88 % the left
89 voltage_drop12 = 100*(grid_voltage - mean(out.voltage12))/grid_voltage;
90 voltage_diff12 = grid_voltage - mean(out.voltage12);
91 power_drop12 = voltage_diff12*mean(out.current12);
```

```
92 power_drop12_percent = 100*power_drop12/(mean(out.voltage12)*mean(out.
       current12));
93
94 % Calculating the voltage drop and power loss for tunect
95 voltage_drop_tunect = 100*(average_voltage-mean(out.tunect_voltage))/
       average_voltage;
96 voltage_diff_tunect = average_voltage - mean(out.tunect_voltage);
97 power_drop_tunect = voltage_diff_tunect*mean(out.tunect_current);
98 power_drop_tunect_percent = 100*power_drop_tunect/(mean(out.tunect_voltage
       )*mean(out.tunect_current));
99
100 %concatenating the voltage drops in V and calculating minimum and maximum
101 %values
102 voltage_drops = [voltage_diff1;voltage_diff2;voltage_diff3;voltage_diff4;
       voltage_diff5;voltage_diff6; voltage_diff_tunect; voltage_diff7;
       voltage_diff8;voltage_diff9;voltage_diff10;voltage_diff11;
       voltage_diff12;];
103 min_voltage_drop = min(voltage_drops);
104 max_voltage_drop = max(voltage_drops);
105 %concatenating the voltage drops in % and calculating minimum and maximum
106 %values
107 voltage_drops_percent = [voltage_drop1; voltage_drop2; voltage_drop3;
       voltage_drop4; voltage_drop5; voltage_drop6; voltage_drop_tunect;
       voltage_drop7; voltage_drop8; voltage_drop9; voltage_drop10;
       voltage_drop11; voltage_drop12;];
108 min_voltage_percent = min(voltage_drops_percent);
109 max_voltage_percent = max(voltage_drops_percent);
110 %concatenating the power losses in W and calculating minimum and maximum
111 %values
112 power_drops = [power_drop1; power_drop2; power_drop3; power_drop4;
       power_drop5; power_drop6; power_drop_tunect; power_drop7; power_drop8;
       power_drop9; power_drop10; power_drop11; power_drop12];
113 min_power_drop = min(power_drops);
114 max_power_drop = max(power_drops);
115 %concatenating the power losses in % and calculating minimum and maximum
116 %values
117 power_drops_percent = [power_drop1_percent; power_drop2_percent;
       power_drop3_percent; power_drop4_percent; power_drop5_percent;
       power_drop6_percent; power_drop_tunect_percent; power_drop7_percent;
       power_drop8_percent; power_drop9_percent; power_drop10_percent;
       power_drop11_percent; power_drop12_percent];
118 min_power_percent = min(power_drops_percent);
119 max_power_percent = max(power_drops_percent);
120
121 %Display minimum and maximum values
122 disp("Minimum voltage drop in V = " + round(min_voltage_drop,2))
123 disp("Maximum voltage drop in V = " + round(max_voltage_drop,2))
124 disp("Minimum voltage drop in % = " + round(min_voltage_percent,2))
125 disp("Maximum voltage drop in % = " + round(max_voltage_percent,2))
126 disp("Minimum power loss in W = " + round(min_power_drop,2));
127 disp("Maximum power loss in W = " + round(max_power_drop,2));
128 disp("Minimum power loss in % = " + round(min_power_percent,2));
129 disp("Maximum power loss in % = " + round(max_power_percent,2));
130
131 %display voltage drops and power losses for each house, tunect is house 7,
132 %and houses 7-12 thus become 8-13
```

```
133 figure(1)
134 plot(voltage_drops)
135 grid minor;
136 xlabel("House number")
137 ylabel("Drop in V");
138 title("Voltage drop in V for each connection")
139 xlim([1,13])
140
141 figure(2)
142 plot(voltage_drops_percent);
143 grid minor;
144 xlabel("House number")
145 ylabel("Drop in %");
146 title("Voltage drop in % of grid voltage for each connection")
147 xlim([1,13])
148
149 figure(3)
150 plot(power_drops);
151 grid minor;
152 xlabel("House number")
153 ylabel("Drop in W");
154 xlim([1,13])
155 title("Power drop in W for each connection")
156
157 figure(4)
158 plot(power_drops_percent)
159 grid minor;
160 xlabel("House number")
161 ylabel("Drop in %");
162 xlim([1,13])
163 title("Power drop in % for each connection")
```

Bibliography

[1] Timothy Carlin. “Tiny homes: Improving carbon footprint and the American lifestyle on a large scale”. In: *Celebrating Scholarship & Creativity Day* (Apr. 24, 2014). URL: https://digitalcommons.csbsju.edu/elce_cscday/35.

[2] *The International Residential Code*. ICC. Mar. 20, 2015. URL: https://www.iccsafe.org/products-and-services/i-codes/2018-i-codes/irc/ (visited on 06/09/2021).

[3] Heather Shearer and Paul Burton. “Towards a Typology of Tiny Houses”. In: *Housing, Theory and Society* 36.3 (June 24, 2018). Publisher: Routledge, pp. 298–318. ISSN: 1403-6096. URL: https://www-tandfonline-com.tudelft.idm.oclc.org/doi/abs/10.1080/14036096.2018.1487879 (visited on 06/09/2021).

[4] Maria Jebbink. “Life in a shoebox: About people and their motivation to go tiny”. In: *Twente University* (), p. 45. URL: http://essay.utwente.nl/78118/1/Jebbink_BA_BMS.pdf.

[5] Wim Landuyt et al. “tunus - tiny house project: an interdisciplinary approach to architecture”. In: (2021). URL: http://resolver.tudelft.nl/uuid:de3a7d8b-f558-4bd7-affb-27e7fedf3b8f (visited on 04/26/2021).

[6] *microgrid*. URL: https://dictionary.cambridge.org/dictionary/english/microgrid (visited on 06/16/2021).

[7] Zengxun Liu et al. “Development of the interconnected power grid in Europe and suggestions for the energy internet in China”. In: *Global Energy Interconnection* 3.2 (2020), pp. 111–119. ISSN: 2096-5117. DOI: https://doi.org/10.1016/j.gloei.2020.05.003. URL: https://www.sciencedirect.com/science/article/pii/S2096511720300451.

[8] M. Safiuddin. “HISTORY OF ELECTRIC GRID”. In: Jan. 2013, pp. 6–11. ISBN: 978-1-60263-070-3.

[9] IEA. “Global Energy Review 2021”. en. In: 5 (2021). URL: https://www.iea.org/reports/global-energy-review-2021 (visited on 05/10/2021).

[10] Council of European Energy Regulators. “CEER Report on Power Losses”. en. In: (Oct. 2017). URL: https://www.ceer.eu/documents/104400/-/-/09ecee88-e877-3305-6767-e75404637087 (visited on 05/10/2021).

[11] B. Urishev. “Microgrid Control Based on the Use and Storage of Renewable Energy Sources”. en. In: *Applied Solar Energy* 54.5 (Nov. 2018), pp. 388–391. ISSN: 0003-701X, 1934-9424. DOI: 10.3103/S0003701X18050201. URL: http://link.springer.com/10.3103/S0003701X18050201 (visited on 04/19/2021).

[12] Greg Young Morris et al. “Evaluation of the costs and benefits of Microgrids with consideration of services beyond energy supply”. In: *2012 IEEE Power and Energy Society General Meeting*. 2012, pp. 1–9. DOI: 10.1109/PESGM.2012.6345380.

[13] Karina Garbesi, Vagelis Vossos, and Hongxia Shen. *Catalog of DC Appliances and Power Systems*. LBNL-5364E, 1076790. Oct. 13, 2010, LBNL–5364E, 1076790. DOI: 10.2172/1076790. URL: http://www.osti.gov/servlets/purl/1076790/ (visited on 06/10/2021).

[14] Vagelis Vossos, Karina Garbesi, and Hongxia Shen. “Energy savings from direct-DC in U.S. residential buildings”. In: *Energy and Buildings* 68 (Jan. 1, 2014), pp. 223–231. ISSN: 0378-7788. DOI: 10.1016/j.enbuild.2013.09.009. URL: https://www.sciencedirect.com/science/article/pii/S0378778813005720 (visited on 06/10/2021).

[15] IEA. “Energy Access Outlook 2017”. en. In: (2017). URL: https://www.iea.org/reports/energy-access-outlook-2017 (visited on 04/22/2021).

[16] Wikimedia Foundation. *Moscow Method*. Last accessed 30 September 2020. URL: https://en.wikipedia.org/wiki/MoSCoW_method.

[17] *Australian Appliance Usage Guide*. URL: https://www.ausgrid.com.au/-/media/Documents/energy-use/Appliance-energy-use-guide.pdf.

[18] *American Appliance Usage Guide*. URL: https://clallampud.net/wp-content/uploads/2014/12/BrochureTypicalApplianceEnergyUsage_2014-09-26.pdf.

[19] *How much electrical power do I need for my home?* Energuide. URL: https://www.energuide.be/en/questions-answers/how-much-electrical-power-do-i-need-for-my-home/1855/ (visited on 06/11/2021).

[20] *Survey Tiny House Users Results*. URL: https://docs.google.com/spreadsheets/d/1KiGUxui8U1bfwwub4Pw-02Ld4R5QJ1L5STsEnxXLzzE/edit?usp=sharing.

[21] Miguel A. Rodriguez-Otero and Efrain O'Neill-Carrillo. "Efficient Home Appliances for a Future DC Residence". In: *2008 IEEE Energy 2030 Conference*. 2008 IEEE Energy 2030 Conference. University of Puerto Rico, Nov. 2008, pp. 1–6. DOI: 10.1109/ENERGY.2008.4781006. URL: https://ieeexplore-ieee-org.tudelft.idm.oclc.org/document/4781006.

[22] Muhammad Kamran, Muhammad Bilal, and Muhammad Mudassar. "DC Home Appliances for DC Distribution System". In: *Mehran University Research Journal of Engineering and Technology* 36.4 (Oct. 1, 2017). Number: 4, p. 10. ISSN: 2413-7219. DOI: 10.22581/muet1982.1704.12. URL: https://publications.muet.edu.pk/index.php/muetrj/article/view/33 (visited on 06/10/2021).

[23] *Beschikbare data | Liander*. URL: https://www.liander.nl/partners/datadiensten/open-data/data (visited on 06/11/2021).

[24] *The 'good old days' are now: Today's home appliances are cheaper, better, and more energy efficient than ever before*. American Enterprise Institute - AEI. Section: Carpe Diem. Dec. 1, 2012. URL: https://www.aei.org/carpe-diem/the-good-old-days-are-now-todays-home-appliances-are-cheaper-better-and-more-energy-efficient-than-ever-before-2/ (visited on 06/11/2021).

[25] Unni Pillai. "Drivers of cost reduction in solar photovoltaics". In: *Energy Economics* 50 (July 1, 2015), pp. 286–293. ISSN: 0140-9883. DOI: 10.1016/j.eneco.2015.05.015. URL: https://www.sciencedirect.com/science/article/pii/S014098831500167X (visited on 06/10/2021).

[26] Bhubaneswari Parida, S. Iniyan, and Ranko Goic. "A review of solar photovoltaic technologies". In: *Renewable and Sustainable Energy Reviews* 15.3 (Apr. 1, 2011), pp. 1625–1636. ISSN: 1364-0321. DOI: 10.1016/j.rser.2010.11.032. URL: https://www.sciencedirect.com/science/article/pii/S1364032110004016 (visited on 06/10/2021).

[27] *LG Neon R*. LG. URL: https://energie-advies-holland.nl/wp-content/uploads/2021/03/380W-Mono-Neon-R-V5-Data-Sheet-EN.pdf.

[28] *FuturaSun FU 360 M Zebra*. FuturaSun. URL: https://www.futurasun.com/wp-content/uploads/2020/03/2020_FuturaSun_120m_350-360W_Zebra_en.pdf?x97762.

[29] *Trinasolar Vertex*. Trinasolar. URL: https://www.stralendgroen.nl/wp-content/uploads/2020/12/Datasheet-Trina-Vertex-S-TSM-390-405W-DE09.05-1500V-Full-black-preliminary.pdf.

[30] *Sunpower Maxeon 3*. Sunpower. URL: https://sunpower.maxeon.com/int/sites/default/files/2020-09/sp_mst_MAX3-400-395-390_ds_en_a4_mc4_1mcable_536423.pdf.

[31] *REC Solar Alpha 380*. REC Solar. URL: https://www.recgroup.com/sites/default/files/documents/ds_rec_alpha_series_en.pdf?t=1621418248.

[32] Alam Md. Mahbub, ShafiqurMeyer Rehman Josua, and Luai M. Al-Hadhrami. "Wind Speed and Power Characteristics at Different Heights for a Wind Data Collection Tower in Saudi Arabia". In: World Renewable Energy Congress – Sweden, 8–13 May, 2011, Linköping, Sweden. Nov. 3, 2011, pp. 4082–4089. DOI: 10.3384/ecp110574082. URL: https://ep.liu.se/en/conference-article.aspx?series=ecp&issue=57&Article_No=5 (visited on 06/10/2021).

[33] Muhammad Mahmood Aslam Bhutta et al. “Vertical axis wind turbine – A review of various configurations and design techniques”. In: *Renewable and Sustainable Energy Reviews* 16.4 (May 1, 2012), pp. 1926–1939. ISSN: 1364-0321. DOI: 10.1016/j.rser.2011.12.004. URL: https://www.sciencedirect.com/science/article/pii/S136403211100596X (visited on 06/10/2021).

[34] Anna E. Craig, John O. Dabiri, and Jeffrey R. Koseff. “Low order physical models of vertical axis wind turbines”. In: *Journal of Renewable and Sustainable Energy* 9.1 (Jan. 1, 2017). Publisher: American Institute of Physics, p. 013306. DOI: 10.1063/1.4976983. URL: https://aip-scitation-org.tudelft.idm.oclc.org/doi/10.1063/1.4976983 (visited on 06/10/2021).

[35] M.J.A. Slob et al. “GGD-richtlijn medische milieukunde: omgevingsgeluid en gezondheid”. In: (2019). Publisher: RIVM. DOI: 10.21945/RIVM-2019-0177. URL: https://rivm.openrepository.com/handle/10029/623477 (visited on 06/10/2021).

[36] *KNMI Meteorologisch Data Portal*. TU Delft. URL: https://www.tudelft.nl/ewi/over-de-faculteit/afdelingen/electrical-sustainable-energy/photovoltaic-materials-and-devices/dutch-pv-portal/meteorologisch-data-portal (visited on 06/18/2021).

[37] Haoran Zhao et al. “Review of energy storage system for wind power integration support”. In: *Applied Energy* 137 (Jan. 1, 2015), pp. 545–553. ISSN: 0306-2619. DOI: 10.1016/j.apenergy.2014.04.103. URL: https://www.sciencedirect.com/science/article/pii/S0306261914004668 (visited on 06/10/2021).

[38] Kendall Mongird et al. *Energy Storage Technology and Cost Characterization Report*. PNNL-28866, 1573487. July 29, 2019, pp. 1–120. DOI: 10.2172/1573487. URL: http://www.osti.gov/servlets/purl/1573487/ (visited on 06/10/2021).

[39] David Connolly. *Energy Storage Technology and Cost Characterization Report*. 3. Aug. 17, 2009, p. 56. DOI: 10.2172/1573487. URL: http://www.paredox.com/foswiki/pub/Luichart/RedoxTechnicalPapers/David_Connolly_UL_Energy_Storage_Techniques_V3.pdf (visited on 06/10/2021).

[40] *BYD Battery-Box Premium HVM 19.3*. BYD. URL: https://www.europe-solarstore.com/download/byd/BYD-Battery-Box-Premium-HVS-datasheet.pdf.

[41] *SimpliPhi PHI 2.6 kWh Smart-Tech HI Power LFP Battery*. Simpliphi. URL: https://www.amerescosolar.com/simpliphi-phi-26-kwh-smart-tech-lfp-battery.

[42] Sandeep Anand and B. G. Fernandes. “Optimal voltage level for DC microgrids”. In: *IECON 2010 - 36th Annual Conference on IEEE Industrial Electronics Society*. IECON 2010 - 36th Annual Conference on IEEE Industrial Electronics Society. ISSN: 1553-572X. Nov. 2010, pp. 3034–3039. DOI: 10.1109/IECON.2010.5674947. URL: https://ieeexplore-ieee-org.tudelft.idm.oclc.org/document/5674947.

[43] Sonia Moussa, Manel Jebali-Ben Ghorbal, and Ilhem Slama-Belkhodja. “DC voltage level choice in residential remote area”. In: *2018 9th International Renewable Energy Congress (IREC)*. 2018 9th International Renewable Energy Congress (IREC). ISSN: 2378-3451. Mar. 2018, pp. 1–6. DOI: 10.1109/IREC.2018.8362444. URL: https://ieeexplore-ieee-org.tudelft.idm.oclc.org/stamp/stamp.jsp?arnumber=8362444.

[44] *CTC-3k Grid tied controller*. URL: https://www.diytrade.com/china/pd/7943926/Grid_Tie_Controller_for_Small_Wind_3KW.html.

[45] *Tame Power Converter Wesbite*. URL: https://www.tame-power.com/en.

[46] Y. Ito, Y. Zhongqing, and H. Akagi. “DC microgrid based distribution power generation system”. In: *The 4th International Power Electronics and Motion Control Conference, 2004. IPEMC 2004.* The 4th International Power Electronics and Motion Control Conference, 2004. IPEMC 2004. Vol. 3. Aug. 2004, 1740–1745 Vol.3. URL: https://ieeexplore.ieee.org/document/1377011.

[47] Shamini Dharmasena, Temitayo O. Olowu, and Arif I. Sarwat. “Bidirectional AC/DC Converter Topologies: A Review”. In: *2019 SoutheastCon*. 2019 SoutheastCon. ISSN: 1558-058X. Apr. 2019, pp. 1–5. DOI: 10.1109/SoutheastCon42311.2019.9020287. URL: https://ieeexplore.ieee.org/abstract/document/9020287.

[48] *100kW 1200V AC/DC converter battery charger*. URL: https://www.zekalabs.com/products/non-isolated-high-power-converters/ac-dc-converter-100kw-1200v (visited on 06/16/2021).

[49] *Prysmian FG16OR16 0,6/1 kV*. Prysmian. URL: https://docs.rs-online.com/f778/A700000007468380.pdf.

[50] *RS online, electrical component web store*. URL: https://nl.rs-online.com/web/c/cables-wires/electrical-power-industrial-cable/electrical-mains-power-cables.

[51] *Custom Converter Website*. URL: https://www.dwe-oss.nl/.

[52] Dawn Dreams Media. *DC Systems - Solar Micro DC/DC Converter*. DC Systems. URL: https://www.dc.systems/products/dc-dc-converters/195-solar-micro-dc-dc-converter (visited on 06/10/2021).

[53] Sijo Augustine et al. *DC Microgrid Protection: Review and Challenges*. U.S. Department of Commerce, Aug. 1, 2018. URL: https://www.researchgate.net/profile/Matthew-Reno-2/publication/326957897_DC_Microgrid_Protection_Review_and_Challenges/links/5b6db1bfa6fdcc87df7112d2/DC-Microgrid-Protection-Review-and-Challenges.pdf.

[54] Jafar Mohammadi, Firouz Badrkhani Ajaei, and Gary Stevens. “Grounding the DC Microgrid”. In: *IEEE Transactions on Industry Applications* 55.5 (Sept. 2019). Conference Name: IEEE Transactions on Industry Applications, pp. 4490–4499. ISSN: 1939-9367. DOI: 10.1109/TIA.2019.2928278.

[55] Ankan Chandra, G K Singh, and Vinay Pant. “Protection techniques for DC microgrid- A review”. In: *Electric Power Systems Research* 187 (Oct. 1, 2020), p. 106439. ISSN: 0378-7796. DOI: 10.1016/j.epsr.2020.106439. URL: https://www.sciencedirect.com/science/article/pii/S0378779620302443 (visited on 06/10/2021).

[56] Unknown Author. *ansi C84.1 electric power systems and equipment - voltage ranges*. URL: http://www.powerqualityworld.com/2011/04/ansi-c84-1-voltage-ratings-60-hertz.html (visited on 06/10/2021).

[57] Simulink Documentation. *Simulation and Model-Based Design*. 2020. URL: https://www.mathworks.com/products/simulink.html.

[58] *Aeolos-V 2kW Data Sheet*. URL: http://www.heliosystems.it/wp-content/uploads/2014/10/Aeolos-V-2kw-Brochure.pdf.

[59] Battolyser B.V. *Battolyser - Energy Enlightenmentz*. 2019. URL: https://www.battolyserbv.com/ (visited on 01/20/2021).

[60] *TNO Heat battery info*. URL: https://gebruikersplatform.bodemenergie.nl/ (visited on 06/12/2021).

[61] *The Dutch PV Portal 2.0: module orientation*. URL: https://pvportal-2.ewi.tudelft.nl/Pages/Orientation.php (visited on 06/10/2021).

[62] Michael Hartner et al. “East to west – The optimal tilt angle and orientation of photovoltaic panels from an electricity system perspective”. In: *Applied Energy* 160 (Dec. 15, 2015), pp. 94–107. ISSN: 0306-2619. DOI: 10.1016/j.apenergy.2015.08.097. URL: https://www.sciencedirect.com/science/article/pii/S0306261915010338 (visited on 06/10/2021).

[63] T. Nordmann and L. Clavadetscher. “Understanding temperature effects on PV system performance”. In: *Proceedings of 3rd World Conference onPhotovoltaic Energy Conversion, 2003*. Proceedings of 3rd World Conference onPhotovoltaic Energy Conversion, 2003. Vol. 3. May 2003, pp. 2243–2246. URL: https://ieeexplore-ieee-org.tudelft.idm.oclc.org/abstract/document/1305032.

[64] Daniel Zammit et al. “MPPT with Current Control for a PMSG Small Wind Turbine in a Grid-Connected DC Microgrid”. In: TUrbWind 2017 (Research and Innovation on Wind Energy Exploitation in Urban Environment) Colloquium. Italy, June 16, 2017, pp. 1–7. URL: https://www.researchgate.net/publication/317954288_MPPT_with_Current_Control_for_a_PMSG_Small_Wind_Turbine_in_a_Grid-Connected_DC_Microgrid.

[65] Muhammad Husnain Ashfaq, Jeyraj A/L Selvaraj, and Nasrudin Abd Rahim. “Control Strategies for Bidirectional DC-DC Converters: An Overview”. In: *IOP Conference Series: Materials Science and Engineering* 1127.1 (Mar. 1, 2021), p. 012031. ISSN: 1757-8981, 1757-899X. DOI: 10.1088/1757-899X/1127/1/012031. URL: https://iopscience.iop.org/article/10.1088/1757-899X/1127/1/012031 (visited on 06/10/2021).

[66] Sreedhar Srisailam and Devadi Jagadeesh. “A Review on Optimization Algorithms for MPPT in Solar PV System under Partially Shaded Conditions”. In: *IOSR Journal of Electrical and Electronics Engineering* (Jan. 1, 2016), pp. 23–32. ISSN: 2278-1676. URL: https://www.researchgate.net/publication/334534711_A_Review_on_Optimization_Algorithms_for_MPPT_in_Solar_PV_System_under_Partially_Shaded_Conditions.

[67] *Water Pump Pricing Source*. URL: https://www.waterpump.co.uk/.

[68] *LG PV Pricing Source*. URL: https://energie-advies-holland.nl/webshop/380w-mono-neon-r-v5/?gclid=Cj0KCQjw5auGBhDEARIsAFyNm9EGlCUNRu5SIOO3tH_DFg2GAFRb-ltjaT6xPKpx8PQ8-x6N41cNSPAaAg8VEALw_wcB.

[69] *Aeolos Wind Turbine & Converter Pricing Source*. URL: https://www.scribd.com/document/432677719/Aeolos-Vertical-Axis-Wind-Turbine-EXW-Price-List-2019.

[70] *Triple Solar PVT Pricing Source*. URL: https://triplesolar.eu/winkel/product/pvt-paneel-pakket-3-kw/.

[71] *BYD HVM 19.3 Pricing Source*. URL: https://www.europe-solarstore.com/byd-battery-box-premium-hvm-19-3.html.